An Investigation into the Effect of Solid Particulate Phase On the Bioleaching Performance of *Sulfolobus metallicus*

Ashley A.Sissing

Submitted in fulfillment of the requirements for the degree of

MASTER OF SCIENCE IN ENGINEERING

(HALF DISSERTATION)

Department of Chemical Engineering
University of Cape Town
Cape Town, South Africa

Supervisor: Prof. S.T.L. Harrison

October 2002

ABSTRACT

Gold-bearing refractory sulphidic ores require a pretreatment process before extraction of the valuable metal, may be carried out. Bioleaching of the mineral may be used as pre-treatment. Further mineral bioleaching may be used to liberate base metals such as copper from refractory sulphidic ores. The microorganisms used in the high intensity tank-based commercial biohydrometallurgy processes are mainly mesophiles, although moderate thermophiles are currently used at Youanmi Mine in Australia (Brierley, 1997). Extreme thermophiles have been found to exhibit enhanced oxidation kinetics in terms of rate of reaction and extent of solubilisation (Duarte *et al.*, 1993; Norris and Barr, 1988; Konishi *et al.,* 1995). However, these thermophiles appear to be sensitive to hydrodynamic conditions (Clark and Norris, 1996) and the presence of solids (Le Roux and Wakerley, 1988; Nemati and Harrison, 2000). An understanding of this sensitivity would be useful in developing systems to utilise extreme thermophiles in commercial biohydrometallurgy processes.

The main objective of this study was to determine the effect of the solid particulate phase on the bioleaching performance of the extreme thermophile *Sulfolobus metallicus*. The hypothesis of the thesis was as follows:

Archae involved in bioleaching are susceptible to damage in agitated aerated vessels, especially with increasing pulp density.

Nemati and Harrison (2000) investigated the effect of solids loading on the bioleaching performance of *Sulfolobus metallicus* by varying the pulp density of pyrite. In this study, a constant pyrite concentration was used at which complete solubilisation had been achieved at a maximum rate (this occurred at 3% (w/v) pyrite (Nemati and Harrison, 2000)). The different solids concentrations were obtained by varying the concentration of an inert solid, quartz.

The effect of hydrodynamic forces generated with increasing power input and tip speed, mass transfer limitations and the state of the inoculum on the bioleaching performance of *Sulfolobus metallicus,* were also investigated in this study. Preliminary experiments to

determine the extent of chemical leaching at 68°C, and the partitioning of *Sulfolobus metallicus* between the particulate phase and the liquid phase were carried out.

The bioleaching experiments were performed in 1 litre stirred tank reactors equipped with a four pitch-blade stainless steel impeller and a set of four baffles to provide agitation for efficient mass transfer and mixing. The reactors were jacketed and maintained at a temperature between 68 and 70°C, while compressed air was provided at a rate of 2 l min^{-1}. The experiments were started at an agitation rate of 285 rpm (tip speed of 0.85 m s^{-1}) until the microbial cell concentration achieved a set value, and then the agitation rate was increased to 560 rpm (tip speed of 1.67 m s^{-1}) to completely suspend the solids. The bioleach performance was determined by monitoring the iron concentration, microbial cell concentration, pH and redox potential, and calculating the extent of pyrite solubilisation.

The extent of leaching observed in the absence of microorganisms was less than 30%, indicating that chemical leaching is limited at 68°C. Thus the results obtained for the bioleaching performance are due predominantly to biological leaching and the presence of the microorganisms.

Sulfolobus metallicus cells were found to remain in suspension, with association to the concentrate surface being insignificant. Owing to the small size of the archael cells, this implies that potential cell damage is unlikely to be caused by fluid forces as the cell size is much smaller than the eddy size. Damage is most likely a result of solid-cell-solid collision (Scholtz, 1998).

Solids loading was found to effect the bioleach performance. The iron release rate and extent of pyrite solubilisation was best in the presence of 3% (w/v) pyrite. Similar bioleaching results were obtained in the presence of 6 to 18% (w/v) total solids (3% pyrite and the remainder quartz). Bioleaching was progressively impaired with increasing solids loading above 18%(w/v) total solids loading. The growth rates for *Sulfolobus metallicus* were similar in the presence of 3 to 18%(w/v) total solids (3% pyrite and the

remainder quartz). The growth rate decreased by 39% at 24% total solids loading, and no growth was observed in the presence of 27% total solids loading. The yield in terms of microbial cells produced per kg iron oxidised remained constant at 1.6 to $1.9x10^{14}$ cells $(kg\ Fe)^{-1}$ at 3 to 18% (w/v) total solids (3% pyrite and the remainder quartz). The biomass yield decreased with increasing solids loading from 24% total solids loading (3% pyrite and 21% quartz). This decrease suggests that the microorganisms were becoming less efficient at utilising the iron substrate, or required a higher maintenance energy to withstand the hydrodynamic stress generated. The decrease in pyrite oxidation with increasing solids loading was due to a decrease in microbial cell concentration in the stationary phase. In the exponential growth phase, the decreased pyrite oxidation resulted from both a decreased microbial concentration and a decreased specific activity.

A comparison between a pyrite system and a pyrite/quartz system on the bioleaching performance was made to determine the effect of different solid particulate matter. The pyrite bioleaching system failed at 18%(w/v) total solids loading, while the pyrite/quartz system still exhibited iron solubilisation at 27%(w/v) total solids loading (3% pyrite and 24% quartz). The failure of the pyrite system at 18% solids was not due to inhibition from high iron concentration and low pH as the system failed before these were generated. Hydrodynamic stress may therefore be implicated. Higher particulate collision momentum, even though at lower frequency of collisions may have contributed to the failure of the pyrite system at a lower solids loading than the pyrite/quartz system. The higher oxygen demand in the pyrite system than the pyrite/quartz system with a constant oxygen transfer potential and similar mass transfer coefficients, could have resulted in the pyrite system being affected by oxygen limitation.

The oxygen mass transfer coefficient was measured for the solids loading range used in this study and it was found that these values did not vary significantly over this solids range. This implied that oxygen limitation did not contribute to the variation in bioleaching results across the range of solids loading investigated. Carbon dioxide limitation was a major factor affecting bioleaching performance. By reducing CO_2 limitation under conditions of severe hydrodynamic stress, bioleach performance

approached that under the less stressed environment. However, performance is not restored completely indicating that CO_2 limitation was not the only factor affecting reduced performance at high solids loading.

The effect of agitation rate on bioleaching performance was investigated using agitation rates of 560 rpm (tip speed of 1.67 m s^{-1}), 660 rpm (tip speed of 1.97 m s^{-1}) and 760 rpm (tip speed of 2.27 m s^{-1}). It was found that the iron leach rate and extent of pyrite solubilisation was higher at 660 rpm than at 560 rpm. The growth rate at 560 rpm was however slightly higher than at 660 rpm. The activity of the cells was higher at the lower agitation rate. An increase to 760 rpm, resulted in no pyrite solubilisation and cell death. The decrease in cell activity at higher agitation rates may have been due to increased damage on increased energy dissipation.

The difference in inoculum state resulted in significant differences in bioleaching performance. Microbes maintained in a stirred tank achieved an iron release rate of 0.15 kg m^{-3} h^{-1}, while inoculum maintained in a shake flask achieved an iron release rate of 0.028 kg m^{-3} h^{-1}. The improved physiological health of the microbes maintained in the stirred tank reactor resulted in their ability to handle stress better than the microbes maintained in the shake flask.

The general findings of this study were:

- Decreased bioleaching performance resulted from decreased cell number.
- During the exponential phase the cell activity decreased with increased hydrodynamic stress due to increased solids loading or agitation rate.
  During the stationary phase, cell activity was constant.
- An improvement in the condition of the cells resulted in an increased resilience of the cells, making them better able to cope with hydrodynamic stress.

The hypothesis of the study, being that *archae used in agitated aerated vessels, especially with increasing pulp density*, was therefore proved.

To maximise space time utilisation of bioreactors, good performance at high solids loading is required. The significance of these findings in the commercial environment are as follows:

- The results clearly indicate that there is a limitation to the solids loading and to the power input per unit volume that can be loaded on the bioreactors. The latter leads to a compromise with maximising gas mass transfer which is essential to the cells.
- The results suggest that maximising the physiological health of the cells prior to entering the slurry reactor, maximises their resilience to damage.

Acknowledgements

I would like to thank a number of people for assisting me with my work and with my post-graduate life:

My supervisor, Professor Sue Harrison, for everything.

Professor Geoff Hansford, for his useful input and interest in my work.

Sue Jobson, for making the life aspect easier.

The bio's group and especially Shenaaz Moosa and Andrew Robinson for their help and guidance.

The mechanical workshop.

The electrical workshop.

And all my friends who know who they are.

Ashley

Contents

List of figures

List of tables

1. Introduction **1-1**

1.1. Objective of study 1-2

1.2. Thesis structure 1-3

1.3. References 1-4

2. The pretreatment of sulphide minerals **2-1**

2.1. Traditional pretreatment methods 2-2

2.1.1. Roasting 2-2

2.1.2. Pressure leaching 2-2

2.2. Bioleaching / biooxidation 2-3

2.2.1. Mechanism of bioleaching 2-4

2.2.1.1. Direct bioleaching 2-4

2.2.1.2. Indirect bioleaching 2-5

2.2.1.3. Chemical leaching 2-6

2.2.2. Microorganisms employed in bioleaching 2-6

2.2.2.1. Mesophiles 2-7

2.2.2.2. Moderate thermophiles 2-8

2.2.2.3. Extreme thermophiles 2-8

2.3. Conclusion 2-10

2.4. References 2-10

3. Thermophilic bioleaching **3-1**

3.1. Specific characteristics of archae 3-2

3.1.1. *Sulfolobacae* family 3-2

3.1.2. Genus *Sulfolobus* 3-3

3.1.2.1. Morphology of *Sulfolobus* 3-3
3.1.2.2. Nature of cell wall 3-3
3.2. Structural differences between thermophiles and mesophiles 3-4
3.3. Advantages of thermophilc bioleaching 3-5
3.3.1. Oxidation kinetics 3-5
3.3.2. Cooling requirements 3-7
3.4. Disadvantages of thermophilic bioleaching 3-7
3.4.1. The effect of reactor configuration on thermophilic bioleaching 3-8
3.4.2. The effect of chemical toxicities on thermophilic bioleaching 3-8
3.4.3. The effect of solid loading on thermophilc bioleaching 3-9
3.4.4. The effect of particle size on thermophilc bioleaching 3-10
3.5. Conclusion 3-11
3.6. References 3-11

4. The use of microorganisms in slurry reactors 4-1
4.1. Factors affecting microbial cells in slurry reactors 4-2
4.1.1. Hydrodynamic effects 4-2
4.1.1.1. Sparging 4-3
4.1.1.2. Agitation intensity 4-3
4.1.1.3. Impeller flow pattern 4-4
4.1.2. Effect of solid particles 4-5
4.1.2.1. Particle size 4-6
4.1.2.2. Pulp density 4-7
4.1.2.3. Inhibitory effects of the particulate material 4-9
4.1.3. Mechanisms of mechanical damage to the microorganisms 4-10
4.1.3.1. Cell-bubble interactions 4-10
4.1.3.2. Cell-fluid eddy interactions 4-11
4.1.3.3. Cell-solid particle interactions 4-11
4.1.3.4. Cell-reactor component interactions 4-12

4.1.4. Mass transfer 4-12
4.1.4.1. Oxygen transfer potential versus demand 4-14
4.1.4.2. Effect of viscosity on k_La 4-15
4.1.4.3. Effect of diffusivity on k_La 4-16
4.1.4.4. Investigations into mass transfer limitations 4-16
4.1.4.5. Availability of carbon dioxide 4-18
4.2. Hypothesis and objectives 4-18
4.3. References 4-20

5. Materials and methods 5-1
5.1. Microorganisms and culture maintenance 5-1
5.2. Experimental methodology 5-2
5.2.1. Bioleaching experimental set-up 5-2
5.2.2. Methodology 5-4
5.2.2.1. Chemical leaching 5-4
5.2.2.2. Adsorption 5-4
5.2.2.3. Bioleaching experiments investigating pulp density 5-5
5.2.2.4. Mass transfer recordings 5-6
5.2.2.5. Bioleaching experiments investigating carbon dioxide limitation 5-6
5.2.2.6. Bioleaching experiments investigating the effect of agitation rate 5-6
5.2.2.7. Bioleaching experiments investigating the state of the inoculum 5-6
5.3. Analytical procedures 5-7
5.3.1. Ferrous iron concentration 5-7
5.3.2. Total iron and ferric iron concentrations 5-8
5.3.3. Bacterial concentration 5-9
5.4. Summary 5-10
5.5. References 5-10

6. Results and discussion 6-1

6.1. Reproducibility of bioleaching experiments 6-2

6.2. Chemical leaching 6-3

6.3. Partitioning of *Sulfolobus* between concentrate surface and Liquid phase 6-6

6.4. Effect of solids loading on bioleaching performance 6-10

6.4.1. Bioleaching performance as a function of solids loading 6-10

6.4.2. Effect of solids loading on bioleach performance – Iron release and microbial cell concentration 6-18

6.4.2.1. Iron release at various solids loading 6-18

6.4.2.2. Microbial cell concentration at various solids loading 6-19

6.4.2.3. pH and redox potential 6-22

6.4.3. Comparison of current research with literature 6-25

6.4.3.1. Bioleaching performance at 3% pyrite 6-26

6.4.3.2. Bioleaching performance at 18% pyrite 6-28

6.4.3.3. Bioleaching performance at 18% pyrite and Pyrite/quartz 6-30

6.4.3.4. Bioleaching performance of pyrite and pyrite/quartz 6-34

6.4.4. Concluding remarks 6-38

6.5. The effect of oxygen and carbon dioxide supply 6-39

6.5.1. Gas - liquid mass transfer in the slurry system 6-39

6.5.2. The effect of carbon dioxide limitation 6-41

6.6. The effect of agitation rate on the bioleach performance 6-44

6.7. The effect of inoculum state on the bioleach performance 6-47

6.8. Conclusion 6-51

6.9. References 6-52

7. Conclusion 7-1

7.1. Chemical leaching 7-1

7.2. Partitioning of *Sulfolobus* between concentrate surface and Liquid phase 7-2

7.3. The effect of solilds loading on bioleaching performance 7-3

7.3.1. Interactions between solids loading and physicochemical conditions and their effect on bioleaching 7-6

7.4. Mass transfer 7-10

7.5. The effect of agitation rate on bioleaching performance 7-11

7.6. The effect of inoculum state on bioleaching performance 7-13

7.7. Summary of findings 7-13

7.8. Recommendations for further study 7-16

7.8.1. Improved experimental conditions in the laboratory 7-16

7.8.2. Implementing findings at a commercial scale 7-16

7.9. References 7-17

Appendices

List of Figures

4.1. Effect of specific surface area of ore particle on leaching rate at pH 2.3, 35°C and 6% solid (Torma *et al.*, 1971)

4.2. Schematic diagram of oxygen transfer demand vs. solids concentration (Bailey and Hansford, 1994)

4.3. Slurry viscosity vs. solids concentration (Rao, 1966)

6.1. (a & b) Reproducibility of the bioleaching of 3% pyrite in the presence of 12% quartz by *Sulfolobus metallicus* in terms of iron release and microbial cell concentration

6.2. Bioleaching profiles of *Sulfolobus metallicus* at 68°C in the presence of 3% pyrite as a function of pH and redox potential, microbial cell count, iron release and ferrous iron concentration

6.3. Bioleaching profiles of *Sulfolobus metallicus* at 68°C in the presence of 3% pyrite and 6% quartz as a function of pH and redox potential, microbial cell count, iron release and ferrous iron concentration

6.4. Bioleaching profiles of *Sulfolobus metallicus* at 68°C in the presence of 3% pyrite and 15% quartz as a function of pH and redox potential, microbial cell count, iron release and ferrous iron concentration

6.5. Bioleaching profiles of *Sulfolobus metallicus* at 68°C in the presence of 3% pyrite and 21% quartz as a function of pH and redox potential, microbial cell count, iron release and ferrous iron concentration

6.6. Bioleaching profiles of *Sulfolobus metallicus* at 68°C in the presence of 3% pyrite and 24% quartz as a function of pH and redox potential, microbial cell count, iron release and ferrous iron concentration

6.7. Total iron release as a function of time at various solids loading

6.8. Microbial cell concentration profiles for various solids loading

6.9. Microbial cell activity in terms of specific pyrite oxidation rate as a function of solids loading and duration of experiment

6.10. pH profiles for various solids loading

6.11. Redox potential profiles for various solids loading

6.12. (a & b) Comparison of iron release and microbial cell profiles for 3% pyrite reported by Nemati and Harrison (2000) and in the current system
6.13. (a & b) Comparison of iron release and microbial cell profiles for 18% pyrite reported by Nemati and Harrison (2000) and in the current system
6.14. (a & b) Comparison of iron release and microbial cell profiles for 18% pyrite and 18% pyrite/quartz in the current system
6.15. (a) Bioleaching performance as a function of solids loading – pyrite system
6.16. (b) Bioleaching performance as a function of solids loading – pyrite/quartz system
6.17. (a & b) Iron release and microbial cell profiles for various agitation rates
6.18. Activity of microbial cells (iron release per hour per cell) at various agitation rates
6.19. Particle size distribution of quartz fraction used
6.20. (a & b) Iron release and microbial cell concentration profiles using shake flask and stirred tank inoculum after increase of agitation rate
7.1. Bioleach rate and extent of iron solubilisation as a function of total solids loading
7.2. Microbial growth rate and biomass yield in terms of microbial cells produced per kg iron oxidized as a function of total solids loading
7.3. Microbial cell activity in terms of specific pyrite oxidation rate as a function of solids loading and duration of experiment
7.4. (a) Rate of iron release and extent of pyrite dissolution at various agitation rates
7.5. (b) Specific growth rate and microbial activity at various agitation rates

List of Tables

3.1. Solubilisation rates obtained for thermophiles and mesophiles

3.2. Metal additions required to cause moderate inhibition of iron –oxidising acidophiles (Norris *et al.,* 1986)

5.1. Composition of medium (Nemati and Harrison, 2000)

6.1. Chemical leaching of pyrite at 70°C under bioleaching conditions

6.2. Adsorption of *Sulfolobus metallicus* to pyrite

6.3. Adsorption experiments showing the change in free cell concentration with time

6.4. Average pyrite leach rate and extent of pyrite solubilisation at the various solids loading

6.5. Microbial cell data for various solids loading

6.6. Comparison of bioleaching performance of nemati and Harrison (2000) and the current work

6.7. Comparison of bioleaching performance using 18% pyrite and 3% pyrite and 15% quartz

6.8. Mass transfer coefficient measurement at various solids loading

6.9. Percentage depression in the absence of carbon dioxide enrichment relative to enrichment with carbon dioxide

6.10. The effect of inoculum state on the bioleach performance

CHAPTER 1

INTRODUCTION

The use of biotechnological methods for pre-treatment in hydrometallurgy has been employed for the past 40 years and research is continuing in this field. Refractory sulphidic ores require a pre-treatment process before extraction of valuable metals, such as copper and gold, may be carried out. A description of the possible pre-treatment methods is described in Chapter 2 where the potential value of biohydrometallurgical technologies is also identified. The micro-organisms used in the commercial biohydrometallurgy processes are mainly mesophiles, although moderate thermophiles are currently used at the Youanmi Mine in Australia (Brierley, 1997). The study of the use of mesophiles for mineral bioprocessing has been extensively researched (van Aswegen *et al.* 1991, Gormely and Branion, 1989). Study into the use of extreme thermophiles for mineral bioprocessing has been attracting increasing interest over recent years. Thermophiles grow at higher temperatures than the mesophiles, 65-85°C compared to 30-45°C. The oxidation reactions involved in the solubilisation of mineral sulphides are exothermic, hence the ability of the thermophiles to grow at higher temperatures is advantageous in providing an improved driving force for heat removal. In addition, enhanced oxidation kinetics in terms of rate of reaction and extent of solubilisation is a potential advantage of thermophilic bioleaching (Duarte *et al.*, 1993; Norris and Barr, 1988; Konishi *et al.*, 1995).

The study of the use of thermophiles in minerals bioprocessing has thus far largely confined to the extent and rate of solubilisation and the comparison of mesophilic and thermophilic minerals bioleaching (Konishi *et al.*, 1995; Norris and Barr, 1988; Le Roux and Wakerley, 1987). The potential disadvantages of thermophilic bioleaching are that the thermophiles used for bio-oxidation appear to be sensitive to hydrodynamic conditions (Clark and Norris, 1996) and the presence of solids (Le Roux and Wakerley, 1988; Nemati and Harrison, 2000). These disadvantages may be due to the fact that the *Sulfolobus* lack a rigid peptidoglycan cell wall

(König, 1988). In addition, an increase in temperature causes the fluidity of cellular membranes to increase (Kelly and Deming, 1988) and the mass transfer of oxygen to decrease owing to decreasing solubility.

Maximum rates of mineral concentrate leaching have been obtained with a solids concentration of 6-8 % w/v pyrite (Norris, 1997) and 9% w/v pyrite (Nemai and Harrison, 2000). Nemati and Harrison (2000) obtained mineral solubilisation at 15 % w/v pyrite in two distinct stages of solubilisation: one at 0.07 kg iron $m^{-3}h^{-1}$ and the other at 0.0017 kg iron $m^{-3}h^{-1}$. The bioleaching rate at 9 % w/v pyrite was 0.09 kg iron $m^{-3}h^{-1}$. The preferred minimum mineral concentration for industrial application is 10 % w/v mineral (Norris, 1997). Current mesophilic bioleaching processes are operated at 18-20% w/v concentrate (Oguz *et al.*, 1987). Knowledge of the effect of solids concentration on thermophilic bioleaching performance is therefore critical for optimisation of thermophilic bioleaching for industrial application.

Several factors affect microbial cells in slurry reactors. A review of these factors and their effect on various organisms may assist in identifying factors that affect thermophiles in slurry reactors. These factors include:

1. hydrodynamic effects - sparging, agitation intensity and impeller flow pattern;
2. effect of solids - particle size, solids concentration and the inhibitory effects of the particulate material (toxicity); and
3. mass transfer effects which depend on the power input per unit volume, the gas sparge rate, the liquor viscosity and the liquid-phase diffusivity of oxygen.

In a three-phase system, solids affect the mass transfer through the particle type and size, solids concentration and operating conditions.

1.1. OBJECTIVE OF THE STUDY

The objective of this work is to determine the effect of solids concentration on the bioleaching performance of thermophilic micro-organisms, namely *Sulfolobus metallicus*. Nemati and Harrison (2000) investigated the effect of solids loading on the bioleaching performance of

Sulfolobus metallicus by varying the pulp density of pyrite. In this research, a constant pyrite concentration is used at which complete solubilisation has been achieved at a maximum rate (this occurred at 3 % w/v pyrite (Nemati and Harrison, 2000)). The concentration of an inert solid, quartz, will be varied to obtain different solids concentrations. This eliminates possible toxic effects due to the sulphide mineral and the increasing solubilisation of iron and sulphate with increasing solids loading. The density of quartz, however is less than that of pyrite (relative density of 2.6 compared to 5.0). This may lead to changes in the mass transfer, impeller flow pattern, power input and collision momentum in the pyrite-silica system with respect to the system containing only pyrite.

At high solids concentrations, oxygen availability has been identified as a key factor in limiting bio-oxidation (Bailey and Hansford, 1994). The mass transfer of oxygen is thus ascertained at the various solids concentrations. The enrichment of air with carbon dioxide has proved to be beneficial in increasing the bio-oxidation rate at high solids concentrations (Torma *et al.*, 1972). This is also investigated in this research.

Agitation intensity has been found to have an inhibitive effect on *Sulfolobus* activity at 5 % w/v pyrite when comparing solubilisation rates in an airlift vessel and a stirred tank reactor (Norris and Barr, 1988). The effect of agitation intensity using different agitation speeds in a stirred tank reactor is presented in this thesis.

1.2. THESIS STRUCTURE

The pretreatment of sulphide minerals is discussed in Chapter 2, along with a detailed description of bioleaching and the microorganisms employed in bioleaching.

Previous work on thermophilic bioleaching is presented in Chapter 3. The oxidation kinetics are given and a comparison is made of the rate and extent of solubilisation between mesophilic and thermophilic bioleaching. Possible advantages and disadvantages of the use of thermophiles for bioleaching are proposed along with experimental data to validate the factors that could affect

thermophilic bioleaching. Analysis of previous work highlights areas of research not addressed that require further investigation to determine their effect on thermophilic bioleaching.

Factors that could affect microorganisms in slurry reactors are presented in chapter 4. This covers work done mainly on mesophilic bioleaching which is more extensive than work done on thermophilic bioleaching. An understanding of the factors that affect other microorganisms in slurry work may help to identify factors that affect thermophilic bioleaching.

The experimental methods used to examine these objectives are discussed in Chapter 5, with the results and relevant discussions in Chapter 6. The conclusions drawn from this work are presented in Chapter 7.

1.3. REFERENCES

Bailey, A.D. and G.S. Hansford (1994), "Oxygen mass transfer limitation of batch bio-oxidation at high solids concentration", *Minerals Engineering*, **7**, 293-303

Brierley, C.L. (1997), "Mining Biotechnology: Research to commercial development and beyond", in *Biomining: Theory, Microbes and Industrial Processes*, Eds. D.E. Rawlings, Springer-Verlag and Landes Bioscience, 3-17

Clark, D.A. and P.R. Norris (1996), "Oxidation of mineral sulphides by thermophilic micro-organisms", *Minerals Engineering*, **9**(11), 1119-1125

Duarte, J.C., P.C. Estrada, P.C. Pereira and H.P. Beaumont (1993), 'Thermophilic vs. mesophilic bioleaching process performance', *FEMS Microbiology Reviews*, **11**, 97-102

Gormely, L.S. and R.M.R. Branion (1989), "Engineering design of microbiological leaching reactors", *Proceedings of Biohydrometallurgy '89*, Wyoming, USA, 499-515

Kelly, R.M. and J.W. Deming (1988), "Extremely thermophilic archaebacteria: Biological and engineering considerations", *Biotechnology Progress*, **4**(2), 47-62

König, H. (1988), "Archaebacterial cell envelopes", *Canadian Journal of Microbiology*, **34**, 395-406

Konishi, Y., S. Yoshida and S. Asai (1995), "Bioleaching of pyrite by acidophilic thermophile *Acidianus brierleyi*", *Biotechnology and Bioengineering*, **48**, 592-600

Le Roux, N., W. and D.S. Wakerley (1988), "Leaching of Chalcopyrite ($CuFeS_2$) at 70°C using *Sulfolobus*", *Proceedings of Biohydrometallurgy '87,* Eds. P.R. Norris and D.P. Kelly, Science and Technology Letters, Surrey, United Kingdom, 305-317

Nemati, M. and S.T.L. Harrison (2000), "Effect of solid loading on thermophilic bioleaching of sulphide minerals", *Journal of Chemical Technology and Biotechnology,* **75**, 526-532

Nemati, M., J. Lowenadler and S.T.L. Harrison (2000), "Particle size effects in bioleaching of pyrite by acidophilic thermophile *Sulfolobus metallicus (BC)*", *Applied Microbiology and Biotechnology*, **53**: 173-179

Norris, P.R. (1997), "Thermophiles and Bioleaching", in *Biomining: Theory, Microbes and Industrial Processes*, Ed. D.E. Rawlings. Springer-Verlag and Landes Bioscience, 247-258

Norris, P.R. and D.W. Barr (1988), "Bacterial oxidation of pyrite in high temperature reactors", *Proceedings of Biohydrometallurgy '87*, Eds. P.R., Norris and D.P. Kelly, Science and Technology Letters, Surrey, United Kingdom, 532-536

Oguz, H., A. Brehm and W.D. Deckwer (1987), "Gas/liquid mass transfer in sparged agitated slurries", *Chemical Engineering Science*, **42**, (7), 1815-1822

Torma, A.E., C.C. Walden, D.W. Duncan and R.M.R. Branion (1972), "The effect of carbon dioxide and particle surface area on the microbiological leaching of a zinc sulphide concentrate", *Biotechnology and Bioengineering*, **14**, 777-786

van Aswegen, P.C., M.W. Godfrey, D.M. Miller and A.K. Haines (1991), "Developments and innovations in bacterial oxidation of refractory ores", *Minerals Engineering*, **8**, (4), 191-199

CHAPTER 2

THE PRETREATMENT OF SULPHIDE MINERALS

Gold ore is often found in close association with sulphide minerals such as pyrite and arsenopyrite. This ore is known as refractory sulphidic gold ore. The ore is considered to be refractory if, in the absence of a pre-treatment step and after fine grinding, the gold extraction by conventional cyanide leaching is less than 80%. A pre-treatment step is used to destroy the sulphide matrix exposing the gold for contact with cyanide ions facilitating gold dissolution of the gold occurs (Iglesias and Carranza, 1996).

For base metal systems whereby valuable metals are extracted from ore, a pre-treatment step may be required. The mineral sulphide chalcopyrite is very refractory to attack in acidic solutions, and thus requires either the presence of an oxidant, such as ferric ion (Gómez *et al.,* 1996), or oxygen pressure leaching at temperatures exceeding 200°C (Hackl *et al.*, 1995).

Oxidative pre-treatment can be achieved by roasting, pressure oxidation and bio-oxidation (Poulin and Lawrence, 1996). These are discussed below with details of the advantages and disadvantages of each process. Since the focus of the study is on bioleaching, a detailed description of the bioleaching mechanisms is given in Section 2.2 along with the micro-organisms used in bioleaching.

2.1. TRADITIONAL PRETREATMENT METHODS

2.1.1 Roasting

Roasting removes harmful constituents by oxidation or vaporisation, releasing metals from pyrite at temperatures of 600-800°C. For metals, such as gold, that require subsequent cyanide leaching, this method can result in poorer metal recovery if compounds, such as metallic copper and copper compounds that consume cyanide in the metal recovery stage, are formed (Lawrence and Bruynesteyn, 1983).

The capital and operating costs of roasting are intensive and the process has a negative impact on the environment (Iglesias *et al.*, 1993). Gas scrubbers are required to capture sulphur dioxide and arsenic trioxide emissions (Poulin and Lawrence, 1996).

2.1.2. Pressure Leaching

In this process, sulphide minerals are broken down in an autoclave using steam and oxygen injection at pressures in the region of 20 atmospheres and approximately 200°C. It is combined with chemical leaching, due to the increased activity of oxygen as a chemical leaching agent at high pressures. Pressure leaching results in good recoveries but cannot be used when carbonaceous material is present. Capital costs are high as advanced materials of construction are required for autoclaves, and an associated oxygen plant is necessary. Operator costs are high due to the high level of operator training and skill required, whilst the safety requirements related to handling high pressures and temperatures (Poulin and Lawrence, 1996) also need to be considered.

2.2. BIOLEACHING/BIOOXIDATION

In bioleaching, micro-organisms leach a valuable metal such as copper, zinc, uranium, nickel and cobalt from a sulphide mineral. The valuable metal moves into the liquid phase during bioleaching. This solution is then treated further for maximum recovery of the metal, while the solid residue is discarded (Brierley, 1997).

Mineral bio-oxidation is a pre-treatment process which catalyses the degradation of mineral sulphides, usually pyrite and arsenopyrite which host gold, silver or both, using the same bacteria used in bioleaching. The valuable metals are left in the solid phase but are amenable to leaching such as cyanide leaching. The solution is discarded (Brierley, 1997).

The micro-organisms used in bioleaching to date are usually mesophiles – *Acidithiobacillus ferrooxidans* and *Leptospirillium ferrooxidans*. Increasing interest is developing in moderate and extreme thermophiles – *Sulfobacillus, Acidianus* and *Sulfolobus*. Bioleaching and bio-oxidation can be applied to high grade mineral concentrates (the grade depending on the sulphide content, with higher grade minerals containing higher sulphide quantities), and ores, in stirred tank or airlift bioreactors, where the ore is suspended as finely ground particles in a nutrient medium containing the microorganisms. With low-grade ores, bioleaching or bio-oxidation is used to treat the ore in heap leaching operations (Brierley, 1997).

Mine operators have cited advantages for using stirred-tank bio-oxidation over conventional roasting and pressure autoclave technologies as follows (Brierley, 1997):

- lower capital and operating costs
- greater gold recovery
- shorter construction period
- robust process
- environmental requirements less demanding
- production of a stable iron/arsenic residue

- simple operation requiring less skilled labour
- plants safer and healthier.

Bio-oxidation processes are, however, sensitive to water quality, especially salt content, cyanide and thiocyanate content. Power and neutralisation costs may thus be high (Poulin and Lawrence, 1996). Long residence times of the order of days are required for bio-oxidation plants, increasing operating costs. Improving the kinetics of bio-oxidation would therefore be desirable (Iglesias and Carranza, 1996).

2.2.1. Mechanism for Bioleaching

The role of the microorganisms used in bioleaching is not clearly understood and thus not precisely defined. Two theories exist on the mechanism of the leaching process. The 'direct' leaching hypothesis proposes that the microbes attach to the mineral surface and directly oxidise the mineral. The 'two-step' or 'indirect' mechanism hypothesis proposes that the microbes generate ferric iron, which then oxidises the mineral (Brierley and Brierley, 1986). The microbes continually regenerate the ferric leaching agent from the ferrous product. Chemical ferric leaching takes place to an extent that is dependent on the mineral. The mechanisms employed are dependent on parameters such as temperature, pH, redox potential and solids concentration.

2.2.1.1. Direct Bioleaching

The direct mechanism proposes enzymatic attack on the mineral induced by the microbe adhered to the mineral surface. The overall reaction on pyrite is:

$$FeS_2 + 3\frac{1}{2}O_2 + H_2O \rightarrow FeSO_4 + H_2SO_4 \qquad (eqn.2.1)$$

The solubilisation of iron results. The iron is subsequently oxidised back to ferric iron by the microbes, and this ferric iron then participates in the 'indirect' leaching process (Brierley and Brierley, 1986). The microorganisms cause the release of metal ions from

the mineral, while using oxygen and carbon dioxide and releasing sulphate ions (Boon and Heijnen, 1993).

2.2.1.2. Two-step or Indirect Bioleaching

In the two-step mechanism, microbial energy generation occurs on oxidation of ferrous iron to ferric iron in acidic conditions (Moses and Cape, 1991):

$$4FeSO_4 + O_2 + 2H_2SO_4 \rightarrow 2Fe_2(SO_4)_3 + 2H_2O \qquad (eqn.2.2)$$

The ferric iron produced acts as a chemical leaching agent. The ferric iron is a strong oxidising agent and can oxidise minerals such as pyrite (FeS_2) or chalcopyrite ($CuFeS_2$):

$$FeS_2 + 14Fe^{3+} + 8H_2O \rightarrow 15Fe^{2+} + 2SO_4^{2-} + 16H^+ \qquad (eqn.2.3)$$

$$CuFeS_2 + 2Fe_2(SO_4)_3 \rightarrow CuSO_4 + 5FeSO_4 + 2S \qquad (eqn.2.4)$$

The soluble metals and sulphates are recovered by solvent extraction, ion exchange or other methods. The ferrous iron in solution is reoxidised to ferric iron by the microorganisms and recycled in the leaching process. Ferrous iron oxidation is slow at low pH, but bacteria greatly accelerate the process.

$$2Fe^{2+} + 0.5O_2 + 2H^+ \xrightarrow{bacteria} 2Fe^{3+} + 2H_2O \qquad (eqn.2.2)$$

Microorganisms also oxidise elemental sulphur, producing sulphuric acid and exposing the metal for further leaching (Moses and Cape, 1991).

$$S_0 + 1.5O_2 + H_2O \xrightarrow{bacteria} H_2SO_4 \qquad (eqn.2.5)$$

Elemental sulphur that is formed or remains after the pre-treatment process is undesirable in the cyanide leach step as it produces thiocyanate ions that increase cyanide

consumption (Iglesias and Carranza, 1996). The elemental sulphur can interact with copper to form a copper polysulphide that covers the surface of chalcopyrite, causing passivation (Hackl *et al.*, 1995).

2.2.1.3. Chemical Leaching

In the 'indirect' bioleaching mechanism, chemical oxidation of the mineral forms the primary attack on the mineral. The rate of chemical oxidation of mineral sulphides by ferric iron is thus important. The chemical oxidation of pyrite is as follows:

$$FeS_2 + 14Fe^{3+} + 8H_2O \rightarrow 15Fe^{2+} + 2SO_4^{2-} + 16H^+ \qquad (eqn.2.3)$$

According to the Arrhenius equation, the rate of most chemical reactions increases exponentially with temperature. Zheng *et al.* (1986) demonstrated that the rate of chemical leaching of pyrite is also a function of the ferric iron concentration, the ratio of ferric to ferrous iron and the sulphate ion concentration.

Boogerd *et al.* (1991) determined the relative contributions of biological and chemical leaching to the overall rate of pyrite oxidation at 30, 45 and 70°C in shake flasks at pH 1.5. The chemical contribution to oxidation of pyrite by (biologically produced) ferric iron was 2, 8-17 and 43% respectively. Chemical leaching of pyrite at 70°C was found to be 33% according to Vitaya *et al.* (1994). The ferrous iron formed during the reaction reduced the rate of oxidation of pyrite by ferric iron. The extent of this effect decreased with increasing temperature (Boogerd *et al.*, 1991).

2.2.2. Micro-organisms Employed in Bioleaching

The organisms used in the bioleaching process are those capable of oxidising reduced iron and sulphur compounds. These organisms are strictly aerobic chemoautotrophs deriving energy from the oxidation of reduced iron and/or sulphur and fixing carbon

dioxide from the atmosphere. The production of energy from the ferrous iron oxidation is coupled to the carbon dioxide fixation reactions (Moses and Cape, 1991).

There are three groups of organisms used for bioleaching, namely mesophilic, moderately thermophilic or extremely thermophilic microorganisms. These have optimum growth temperature ranges of 30-45, 45-55 and >55°C, respectively. The microorganism chosen may be limited by operating conditions. For instance, higher leach rates of up to five fold the rate of mesophiles are achieved with thermophiles (Norris and Barr, 1988). However optimum conditions for thermophilic bioleaching have been found to be at a low pulp density of between 6 and 8% w/v (Norris, 1997) and 9% w/v (Nemati and Harrison, 2000), which restricts industrial application.

For a microorganism to be successfully implemented in a bioleaching system, it should display the following characteristics (Lawrence and Marchant, 1988):

- Ability to oxidise ferrous iron and/or reduced sulphur compounds
- Fast oxidation kinetics
- Tolerance to high pulp densities
- Tolerance to low pH and high metal concentrations

A description of the different groups of micro-organisms in terms of their optimum growth temperatures is given below.

2.2.2.1. Mesophiles

Mesophilic chemoautotrophic bacteria such as *Acidithiobacillus ferrooxidans* (previously *Thiobacillus ferrooxidans*), *At. thiooxidans* (previously *T. thiooxidans*) and *Leptospirillum ferroxidans* are commonly isolated from inorganic environments. These bacteria are used at temperatures between 35 and 45°C and pH between 1.2 and 1.8. High temperatures have a negative effect on the activity of the mesophiles due to protein denaturation (Torres *et al.*, 1995). *At. ferrooxidans* and *At. thiooxidans* are rod shaped, ranging in size from 0.3 to 0.8 μm in diameter and 0.9 to 2.0 μm in length (Barrett *et al.*, 1993).

At. ferrooxidans is able to use either ferrous iron or reduced sulphur compounds as electron donors to obtain energy. *At. thiooxidans* can only use reduced sulphur compounds as an electron donor, while *L. ferrooxidans* can only use ferrous iron. *At. ferroxidans* can therefore produce more energy per mole of pyrite oxidised than either *A. thiooxidans* or *L. ferrooxidans*. *At. ferroxidans*, however, displays a delay when switching from sulphur to iron substrates and *vice versa* (Breed, 2000).

2.2.2.2. Moderate Thermophiles

Moderately thermophilic bacteria are usually isolated from sulphide ore dumps, volcanic regions and thermal springs. The use of moderate thermophiles in bioleaching operations may be economically viable as these bacteria exhibit accelerated rates of biological and chemical reactions compared to mesophiles, whilst solubility of oxygen and carbon dioxide is higher than growth conditions of extreme thermophiles (Breed, 2000).

The moderately thermophilic bacteria most commonly used in bioleaching are *T. caldus* and *S. thermosulfidooxidans*. *At. caldus* operate at temperatures of between 30 and 40°C. The cells are short, motile, Gram-negative rods. They are capable of chemolithoautotrophic growth on reduced sulphur substrates such as thiosulphate, tetrathionate, sulphide, sulphur and molecular hydrogen, and have been described as the moderately thermophilic equivalent of *At. thiooxidans* (Hallberg, 1995). *S. thermosulfidooxidans* are Gram-positive and generally occur as straight rods of 0.5–1.0 μm by 1.0-6.0 μm (Karavaiko *et al.*, 1988). This species are facultatively autotrophic, aerobic eubacteria. They are unable to assimilate sulphate into proteins, and thus cannot grow on pyrite or ferrous iron unless a source of reduced sulphur is present (Norris and Barr, 1985). They are able to grow under heterotrophic conditions without losing their ability to catalyse mineral oxidation. The different strains of *S. thermosulfidooxidans* grow at temperatures of between 50 and 60°C.

2.2.2.3. Extreme Thermophiles

The use of extreme thermophiles in bioleaching has the potential of increased rates of biological and chemical reactions over those possible at lower temperatures. Operating at

higher temperatures would have the added advantage of reduced cooling requirements (Miller, 1997).

Operating at higher temperatures, however, leads to the disadvantages of thermophilic bioleaching, namely:

1. the reduced solubility of both oxygen and carbon dioxide,
2. increased evaporative loss, and
3. highly oxidising acidic slurries at temperatures above 50°C require appropriate materials of construction.

The acidophilic extreme thermophiles are archae. Archae have been isolated from geothermal hot springs and burning coal tips. Temperatures in the region of 50-80°C have been measured in heap leach operations, suggesting that extreme thermophiles may occur naturally in these environments. Archae inhabit extreme conditions, including high temperatures, acidic conditions and high halide concentrations.

In biohydrometallurgy, the archae of importance are *Sulfolobus* and *Acidianus* (Barrett *et al.,* 1993). They have a negative response to the gram staining test, but cannot be described as Gram-negative. *Sulfolobus* and *Acidianus* are coccoid-shaped and have diameters of approximately 1 μm. They are both immotile and neither have flagella. *Sulfolobus* does, however, have pili-like structures that are thought to be involved in the mechanism of attachment to surfaces.

S. acidocaldarius and *A. brierleyi* are facultative chemolithoautotrophs and grow under autotrophic, mixotrophic or heterotrophic conditions (Barrett *et al.,* 1993). *S metallicus* is strictly chemolithoautotrophic (Huber and Stetter, 1991). *S. acidocaldarius* can oxidise elemental sulphur under anaerobic conditions, using ferrous iron as the terminal electron acceptor. *A. brierleyi* can grow anaerobically on sulphur, producing H_2S from this energetic pathway. *S. metallicus* (Huber and Stetter, 1991) is considered to be a strict aerobe. The temperature ranges for growth of both *S. acidocaldarius* and *A. brierleyi* are

55-80°C with an optimum growth temperature of 70°C, while that of *S. metallicus* is 50-75°C with an optimum of 65°C.

2.3. CONCLUSION

For refractory sulphidic gold ores and base metal systems, whereby valuable metals are extracted from the ore, a pre-treatment step may be required. Oxidative pre-treatment, which can be achieved by roasting, pressure oxidation and bio-oxidation, have been described in this chapter. The advantages of using bio-oxidation over the former methods include lower capital and operating costs, greater gold recovery and less demanding environmental requirements. The microorganisms that can be used for bioleaching/bio-oxidation, namley mesophiles, moderate thermophiles and extreme thermophiles, were discussed with the indication that extreme thermophiles could potentially be the most beneficial microorganism to use. Bioleaching using extreme thermophiles will be discussed in Chapter 3.

2.4. REFERENCES

Barrett, J., M.N. Hughes, G.I. Karavaiko and P.A. Spencer (1993), Metal Extraction by Bacterial Oxidation of Minerals, Ellis Horwood, New York

Boogerd, F.C., C. van den Beemd, T. Stoellwinder, P. Bos and J.G. Kuenen (1991), "Relative contributions of biological and chemical reactions to the overall rate of pyrite oxidation at temperatures between 30°C and 70°C", *Biotechnology and Bioengineering*, **38**, 109-115

Boon , M. and J.J. Heijnen (1993), "Mechanisms and rate limiting steps in bioleaching of sphalerite, chalcopyrite and pyrite with *Thiobacillus ferrooxidans*", in *Biohydrometallurgical Technologies* Eds. A.E. Torma, J.E. Wey and V.L. Laksmanan, The Minerals, Metals and Materials Society, 217-235

Breed, A.W. (2000), "Studies on the mechanism and kinetics of bioleaching with special reference to the bioleaching of refractory gold-bearing arsenopyrite/pyrite concentrates", Thesis for Doctor of Philosophy, University of Cape Town

Brierley, C.L. (1997), "Mining Biotechnology: Research to commercial development and beyond", in *Biomining: Theory, Microbes and Industrial Processes*, Eds. D.E. Rawlings, Springer-Verlag and Landes Bioscience, 3-17

Brierley, J.A. and C.L., Brierley (1986), "Microbial mining using thermophilic micro-organisms", in *Thermophiles: General, Molecular and Applied Microbiology*, T.D. Brock, John Wiley & Sons, New York, 279-305

Gómez, E., M.L. Blázquez, A. Ballester and F. González (1996), "Study by SEM and EDS of chalcopyrite bioleaching using a new thermophilic bacteria", *Minerals Engineering*, **9**, (9), 985-999

Hackl, R.P., D.B. Dreisinger, E.Peters and J.A. King (1995), "Passivation of chalcopyrite during oxidative leaching in sulphate media", *Hydrometallurgy*, **39**, 25-48

Hallberg, K.B. (1995), "Role of arsenic toxicity to and residence of thermophilic bioleaching micro-organisms", Thesis for Doctor of Philosophy, Umeå University, Umeå

Huber, G. and K.O. Stetter (1991), "*Sulfolobus metallicus*, sp. nov., a novel strictly chemolithoautotrophic thermophilic archael species of metal-mobilizers", *System Applied Microbiology,* **14**, 372-378

Iglesias, N. and F. Carranza (1996), "Treatment of a gold bearing arsenopyrite concentrate by ferric sulphate leaching", *Minerals Engineering*, **9,**(3), 317-330

Iglesias, N., I. Palencia and F. Carranza (1993), "Removal of the refractoriness of a gold bearing pyrite-arsenopyrite ore by ferric sulphate leaching at low concentration", *EPD Congress*, Eds. J.P. Hager, The Mineral, Metals and Materials Society

Karavaiko, G.I., R.S. Golovacheva, T.A. Pivovarova, I.A. Tzaplina and N.S. Vartanjan (1988), "Thermophilic bacteria of the genus *Sulfobacillus*", *Biohydrometallurgy*, Eds. P.R. Norris and D.P. Kelly, 29-41

Lawrence, R.W. and A. Bruynesteyn (1983), "Biological pre-oxidation to enhance gold and silver recovery from refractory pyritic ores and concentrates", *CIM Bulletin*, September, **76**(857), 107-110

Lawrence, R.W. and P.B. Marchant (1988), "Comparison of mesophilic and thermophilic oxidation systems for the treatment of refractory gold ores and concentrates", in *Biohydrometallurgy 1987*, Eds. P.R. Norris and D.P. Kelly, *Science and Technology Letters*, Warwick, United Kingdom, 359-374

Miller, P.C. (1997), "The design and operating practice of bacterial oxidation plant using moderate thermophiles (The BacTech Process)", in *Biomining: Theory, Microbes and Industrial Processes*, Eds. D.E. Rawlings, Springer-Verlag and Landes Bioscience, 81-101

Moses, V. and R.E. Cape (1991), *Biotechnology: The Science and the Business*, Harwood Academic Publishers, United Kingdom

Nemati, M. and S.T.L. Harrison (2000), "Effect of solid loading on thermophilic bioleaching of sulphide minerals", *Journal of Chemical Technology and Biotechnology*, **75**, 526-532

Norris, P.R. (1997), "Thermophiles and bioleaching", in *Biomining: Theory, Microbes and Industrial Processes*, Eds. D.E. Rawlings, Springer-Verlag and Landes Bioscience, 247-258

Norris, P.R. and D.W. Barr (1988), "Bacterial oxidation of pyrite in high temperature reactors", *Biohydrometallurgy '87*, Eds. P.R., Norris and D.P. Kelly, *Science and Technology Letters*, Surrey, United Kingdom, 532-536

Poulin, R. and R.W. Lawrence (1996), "Economic and environmental niches of biohydrometallurgy", *Minerals Engineering*, **9**(8), 799-810

Torres, F., M.L. Blazquez, F. Gonzalez, A. Ballester and J.L. Mier (1995), "The bioleaching of different sulphide minerals using thermophilic bacteria", *Metallurgical and Materials Transactions B*, **26B**, June, 455-465

Vitaya, V.B., J. Loizumi and K. Toda (1994), "A kinetic assessment of substantial oxidation by *Sulfolobus acidocaldarius* in pyrite dissolution", *Journal of Fermentation Bioengineering*, **77**(5), 528-534

Zheng C.Q., C.C. Allen and R.G. Bautista (1986), "Kinetic study of the oxidation of pyrite in aqueous ferric sulphate", *Industrial Engineering Chemical Process Des. Dev.* **25**, 308-317

CHAPTER 3

THERMOPHILIC BIOLEACHING

Thermophiles perform similar reactions to the mesophiles, *Acidithiobacilli*. The contribution of the thermophiles to metal extraction in commercial leaching operations has not yet been demonstrated, but laboratory examination indicates that these microorganisms can contribute significantly to the extraction of metal from mineral matrices. As the thermophiles function at higher temperatures, the kinetics of biological and chemical reactions, which are both important in leaching operations, are enhanced and thus residence times are reduced (Brierley and Brierley, 1986).

Earlier studies investigating the dissolution of mineral concentrates by strains of *Sulfolobus* at 70 °C were carried out at low mineral concentrations (up to 5% w/v) (Norris and Barr, 1988). Since then, unpublished data of Norris illustrated maximum rates of mineral concentrate leaching with 6-8% w/v pyrite in stirred reactors (Norris, 1997). Nemati and Harrison (2000) report leaching of pyrite to be unaffected by mineral concentrations in the range of 3-9% w/v, with leaching at 12 and 15% w/v pyrite being typified by a biphasic rate profile. The mineral concentrations preferred for industrial application is at least 10% w/v mineral (Norris, 1997).

The archae used in thermophilic bioleaching tend to be sensitive to shear. This shear sensitivity could be due to the lack of a rigid peptidoglycan cell wall (König, 1988) and the increase in fluidity of cellular membranes with temperature increase (Kelly and Deming, 1988).

The specific characteristics of archaebacteria, which are the main thermophilic organisms, are presented and discussed. A comparison is made between the morphology and structure of the cell envelope of *Sulfolobus* and the mesophile *Acidithiobacillus ferrooxidans*. The advantages and disadvantages of using thermophilic bioleaching are discussed in this chapter. Information from this chapter provides motivation for research in this area.

3.1. SPECIFIC CHARACTERISTICS OF ARCHAE

Extreme thermophilic organisms are mainly archaeobacteria from the *Sulfolobacae* family. Archaeobacteria have been recognised as a phylogenetically distinct group of organisms. They are distinct from the eubacteria and from the eucaryotes (Woese, 1987). The taxonomy of these organisms is developing continuously as more organisms are isolated and characterised. The archaeobacteria (Greek *archaois*, ancient, and *bakterion*, a small rod) are a diverse group in terms of morphology and physiology. These organisms usually prefer restricted or extreme aquatic and terrestrial habitats. Archae inhabit extreme conditions, including high temperatures, acidic conditions and high halide concentrations (Prescott *et al.*, 1993).

3.1.1. *Sulfolobacae* Family

The *Sulfolobacae* family is characterised by a coccoid shape, tolerance of the thermoacidophilic environment, ability to oxidise elemental sulphur and ferrous iron (de Rosa and Gambacorta, 1975) and a cell envelope comprised of glycoprotein sub-units. The *Sulfolobales* consist of the genera *Sulfolobus*, *Acidianus*, *Desulfurolobus*, *Sulfurococcus* and *Metallosphaera* (Huber *et al.*, 1989). As indicated in Chapter 2, the most common extreme thermophiles used for bioleaching are from the *Sulfolobus* and *Acidianus* genera. The micro-organisms used in this study are *Sulfolobus metallicus,* hence the genus *Sulfolobus* is discussed in greater detail.

3.1.2. The Genus *Sulfolobus*

These organisms are extremely thermophilic and grow at temperatures above 55°C and a pH between 1.0-5.9 where an oxidisable energy source of either ferrous iron or sulphur is available (Brierley *et al.*, 1980). The oxidation of ferrous iron produces extensive precipitates of jarosite. Under microaerophilic conditions, *Sulfolobus* is able to reduce ferric iron, which then acts anaerobically as an electron acceptor. Many *Sulfolobus* isolates can grow autotrophically and some are able to grow heterotrophically by aerobic respiration of organic material (Brock, 1986).

3.1.2.1. Morphology of *Sulfolobus*

Sulfolobus cells are generally spherical in shape, although they often appear irregular. The diameter of these cells is 0.8-1.0 μm and little size variation is reported. *Sulfolobus* cells show no signs of budding or hyphae (Brock, 1986).

3.1.2.2. Nature of Cell Wall

The wall structure of *Sulfolobus* is atypical. The characteristic peptidoglycan layer seen in other bacteria is not present. An enlarged portion of the cell wall shows the presence of a diffuse electron transparent layer of subunits. From studies on the effects of various enzymes and extraction agents on cell walls, Weiss (1974) concluded that the cell wall of *Sulfolobus* appears to be a protein-lipid complex. He found that the cell wall protein is enriched with charged amino acids (aspartate, glutamate, lysine) and branched-chain hydrophobic amino acids (valine, leucine, isoleucine). The cell wall components typical of bacteria are diaminopimelic and muramic acids. Weiss (1974) did not find significant amounts of amino acids in the bacterial cell wall.

3.2 STRUCTURAL DIFFERENCES BETWEEN THERMOPHILES AND MESOPHILES

Thermophiles are small, spherical cells, with a primitive sub-microscopic morphology, lacking true cell walls and being surrounded by a plasma membrane and a very fine extracellular coat (Brierley *et al.*, 1980). Berry and Murr (1980) observed the cell envelope of a *Sulfolobus*-like microorganism having a cell envelope structure very similar to *Sulfolobus acidocaldarius* and *Caldariella MT.* The membrane comprises a layer of cytoplasm 50Å thick. A hollow periplasmic space of 125Å exists between the plasma membrane and the extracellular coat. The outside extracellular coat had a well arrayed subunit structure 150Å thick. The arrays form a hexagonal crystalline structure and the subunits provide a good covering for the underlying cell wall. The *Sulfolobus*-like microorganism is described as part of a major division of bacteria having morphologically distinct outer subunit cell envelope structure with the absence of a peptidoglycan layer (Berry and Murr, 1980). Weiss (1974) suggested that peptidoglycan is unstable in unusual habitats such as low pH and high temperature, and thus a cell wall devoid of peptidoglycan helps in the adaption of *Sulfolobus* and *Sulfolobus*-like microorganisms to those extreme conditions.

The mesophiles *Acidithiobacillus ferrooxidans* and *At. thiooxidans* are rod-shaped bacteria about 0.5x1.0 μm in size (Brierley, 1978). The cell envelope of *At. ferroxidans* consists of an inner cytoplasmic membrane, a dense peptidoglycan layer, an outer membrane and an extracellular coat. The peptidoglycan layer is approximately 50Å and is considered to provide strength to the bacterial cell wall. The outer membrane of *At. ferroxidans* is loosely bound and separate from the inner layers, unlike the well-defined arrayed outer membrane of the *Sulfolobus*-like microorganism (Berry and Murr, 1980).

3.3. ADVANTAGES OF THERMOPHILIC BIOLEACHING

The potential advantages of thermophilic bioleaching include better oxidation kinetics in terms of rate and extent of leaching (Duarte *et al.*, 1993; Konishi *et al.*, 1995; Le Roux and Wakerley, 1987), and to a lesser extent, reduced cooling requirements (Miller, 1997).

3.3.1. Oxidation Kinetics

A comparison of the oxidation kinetics for mesophilic and thermophilic microorganisms is presented in Table 3.1 to assess the advantages of using thermophilic bioleaching.

Table 3.1: Solubilisation rates obtained for thermophiles and mesophiles

Organism	Conditions	Maximum solubilisation rate	Extent of solubilisation	Reference
Acidianus brierleyi	1%(w/v) pyrite (25-44μm) in 1L stirred reactor (500rpm), 65°C	83 mg L^{-1} h^{-1} iron	Over 50% leaching of pyrite in 2.5 days – complete dissolution within 5 days	Konishi *et al.*, 1995
Acidithiobacillus	1%(w/v) pyrite in 1L stirred reactor (500rpm), 30°C	23 mg L^{-1} h^{-1} iron	50% leaching of pyrite in 9 days	Konishi *et al.*, 1995
Sulfolobus BC	5%(w/v) pyrite (<75μm) in an air-lift vessel, 70°C	200 mg L^{-1} h^{-1} iron		Norris and Barr, 1988
Sulfolobus BC	1%(w/v) pyrite in 1L stirred reactor (100rpm), further pyrite additions to 9%, 70°C	40 mg L^{-1} h^{-1} iron		Norris and Barr, 1988
Mesophile	1%(w/v) pyrite in 1L stirred reactor (100rpm), further pyrite additions to 9%, 30°C	40 mg L^{-1} h^{-1} iron		Norris and Barr, 1988
Sulfolobus BC	5% chalcopyrite (-90μm) 1L stirred reactor (500rpm), 68°C	11.5 mg L^{-1} h^{-1} copper	83% copper extraction	Le Roux and Wakerley, 1987
Acidithiobacillus	5% chalcopyrite 1L stirred reactor (500rpm), 30°C	2.5 mg L^{-1} h^{-1} copper	19% copper extraction	Le Roux and Wakerley, 1987

Findings of Konishi *et al.* (1995) demonstrate that the thermophilic bioleaching of pyrite, using *Acidianus brierleyi,* resulted in a greater extent of solubilisation, as well as a faster solubilisation rate than mesophilic bioleaching, under similar conditions (excluding temperature and micro-organism) in a stirred tank reactor.

Norris and Barr (1988) obtained results that indicate that thermophilic bioleaching holds no advantage over mesophilic bioleaching in terms of leach rates. Unpublished data by Norris (1987), however, suggests that the leaching rate of *Sulfolobus*-like organisms was 3 to 5 times faster than by *Acidithiobacillus*.

The work of Le Roux and Wakerley (1987) showed that almost complete copper dissolution was obtained using thermophilic bioleaching of chalcopyrite, whereas only 19% was achieved using mesophilic bioleaching. The rate of dissolution of copper under thermophilic conditions was approximately 36 mg l^{-1} h^{-1} initially, decreasing to 8 mg l^{-1} h^{-1}, giving an overall rate of leaching of 11.5 mg l^{-1} h^{-1} for the thermophilic bioleaching. The rate of copper solubilisation by the mesophile was 2.5 mg l^{-1} h^{-1} throughout the test period.

Dew *et al.* (1999) carried out continuous bioleaching of a Chilean chalcopyrite concentrate, consisting of 85% chalcopyrite with a copper content of 31%. The continuous pilot plant comprised 1040 l in total volume, and was made up of two 240 L and four 140 l stirred tank reactors connected in series. A slurry feed solids concentration of 10% by mass was used, and the pilot plant was inoculated with a 78 °C *Sulfolobus*-like archae culture. Copper dissolution of 95% was attained in a total residence time of 14 days. In the first stage of the plant, 66% dissolution was obtained in a residence time of 5 days. For mesophilic bioleaching, the copper dissolution was found to be typically 40% or less. Bioleaching of chalcopyrite is difficult due to passivation of this mineral during leaching.

3.3.2. Cooling Requirements

The oxidation of sulphide minerals is a highly exothermic process and large cooling requirements are needed for a mesophilic process (30°C). The quantity of heat generated is a function of the mineralogy and the degree of sulphide oxidation performed. The heat produced by the oxidation of arsenopyrite is 9 415 kJ/kg, and that from pyrite is 12 884 kJ/kg (Miller, 1997). The quantity of heat to be removed is process-specific and the magnitude of heat generated may be of the order of 3 MW to 12 MW for a plant with a throughput of 100 tpd concentrate. The use of thermophiles operating at a higher temperature (70°C) creates a higher temperature driving force for heat exchange, increasing heat losses and reducing the amount of heat required to be removed by the cooling system. In addition, the temperature does not have to be cooled to as low a temperature. This is a significant process advantage (Miller, 1997).

3.4. DISADVANTAGES OF THERMOPHILIC BIOLEACHING

The microorganisms used in thermophilic bioleaching are reported to be unable to cope with high concentrations of minerals in agitated culture (Nemati and Harrison, 2000, achieved maximum rates with 9% (w/v). The concentration of mineral present (Nemati and Harrison, 2000) and the particle size of the ore (Nemati *et al.*, 2000) have been reported to affect thermophilic bioleaching. This sensitivity to pulp density is postulated to result for several factors including sensitivity to shear forces, physical attrition, chemical toxicities and unfavourable mass transfer phenomena (Clark and Norris, 1996). These factors that adversely affect the performance of thermophilic microorganisms are discussed in greater detail below.

3.4.1. The Effect of Reactor Configuration on Thermophilic Bioleaching

Norris and Barr (1988) investigated the effect of reactor configuration on thermophilic bioleaching by comparing airlift vessels and stirred reactors. These vessels represent different agitation conditions for the bioleaching process. The agitation, which directly affects physical attrition and shear forces, is minimised in airlift vessels. Leaching of 5% (w/v) pyrite (particle diameter of <75μm) at 5% solids with *Sulfolobus* at 70°C gave an iron solubilisation rate of 200 mg L^{-1} h^{-1} in an airlift vessel. This rate was five times greater than that obtained in a stirred reactor (Table 3.1) using 1% solids. Although the solids concentrations were different in the two systems, the airlift reactor, which had a higher solids loading (5%) exhibited a faster solubilisation rate than the stirred reactor (solids loading of 1%).

3.4.2. The Effect of Chemical Toxicities on Thermophilic Bioleaching

The stability of various strains of organisms to heavy metals is non-uniform and is therefore probably associated with the adaption of these organisms in nature. Norris *et al.* (1986) tested the metal additions required to cause a moderate inhibition of exponentially growing iron-oxidising acidophiles. The organisms tested were *Acidithiobacillus ferrooxidans, Leptospirillum ferrooxidans* and *Sulfolobus* (BC). The results of the study are given in Table 3.2. Copper tolerance could be increased by progressive adaptation techniques. Le Roux and Wakerley (1988) increased the tolerance of *Sulfolobus* BC from 3 to 27 g Cu/l (47 to 425mM) in 18 months, making the thermophiles comparable to mesophiles.

Table 3.2: Metal additions required to cause moderate inhibition of iron-oxidising acidophiles (from Norris *et al.*, 1986)

Microorganism	Metal				
	U (mM)	Cu (mM)	Mo (mM)	Ag (μM)	Hg (μM)
Acidithiobacillus ferrooxidans	0.5	100	0.25	0.5	0.25
Leptospirillum ferrooxidans	2.5	1	1	1	2.5
Sulfolobus (BC)	2.5	75	1	0.1	5

An arsenic concentration of over 4 g/l did not inhibit the capacity of *Sulfolobus* BC to oxidise iron (Clark and Norris, 1996). Lindström and Gunneriusson (1990) found that the leaching rate of arsenopyrite by *Sulfolobus* BC decreased with increasing pulp density above a value of 1.5% w/v flotation concentrate. During batch leaching with *Sulfolobus* at 70°C, approximately 80% of the arsenic released remained in solution as arsenate, which corresponded to 18mM arsenate. This decrease in leach rate was attributed to the toxicity of arsenic.

3.4.3. The Effect of Solid Loading on Thermophilic Bioleaching

Nemati and Harrison (2000) investigated the effect of solid loading on thermophilic bioleaching of pyrite (53-75 μm in diameter) using *Sulfolobus metallicus* (BC) in a 1L stirred tank batch reactor. The reactor was maintained at 68 to 70°C and sparged with compressed air at a rate of 1 l min^{-1}. The range of solids loading tested was 3 to 18% (w/v) pyrite. A low agitation speed of 250-300 rpm was provided initially using a four-pitch-blade impeller, providing mild hydrodynamic conditions in the bioreactor and allowing for rapid increase in microbial population. When a shift to exponential growth (indicated by the number of cells present) was observed, the agitation speed was increased to 500-550 rpm. This resulted in complete suspension of solids, observed

visually. Solids loadings of 3, 6 and 9% resulted in constant leach rates of 0.10, 0.11 and 0.09 kg m^{-3} h^{-1} respectively, indicating that the leach rate is not affected up to 9% solids.

Two separate stages of leaching were obtained for loadings of 12 and 15%. In the first stage, leach rates of 0.09 and 0.07 kg m^{-3} h^{-1} were found for 12 and 15% loading respectively. In the second stage, these decreased to 0.02 kg m^{-3} h^{-1} and 0.017 kg m^{-3} h^{-1} for 12% and 15% loading respectively. The decreased leach rate coincided with a cessation of microbial growth.

A decrease in biomass was observed for a loading of 18% during the initial experimental stage when an agitation speed of 250 rpm was used. After 5 days, 150 cm^3 of inoculum replaced the same amount of reactor liquid, leading to an increase in biomass concentration and a shift to exponential phase after 24 h. Increase in agitation speed to 500 rpm with complete suspension of solids led to a decrease in biomass, and over a further 10 days, the concentration of total iron, sulphate and biomass remained unchanged. The extent of bioleaching was 11% within the initial experimental stage when the agitation speed was 250 rpm. Thus, the bioleach rate was unaffected by solids loading in the range of 3-9% w/v. For solids loading of 12-15%, two stages of leach rates were obtained, while 18% resulted in insignificant leach rates and microbial cell death.

3.4.4. The Effect of Particle Size on Thermophilic Bioleaching

Thermophilic bioleaching of various sizes of pyrite using *Sulfolobus metallicus* (BC) in 1L stirred tank batch reactors was investigated by Nemati *et al.* (2000). The reactor was maintained at 68 to 70°C and sparged with compressed air at a rate of 1 l min^{-1}. A solids loading of 3% (w/v) pyrite was used throughout the experiments at an agitation speed of 500-550 rpm using a four-pitch blade impeller. It was observed that fine particle sizes, <25 μm in diameter, negatively affected leach rate and resulted in no biological activity (unpublished data). In the 25-180 μm range, increasing leach rate is observed with decreasing particle size. A leach rate of 0.098 kg m^{-3} h^{-1} was obtained with a dominant

particle diameter in the range of 25-45 μm, while 150-180μm particle diameter experiments had a leach rate of 0.05 kg m^{-3} h^{-1} and a longer lag phase.

3.5. CONCLUSION

As mentioned previously in the chapter, thermophiles perform similar reactions to the mesophiles *Acidithiobacilli*. Commercially, mesophiles are used for bioleaching, but thermophiles have the potential advantage of better oxidation kinetics in terms of rate and extent of leaching. In addition, reduced cooling is required for the highly exothermic bioleaching reaction. Thermophiles have, however, been found to be sensitive to pulp density, a fact that is commercially disadvantageous. The sensitivity is postulated to be due to sensitivity to shear forces, physical attrition, chemical toxicities and unfavorable mass transfer phenomena. To achieve better understanding of the sensitivity of thermophiles to pulp density, this thesis examines the effect of various factors on the bioleaching performance. The factors examined were determined by the current literature available on thermophilic bioleaching, and on factors found to affect bioleaching using mesophiles. Those factors are discussed in Chapter 4.

3.6. REFERENCES

Berry, V.K. and Murr, L.E. (1980), "Morphological and Ultrastructural Study of the Cell Envelope of Thermophilic and Acidophilic Microorganisms as compared to *Thiobacillus ferrooxidans*", *Biotechnology and Bioengineering*, **22**, 2543-2555

Brierley, C.L. (1978), "Bacterial Leaching", *CRC Critical Reviews in Microbiology*, **6**

Brierley, C.L. (1974), "Leaching: Use of a high temperature microbe", *Solution Mining Symposium*

Brierley, J.A. and C.L., Brierley (1986), "Microbial mining using thermophilic micro-organisms", in *Thermophiles: General, Molecular and Applied Microbiology*, T.D. Brock, John Wiley & Sons, New York, 279-305

Brierley, C.L., J.A. Brierley, P.R. Norris and D.P. Kelly, (1980), "Metal-tolerant micro-organisms of hot, acid environments", in *Microbial Growth and Survival in Extremes of Environments* Eds. G.W. Gould and J.E.L. Corry, Academic Press, New York, 39-51

Brock, T.D. (1986), *Thermophiles: General, Molecular and Applied Microbiology*, John Wiley & Sons, New York

Clark, D.A. and P.R. Norris (1996), "Oxidation of mineral sulphides by thermophilic micro-organisms", *Minerals Engineering*, **9**(11), 1119-1125

De Rosa, M. and A. Gambacorta (1975), "Extremely thermophilic acidophilic bacteria convergent with *Sulfolobus acidocaldarius*", *Journal of Industrial Microbiology*, **86**, 156-164

Dew, D.W., C. van Buuren, K. McEwan and C. Bowker (1999), "Bioleaching of base metal sulphide concentrates: a comparison of mesophile and thermophile bacterial cultures", *Proceedings of Biohydrometallurgy, 1999*, 229-238

Duarte, J.C., P.C. Estrada, P.C. Pereira and H.P. Beaumont (1993), 'Thermophilic vs. mesophilic bioleaching process performance', *FEMS Microbiology Reviews*, **11**, 97-102, Elsevier, Lisbon, Portugal

Huber, G., C. Spinnler, A. Ballester and F. Gonzalez (1989), "*Metallosphaera sedula* gen. and sp. nov. represents a new genus of aerobic, metal mobilising, thermoacidophilic archaebacteria", *System Applied Microbiology*, 12, 38-47

Kelly, R.M. and J.W. Deming (1988), "Extremely thermophilic archaebacteria: Biological and engineering considerations", *Biotechnology Progress*, **4**(2), 47-62

König, H. (1988), "Archaebacterial cell envelopes", *Canadian Journal of Microbiology*, **34**, 395-406

Konishi, Y., S. Yoshida and S. Asai (1995), "Bioleaching of pyrite by acidophilic thermophile *Acidianus brierleyi*", *Biotechnology and Bioengineering*, **48**, 592-600

Le Roux, N., W. and D.S. Wakerley (1987), "Leaching of Chalcopyrite ($CuFeS_2$) at 70°C using *Sulfolobus*", in *Biohydrometallurgy '87,* Eds. P.R. Norris and D.P. Kelly, *Science and Technology Letters*, Surrey, United Kingdom, 305-317

Lindström, E.B. and L. Gunneriusson (1990), "Thermophilic bioleaching of arsenopyrite using *Sulfolobus* and a semi-continuous laboratory procedure", *Journal of Industrial Microbiology*, **5**, 375-382

Miller, P.C. (1997), "The design and operating practice of bacterial oxidation plant using moderate thermophiles (The BacTech Process)", in *Biomining: Theory, Microbes and Industrial Processes*, Ed. D.E. Rawlings, Springer-Verlag and Landes Bioscience, 81-101

Nemati, M. and S.T.L. Harrison (2000), "Effect of solid loading on thermophilic bioleaching of sulphide minerals", *Journal of Chemical Technology and Biotechnology,* **75**, 526-532

Nemati, M., J. Lowenadler and S.T.L. Harrison (2000), "Particle size effects in bioleaching of pyrite by acidophilic thermophile *Sulfolobus metallicus (BC)*", *Applied Microbiology and Biotechnology*, **53**: 173-179

Norris, P.R. (1997), "Thermophiles and Bioleaching", in *Biomining: Theory, Microbes and Industrial Processes*, Ed. D.E. Rawlings. Springer-Verlag and Landes Bioscience, 247-258

Norris, P.R. and D.W. Barr (1988), "Bacterial oxidation of pyrite in high temperature reactors", *Biohydrometallurgy '87*, Eds. P.R., Norris and D.P. Kelly, *Science and Technology Letters*, Surrey, United Kingdom, 532-536

Norris, P.R., L. Parrott and R.M. Marsh (1986), "Moderately thermophilic mineral-oxidising bacteria", in *Workshop on Biotechnology for the Mining, Metal-Refining and Fossil Fuel Processing Industries*, Eds. H.L. Ehrlich and D.S. Holmes, *Biotechnol. Bioeng. Symp.* **16**, 253

Prescott, L.M., J.P. Harley and D.A. Klein (1993), "The Bacteria: The Archaebacteria", *Microbiology 2nd edition*, Wm. C. Brown Communications Inc., USA, 492-505

Weiss, R.L. (1974), "Subunit cell wall of *Sulfolobus acidocaldarius*", *Journal of Bacteriology,* **118**, 275-284

Woese, C.R. (1987), "Bacterial evolution", *Microbiology Reviews*, **51**, 221-271

CHAPTER 4

THE USE OF MICROORGANISMS IN SLURRY REACTORS

Use of reactor processes for mineral bioprocessing generally requires the cultivation of microorganisms in the presence of solids. The energy source of the microorganisms is derived from the solids. Slurry reactors allow the control of the physicochemical environment as well as an adequate oxygen supply for aerobic processes to be maintained. Mixing conditions must be sufficient for adequate mass transfer of oxygen and nutrients to the microorganisms as well as suspension of the mineral phase. Excessive mixing may cause damage to the cells due to the fluid mechanical forces.

Biohydrometallurgical processes take place in a three-phase system. The three phases are:

i) An aqueous phase – this consists of a solution of inorganic nutrients to support microbial growth and maintenance for the microorganisms. The microorganisms act as biological catalysts in the oxidation of metal sulphides.

ii) A solid phase – this is the finely ground sulphide mineral concentrate consisting of waste rock and valuable metals combined with sulphur.

iii) A gaseous phase – this is the supply of atmospheric oxygen and carbon dioxide required by the microorganisms through the fine dispersion of air.

In the aqueous phase several elementary processes occur (Rossi, 1999), namely:

1. the growth of the micro-organisms;
2. the encounter of solid particles with the micro-organisms;
3. the encounter of the solid particles with chemically active molecules;
4. the release of metal ions; and
5. the uniform distribution and effective dissolution of oxygen and carbon dioxide.

The three phases and the interactions between them are therefore important factors in the slurry performance.

The performance of the slurry reactor is affected by chemical reactions, other chemical processes such as passivation and factors that affect the microbial cells. The factors that affect microbes include hydrodynamic forces, effect of solids, physiological stress such as toxicology or inhibition and mass transfer.

4.1. FACTORS AFFECTING MICROBIAL CELLS IN SLURRY BIOREACTORS

In bioleaching and bio-oxidation, a negative effect on the microorganisms could be due to the following factors:

- mechanical destruction
- inhibition of the organisms through the build-up of leach metabolites or by the introduction of toxic elements
- the cell concentration of the inoculum being too low with respect to the amount of ore present.

The negative effect on the microorganisms is seen as a reduction in oxidation rate (Bailey, 1993). The main factors affecting the microbial cells in slurry bioreactors are not independent of each other – the presence of one usually affects another, and so these factors must be considered in relation to each other.

The observed effects of certain factors on the performance of the cells and the possible mechanisms of mechanical cell damage are discussed below. Thereafter, the effect of mass transfer limitations on the bioleach performance will be illustrated.

4.1.1. Hydrodynamic Effects

Hydrodynamic forces are created to meet the need for good mixing and adequate mass transfer. They are caused by sparging and agitation and are a function of aeration rate, agitation intensity, and the impeller flow pattern.

4.1.1.1. Sparging

In bubble columns and airlift reactors, aeration intensity is the only form of agitation and must therefore be intense enough to suspend pyrite particles homogeneously in the medium. In stirred tank reactors, however, impellers provide agitation, and so the aeration provided is just adequate to supply dissolved oxygen and carbon dioxide to the microorganisms.

4.1.1.2. Agitation Intensity

In a three-phase slurry reactor system, the agitation must be sufficiently intense to completely suspend the solid particles that are an energy source for the microorganisms. Adequate power input to the system is required to provide adequate agitation. The agitation intensity, the impeller flow pattern and the position of the impeller in the stirred tank affect the shear forces in liquid systems (Hackl *et al.*, 1989). The maximum energy dissipation rate per fluid mass, which is related to the power input per unit volume, occurs in the impeller discharge zone. Hence the highest shear stresses and thus the majority of cell damage due to shear forces are expected to occur in this region.

The effect of agitation intensity on the leach rates of the mesophile, *Acidithiobacilli*, was investigated by Hackl *et al.* (1989) in a pilot plant. The pilot plant consisted of a 700 l feed tank and four 170 l bioleach tanks. The slurry was pumped from the feed tank to the first stage and advanced from one stage to the next by gravity overflow. The concentrate used was mainly arsenopyrite and pyrrhotite in the range of 25-30% (w/v). The researchers found that a tip speed of 5.3 ms^{-1} affected the leach rate negatively, but a reduction in tip speed of the Rushton turbine to 3.3 ms^{-1} resulted in an increase in bioleach rates, that returned to standard values within 4 days. At laboratory scale (1 l), Pearce (1993) found that an impeller tip speed of 2.6 ms^{-1} (630 rpm) with a 6-bladed Rushton turbine, in the presence of 10% w/v pyrite, completely inhibited the growth of *Acidithiobacilli*. In the same study, an impeller tip speed of 1.4 ms^{-1} (350 rpm) was not detrimental to the cells.

Using high agitation intensities during the early stages of *Acidithiobacilli* growth also hinders the attachment of the cells to the mineral particles resulting in inhibited growth and bioleach rates (Gormely and Branion 1989, Hackl *et al.* 1989). Cook

(1964) showed that inhibition of *Acidithiobacillus thiooxidans* by high levels of sulphur (2.0 g per flask) occurs only in shaken, not stationary cultures. Such inhibition is found even where the culture was only shaken for 30 minutes. Growth was restored to these inhibited cultures by allowing a preliminary stationary incubation before shaking, or by the addition of surface-active materials. Cook (1964) concludes that attachment to the sulphur particle is dependent upon a wetting agent, formed by the organism or may be added externally. If too much sulphur is present for the wetting agent to coat to a sufficient depth, even brief shaking, may disperse the wetting agent, resulting in reduced attachment and inhibited growth.

4.1.1.3. Impeller Flow Pattern

The type of impeller used determines the flow pattern and thus the suspension of solid particles. For complete suspension of solids, the power input required depends on the impeller used. Impellers can be classified into two categories, depending on the flow pattern they generate: radial flow and axial flow. Radial flow impellers generate high shear, making them efficient at dispersing oxygen. They have a poor pumping capability and are high power consumers. The Rushton turbine is a radial flow impeller. Axial flow impellers have a high pumping capacity, maximising axial mixing and homogeneity. These consume less power and generate much less shear (Nagata, 1975).

The effect of the impeller flow pattern on a mixed culture of *Acidithiobacillus ferrooxidans*, *Acidithiobacillus thiooxidans* and *Leptospirillum ferrooxidans* was investigated by Hackl *et al.* (1989), at an impeller tip speed of 5.3 ms^{-1} using different impellers. The use of a Rushton turbine resulted in an immediate 14 % reduction in the bioleach rate, while a 45-degree pitched-blade turbine (axial flow impeller) resulted in normal leach rates. Thus, a Rushton turbine caused more damage to the cells at a constant impeller speed of 5.3 ms^{-1}. Pearce (1993) confirmed these results using a Rushton turbine and an axial flow impeller on *Acidithiobacilli* in the presence of 10 % w/v pyrite. Using a tip speed of 2.6 ms^{-1}, the Rushton turbine agitation inhibited cell growth (lag was greater than 20 days), while the lag time for the agitation from the axial flow impeller was 11 days. These findings are consistent with the higher power consumption of the Rushton turbine as well as the higher shear stresses induced at the equivalent agitation speed.

Scholtz (1998) investigated the effect of impeller flow pattern on cell disruption on *S. cerevisiae* using a Rushton turbine and a pitched-blade turbine. The results indicate that for a given power input with a completely suspended solid system, the same cell disruption rates are observed, independently of flow pattern type. For a given impeller speed, the rate of cell disruption is less for the pitched-blade turbine due to the lower power input of this impeller.

4.1.2. Effect of Solid Particles

The effect of solid particles on microbial cells can be observed in terms of the particle size, the pulp density and the inhibitory effects of the particulate material due to toxicity. These parameters will be discussed in reference to microbial systems that illustrate their effects.

Scholtz (1998) completed a recent and thorough study on the disruption of cells in a slurry reactor. This study takes into consideration the possible cell disruption mechanisms and the viability of each. The study was carried out on the yeast *Saccharomyces cerevisiae*. *S. cerevisiae* is a unicellular eukaryote that has a rigid cell wall. Hunter and Asenjo (1988) have described the cell wall of yeast as one of the most tough and rigid of all microbial cell walls. The yeast cell is 5-10 μm and is able to tolerate high shear stress in the order of $8x10^7$ N/m^2 (Buschelberger *et al.*, 1989). This organism is thus very different from archaebacteria, and the results obtained in this cell disruption work cannot be conclusively compared to any work on the archaebacteria, although the effects on archae can be expected to be magnified over those on *S. cerevisiae.*

Scholtz (1998) investigated the disruption of *S. cerevisiae* in a stirred tank reactor. It was found that negligible cell disruption occurs in the absence of solid particles, suggesting that cell disruption in the slurry reactor is caused by interaction between the cells and solid particles. Complete suspension of solids results in cell disruption from solid-cell-solid collisions (attrition caused by the cell caught between two solid particles), solid-cell collisions (attrition from solid particle rubbing against the cell)

and solid-cell-reactor collisions. The conclusions drawn from this work indicate that the mechanism of cell disruption found to be dominant in the slurry reactor is solid-cell-solid collisions. The significance of this mechanism increases with increasing solids loading, but is unaffected by changes in the agitation intensity. The effect of cell-eddy interaction was found to be negligible.

4.1.2.1 Particle Size

Hansford and Chapman (1992) investigated the effect of particle size at constant surface area concentrations on batch biooxidation studies in air-lift reactors (pachucas). *Acidithiobacillus ferrooxidans* was used to leach iron from pyrite. The following three size fractions were studied: +53-75 μm, +38-53 μm and –38 μm. The solids concentrations used were adjusted to obtain approximately the same surface area concentration of 2700 $m^2.m^{-3}$ for the three size fractions. Only a slight increase in rate based on surface area was observed with increasing particle size, the surface area rates being $1.11x10^{-3}$, $1.20x10^{-3}$ and $1.36x10^{-3}$ kg FeS_2 m^{-2} d^{-1} from smallest to largest size fraction, respectively. The mass rates of iron release for the smallest to largest size fractions are 1.38, 1.50 and 1.70 $kg.m^{-3}$ d^{-1}, respectively. Thus the particle size at constant surface area concentration at this range of particle sizes does not greatly affect the biooxidation rate.

The effect of particle size at constant solids concentration was also investigated by Hansford and Chapman (1992) using the same system as described above, but under continuous operation. The particles used had similar surface area concentrations. After a residence time of approximately 10 days, the mass rates for iron release were almost constant at 2.14, 2.21 and 2.39 $kg.m^{-3}d^{-1}$ from largest to smallest particle size. This suggests that the particle size at constant solids concentration does not greatly affect the biooxidation rate within this range of particle size.

The effect of the initial specific surface area on the extraction rate of zinc from a zinc sulphide concentrate using *Acidithiobacillus ferrooxidans* was studied by Torma *et al.* (1970). Different size fractions (between 0.29 and 6.90 m^2g^{-1}) were leached at an initial pulp density of 16%. Plots of zinc extraction rates as a function of specific surface area are shown in Figure 4.1. This figure suggests that where the specific

surface area is low, i.e. large particles, the extraction rates were limited by the availability of particulate surface. Since the bacteria must contact the surface for the solubilisation of zinc to occur, if only a certain amount of surface is exposed, it can become the rate-limiting factor. As the specific surface area increases, the rate tends towards a constant value, suggesting that some other factor has become rate limiting. It was also found that the data complemented those obtained in the pulp density experiments. The curves of zinc extraction rate versus total surface area of solids per unit volume of solution, coincided in the region of low surface area per unit volume, i.e. at low pulp densities or for particles having low values of specific surface. Thus the true rate-limiting factor associated with the energy source is the amount of surface area available per unit volume of leach solution (Torma *et al.*, 1970).

4.1.2.2. Pulp Density

As the pulp density of a system increases, the agitation intensity required for complete suspension of the solid particles increases, and thus the power input supplied to the impellers increases. Energy dissipation increases and subsequently cell damage may be expected to increase.

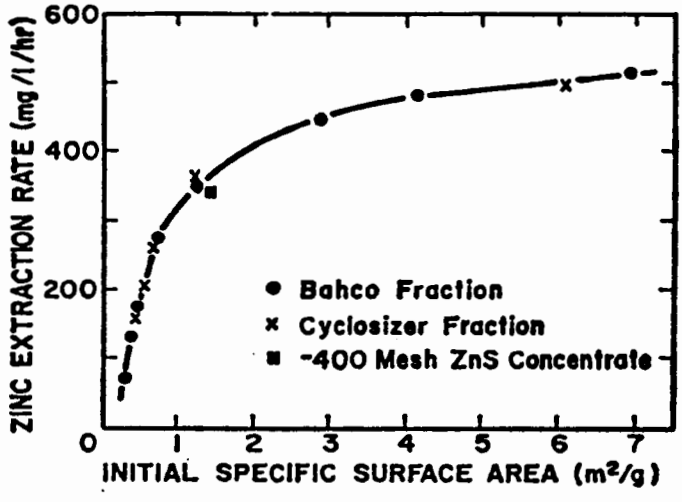

Figure 4.1: Effect of specific surface area of ore particle on leaching rate at pH 2.3, 35°C and 16% solid (Torma *et al.*, 1971)

The effect of pulp density on the rate of bioleaching by *Acidithiobacillus ferrooxidans* was studied by Torma *et al.* (1970) using concentrations of 0 to 27% w/v of zinc sulphide concentrate containing 33% sulphur. For a solids concentration below 14% w/v, the zinc extraction rate was directly proportional to the solids concentration. The extraction rate was independent of the solids concentration between 14 and 20% w/v solids, and decreased above 20% w/v. Torma *et al.* suggest that at high pulp densities, the decrease in extraction rate could be attributed to the interference of the solids with the mass transfer of oxygen and carbon dioxide to the organism. Bailey (1993) supports this postulation. His investigations were carried out on two high-grade pyrite concentrates (>28% Sulphur) in a fluidised bed reactor using a mixed culture of *Acidithiobacillus ferrooxidans*, *Acidithiobacillus thiooxidans* and *Leptospirillum ferrooxidans.* Overall system solids concentrations of 17 and 45 kg m^{-3} were used, and in both cases, the bed solids concentration was 200 kg m^{-3} (20% solids). This allowed for the oxygen transfer potential to be varied whilst not affecting other factors that could alter the bio-oxidation rate. He found that at the higher solids concentration, the bio-oxidation rate was affected by the oxygen availability in the reactor. Although the oxygen and carbon dioxide availability may limit the bio-oxidation rate at high solids concentrations, the influence of mechanical stress should not been discounted.

Beyer *et al.* (1986) investigated the influence of solids concentration on microbial coal desulphurisation in a stirred tank reactor. At 10 % solids, 1 vvm air and 400 rpm, pyrite was microbiologically removed from coal by *Acidithiobacillus ferrooxidans* at a maximum rate of 350 mg pyritic S l^{-1} d^{-1}. At 20% solids almost no pyrite oxidation took place and the cell concentration decreased rapidly with time. Vigorous mixing in the stirred tank reactor seemed to cause decreasing viability of the microorganisms.

High shear levels, which are dependent on the reactor geometry, agitation conditions and solids concentration, are an important cause of bacterial trauma resulting in decreased oxidation rates and growth rates. An increase in solids concentration is likely to cause the predominance of shear effects. High shear conditions are desirable for good oxygen and carbon dioxide mass transfer.

Dispirito *et al.* (1981) investigated the inhibitory effects of particulate materials in growing cultures of *Acidithiobacillus ferrooxidans* on ferrous iron using various particulate materials - pyrite, sulphur, fluorapatite and glass beads of similar sizes. It was found that particles of various chemical compositions inhibited bacterial iron oxidation, the extent of inhibition dependent on the type and concentration of the particulate material, as well as culture conditions. Except for pyrite, direct contact with particles and bacteria was requisite for inhibition, indicating that bacterial activities at the liquid-solid interface may be different to those in the aqueous phase. The sorption of cells to certain particulates may thus affect metabolic activity. Pyrite and sulphur were the most toxic materials under all conditions, and inhibited the bacteria at concentrations as low as 0.1 %. Bacterial oxidation was completely inhibited for at least 5 weeks at concentrations above 1 % pyrite. The inhibition caused by 1 % sulphur was overcome after 16 days, but complete inhibition was observed with higher levels (2-5%). Fluorapatite completely inhibited the cells at 1-4 %, but had little inhibition at 5 % concentrations. When the concentration of glass beads was increased above 4 %, no growth was detected. Below 4 % the rate decreased linearly with increasing solids concentration, suggesting mechanical damage affected the bacteria.

4.1.2.3. Inhibitory Effects of the Particulate Material (Toxicity)

The presence or absence of certain substances or the build-up of toxic oxidation products has been found to be inhibitory to the microorganisms. Roy and Mishra (1981) studied the oxidation of pyrite by *Acidithiobacillus ferrooxidans* in shake flask with a working volume of 100 ml. They found that the oxidation was synchronous with the bacterial growth, and thus the iron leach curves reflected the exponential increase of the bacterial activity. However, at an iron concentration of 1 mg ml^{-1}, the iron leach rate did not increase, leaching at a linear rate. Thus at this iron concentration, the iron oxidation was not coupled to the bacterial growth as observed at lower iron concentrations. Roy and Mishra also found that the absence of nitrogen, phosphorous and potassium reduced the oxidation rate significantly. This was contrary to the findings of Tuovinen *et al.* (1971), who observed an almost two-fold increase in the rate of ferrous iron oxidation by *Acidithiobacillus ferrooxidans* in the absence of nitrogen in the 2.0 g l^{-1} Fe^{2+} basal medium. A supply of 0.1 or 0.01 g l^{-1} of $Ca(NO_3)_2.4H_2O$ or $NaNO_3$ did not increase the oxidation rate. It was, however,

pointed out that the acid medium was very efficient in absorbing ammonia from the atmosphere. Higher concentrations of nitrate (0.5 g l^{-1}) have been shown to decrease the iron oxidation rate and inhibit the microorganisms, although gradual adaption to higher nitrate concentrations is possible. Tuovinen *et al.* (1971) also investigated the effect of the absence of phosphorus and found a 20% reduction in the iron oxidation rate after 13 subcultures in P-free solution during logarithmic growth. Sulphate and magnesium were found to be essential nutrients with the lowest unlimiting concentration being 2.0 g l^{-1} SO_4^{2-} and 2.0 mg Mg^{2+} l^{-1} for a biomass concentration of 10^8 cells ml^{-1}.

4.1.3. Mechanisms of Mechanical Damage to the Microorganisms

Various mechanisms of cell damage have been proposed in the literature. These are described below.

4.1.3.1. Interactions Between the Cells and Bubbles

The provision of dissolved oxygen for microbial cells is achieved by sparged aeration, which provides mild agitation. Simultaneously the air bubbles may interact with the microbial cells and can cause mechanical damage to the cells. Bubble rupture at the free gas-liquid interface has been shown to be the dominant cause of animal and insect cell damage when interaction between the cells and bubbles occur (Papoutsakis, 1991). Shear stress in the bubble column or stirred tank reactor has been shown to be greatest on the drainage of lamella during bubble break-up at the medium surface. This may result in cell damage where the cells are adsorbed onto the bubble surfaces, due to hydrophobic interactions between the cells and the bubbles or because the cells are captured in the wake of the moving bubbles. The rupturing film of the bubble damages the trapped cells by large compressional forces which occur when the rupturing rim breaks into threads. In addition, the hydrodynamic conditions due to shear, created in the boundary layer around the walls of the bubble cavity, are sufficiently large to kill insect cells (Chalmers and Bavarian, 1991). As a breaking bubble releases accumulated surface energy, a potentially damaging shockwave may also be formed (Yang *et al.,* 1990).

4.1.3.2. Interactions Between the Cells and Fluid Eddies

For good mixing to occur, turbulent flow is required. The turbulent flow fields result in fluid eddies. The size of the fluid eddies determines the potential for cell damage. Eddies larger than the suspended cells or the solid particles to which cells are attached entrain the cells or the solid particles rotating and translating them in a way that reduces the net forces on their surface. Eddies smaller than the suspended cells or solids are dissipated on the surface of the suspended cells, and are thus more likely to damage the individual cells (Croughan *et al.*, 1987).

The size of the smallest energy-containing eddy (λ), called the Kolmogorov eddy size, is given as follows (Kolomogorov, 1941):

$$\lambda = \left[\frac{\nu^3}{\varepsilon}\right]^{1/4} \qquad (eqn.4.1)$$

where: ν is the kinematic fluid viscosity (m^2s^{-1})

ε is the energy dissipation rate per unit volume (Wm^{-3})

Kolmogorov eddies must therefore be smaller than the cell diameter to impose shearing forces on the cell and cause cell damage.

If the fluctuating velocity of the fluid changes rapidly with time or position, strong hydrodynamic forces, although short-term, can result, which damage the cells.

4.1.3.3. Interactions Between the Cells and the Solid Particles

Animal cells are damaged by solid particles when the microcarrier particles on which the cells are immobilised collide, or when the microcarrier particles pass each other in close proximity (Croughan *et al.* 1988). This mechanism was found by Croughan *et al* (1988) to be significant above a solids concentration of approximately 0.5 % (v/v) at agitation intensities of 150 rpm (impeller tip speed of 0.42 m s^{-1}) using 125 ml spinner vessels. The frequency and force of the collisions between cells and solid particles are important parameters in the mechanism of cell damage.

4.1.3.4. Interactions Between the Cells and Reactor Components

Collisions between the cells and the solid components of the vessel cause cell damage in a similar way to the solid particles (Croughan *et al.*, 1988, 1989). The kinetic energy and the frequency of the collisions are important parameters to determine the damage from this mechanism. The microcarriers are assumed to collide with the impeller only if they passed within one bead radius of the impeller surface. This region where collisions between the microcarriers and the impeller occur is termed the 'window area'. The collision frequency is estimated from the time the microcarriers take to flow through the entire reactor volume along the set of streamlines that are in the window area. Croughan *et al.* (1989), however, suggest that interactions between the microcarriers and the reactor components are insignificant as a damage mechanism as the microcarriers do not rapidly penetrate the boundary layers surrounding the reactor internals.

4.1.4. Mass Transfer

The volumetric oxygen mass transfer coefficient, k_La, is dependent on the power input per unit volume, the gas sparge rate, the liquor viscosity and the liquid-phase diffusivity of oxygen (Bailey and Ollis, 1987). The power input per unit volume is affected by the agitation and aeration rates, the vessel geometry, type of impeller and baffles used. The effect of the presence of solids on k_La depends on the particle type, size, concentration and operating conditions (Oguz *et al.*, 1987). The actual influence of solids on oxygen availability during bacterial oxidation occurs in two ways. Firstly the sulphide content of the particles determines the oxygen demand, hence as the solids concentration increases, the oxygen demand increases. Secondly, the presence of solids affects the oxygen mass transfer rate by adjusting the interfacial turbulence at low solids concentrations. At higher solids concentrations, an increase in the apparent viscosity and the alteration of bubble coalescence rates affect the interfacial area. The size of the particle may block the diffusion of oxygen (Lee *et al.*, 1982). At high solids concentrations, Mills *et al.* (1987) observed a decrease in gas hold-up, contributing to a decrease in the oxygen transfer area.

Through understanding the effects on oxygen demand and oxygen transfer potential, one can ascertain whether a system is oxygen transfer limited. Hence the oxygen demand and the oxygen transfer potential (OTP) for the system must be determined.

Oxygen Demand

The bio-oxidation rate has been shown to be directly proportional to the surface area concentration, or more specifically, directly proportional to the sulphide surface area available for oxidation. Hansford and Drossou (1988) showed that the relationship holds until a certain solids concentration at which the bio-oxidation is limited by some factor. The pyrite bio-oxidation rate can be based on the pyrite surface area, as follows:

$$\text{Pyrite oxidation rate} \propto \text{P (kg pyrite)}(\text{m}^2\text{ pyrite})^{-1}\text{d}^{-1}$$

The reaction stoichiometry indicates that the overall bacterial oxidation of pyrite occurs as follows:

$$4FeS_2 + 15O_2 + 2H_2O \rightarrow 2Fe_2(SO_4)_3 + 2H_2SO_4 \qquad (eqn.4.2)$$

To oxidise 1 kg of pyrite, 1 kg of oxygen is required. Thus an oxygen utilisation rate may be determined from the pyrite bio-oxidation:

$$\text{Oxygen utilisation rate} = \text{R (kg } O_2)(\text{m}^2\text{ pyrite})^{-1}\text{d}^{-1}$$

The pyrite surface area (A), which is dependent on the solids concentration, particle size and ore grade, can be used to determine the oxygen demand for a particular system:

$$\text{Oxygen demand} = \text{R x A (kg } O_2)(\text{m})^{-3}\text{d}^{-1}$$

For a particular size ore, the oxygen demand is linearly dependent on the solids concentration. The actual slope of the oxygen demand line is dependent on the sulphide content of the ore. A high sulphide content (approximately 30 %) results in a steep slope, while a low sulphide content (approximately 1 %) results in a more gradual slope (Bailey and Hansford, 1994).

Oxygen Transfer Potential

The oxygen transfer rate (OTR) is the product of the mass transfer coefficient, k_La, and the concentration driving force (Bailey and Ollis, 1987):

$$OTR = k_La\ (C^* - C) \qquad (eqn.4.3)$$

where C^* is the saturated dissolved oxygen concentration (mg $O_2.l^{-1}$)

C is the liquor dissolved oxygen concentration (mg $O_2.l^{-1}$)

C^* is dependent on the oxygen concentration in the gas used for sparging (air or enriched air) according to Henry's Law, and on the operating temperature and pressure in the reactor.

The maximum possible driving force in a particular system is the difference between C^* and a critical dissolved oxygen concentration, C_{CRIT}, below which the growth and metabolism of microorganisms are adversely affected by the low dissolved oxygen concentrations. The oxygen transfer potential (OTP) of a system is therefore:

$$OTP = k_La\ (C^* - C_{CRIT}) \qquad (eqn.4.4)$$

4.1.4.1. Oxygen Transfer Potential Versus Demand

Bailey and Hansford (1994) compared oxygen demand and oxygen transfer potential across a range of solids concentrations in the bioleach system using Equations 4.2 and 4.3 (Figure 4.2). Figure 4.2 illustrates where the oxygen demand is less than the oxygen transfer potential, the system is not oxygen limited. To the right of the intersection of the demand and transfer potential lines (shaded area of the diagram), in the high solids loading region of the diagram, the system will be oxygen limited. The maximum oxidation rate in this region is described by the oxygen transfer potential.

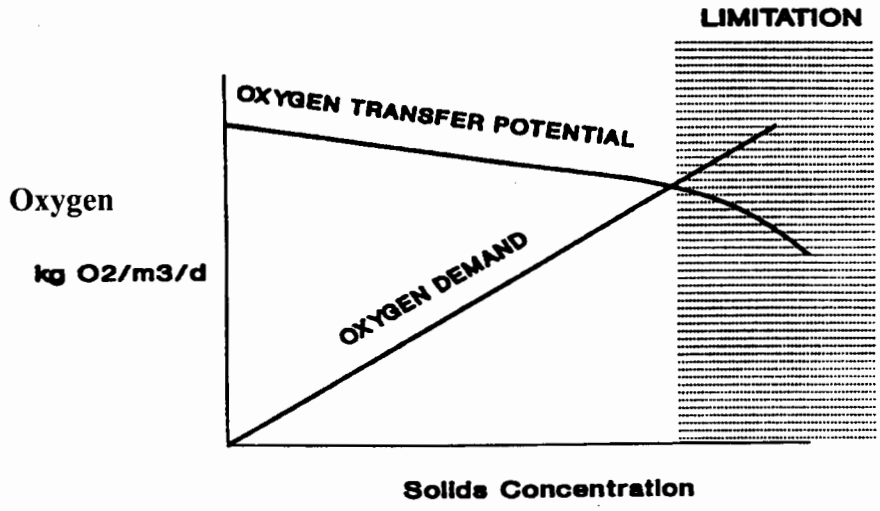

Figure 4.2: Schematic Diagram of Oxygen Transfer and Demand vs. Solids Concentration (Bailey and Hansford, 1994)

4.1.4.2. Effect of Viscosity on k_La

Oguz *et al.* (1987) extended the standard correlation of mass transfer coefficient as a function of power input per unit volume and gas sparge rate to relate relative slurry viscosity (μ_{rel}) to the mass transfer coefficient:

$$k_L a = 6.6x10^{-4}(\mu_{rel})^{-0.39}(Q)^{0.5}(P/V)^{0.75} \qquad (eqn.4.5)$$

where Q is the gas sparge rate ($l.min^{-1}$)

(P/V) is the power input per unit volume ($kW.m^{-3}$)

Rao (1966) collected data sets of the apparent viscosity of silica and pyrite slurries in water (Figure 4.3). Initially the relative slurry viscosity is only slightly affected by increasing solids concentration, but at a certain point (approximately 1.3 pulp specific gravity for silica and 2.2 for pyrite), a transition occurs whereby a relatively large increase in slurry viscosity results from a relatively small increase in solids concentration. According to Equation 4.5, the increase in slurry viscosity corresponds to a decrease in k_La, thus a lowering of oxygen mass transfer potential. Since the relative viscosity of a mineral slurry is dependent on the volume fraction of solids (Hansford *et al.* 1976), the transition point to a relatively large viscosity increase,

corresponding to a thus sharp decrease in k_La, occurs at a lower pulp density for silica than pyrite (relative density of silica is 2.6 as opposed to 5.0 for pyrite).

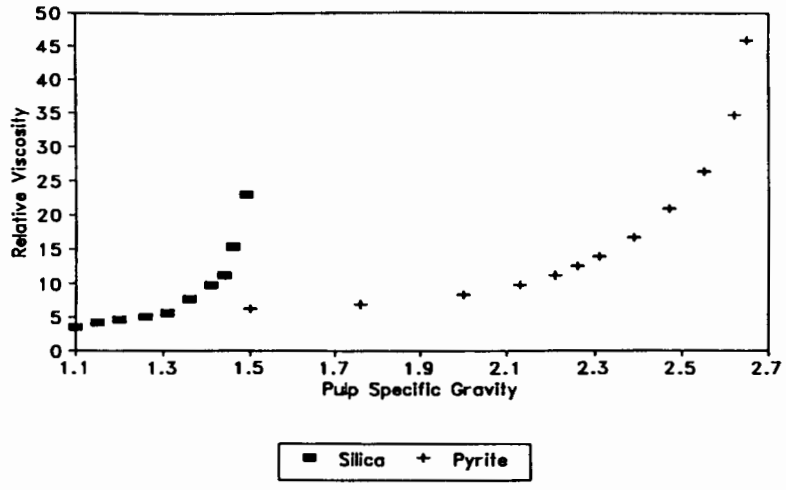

Figure 4.3: Slurry viscosity vs. solids concentration (data of Rao, 1966)

4.1.4.3. Effect of Diffusivity on k_La

The diffusion coefficient varies with ionic strength and with the concentration of solutes that affect viscosity of the suspending medium (Bailey and Ollis, 1987). In a mineral bio-oxidation system, essentially all of the iron present is in the ferric form. Bailey (1993) determined the effect of ferric sulphate on oxygen mass transfer using different concentrations of ferric sulphate solutions in a stirred tank reactor. A temperature of 35°C was used, with the pH adjusted to 2 using sulphuric acid. An air sparge rate of 3 $l.min^{-1}$ was used throughout all tests in a reactor working volume of 4 l. On introduction of a ferric sulphate solution of 9.77 $g.l^{-1}$ (3.8 g $Fe.l^{-1}$ and 0.10 (moles SO_4^{2-}).l^{-1}), the k_La measured was reduced by 26% with respect to that measured in the distilled water slurry. Similar reductions in measured k_La values were observed with concentrations of sulphate of 0.2 and 0.4 $mol.l^{-1}$.

4.1.4.4. Investigations into Mass Transfer Limitations

Bio-oxidation of high sulphide content materials (>25 %S) have been found to have maximum oxidation rates at approximately 20% solids concentration (Torma *et al.* 1970). Van Aswegen *et al.* (1991) analysed the bio-oxidation rate data of Pinches *et*

al. (1991) and van Staden (1991) and revealed a link between the sulphide grade of the material and the solids concentration at which the bio-oxidation rate was maximal. A low grade material of 1 % Sulphur was oxidised at a solids concentration of 55 %. Bailey and Hansford (1993) used a fluidised bed (whereby solids and liquids can be controlled independently) to investigate the effect of oxygen availability on the bio-oxidation rate of a high sulphide content material (20 % Sulphur). They found that if an adequate oxygen supply was provided to the reactor, the specific bio-oxidation rate was constant and independent of solids concentration over the range of 20 to 45% solids that was tested.

Bailey and Hansford (1994) investigated the oxygen mass transfer limitation of batch bio-oxidation at high solids concentrations. Stirred tank reactors with a 3 l working volume were used, at a tip speed of 1.97 $m.s^{-1}$, i.e. well below the tip speed of 5.3 $m.s^{-1}$ that Hackl *et al.* (1989) reported to be inhibitory to bacterial growth. A mixed culture of mesophilic bacteria including *A. ferrooxidans, A. thiooxidans* and *L. ferrooxidans* were used. The first factor studied was the effect of solids concentration on the bio-oxidation rate when processing low-grade material (1.24 % Sulphur) at 20, 40 and 60% (w/v) solids loading. Bio-oxidation rates were predicted using Equation 4.2. Measured bio-oxidation rates correlated well with these predictions, indicating that the bio-oxidation rate was proportional to the solids concentration. At 60 % solids, the oxygen transfer potential was measured to be 29.68 (kg O_2).m^{-3}.d^{-1}, while the oxygen demand was determined from the pyrite oxidation rate to be 0.591 (kg O_2).m^{-3}.d^{-1}. The oxygen supply thus exceeded the demand and oxygen limitation was not expected in this system. The results suggest that where sufficient oxygen is available, the bio-oxidation rate is proportional to the solids concentration. In addition, a bio-oxidation system processing low-grade sulphide material can operate at a higher solids concentration (60 %) than a high-grade sulphide material that can operate at a solids concentration of only 20 % (w/v).

Bailey and Hansford (1994) also carried out batch bio-oxidation studies using mixtures of pyrite concentrate (47.8 % Sulphur) and quartz. The quartz acted as an inert solid that allowed the effect of the total solids concentration on the bio-oxidation rate to be assessed, while keeping the pyrite concentration constant. The total solids concentrations tested were 10, 20 and 30 % (w/v) with each containing 10 % pyrite.

The bio-oxidation rates obtained, were expressed in terms of the specific oxidation rate based on the amount of pyrite present in the reactor. The results at the three different overall solids concentrations agreed with each other. The oxygen demand at 10 % overall solids was 4.01 (kg O_2).$m^{-3}d^{-1}$ and the dissolved oxygen concentration was, on average, 4.7 $mg.l^{-1}$. It was predicted that oxygen limitation would be expected to occur at 26 % concentrate. However, the specific pyrite oxidation rate at 30 % overall solids was the same as that at 10 % solids, indicating that the oxygen transfer potential still exceeded the oxygen demand at those conditions.

4.1.4.5. Availability of Carbon Dioxide

The microorganisms used in bio-oxidation are autotrophs, using carbon dioxide as their carbon source. An adequate supply of carbon dioxide to the microorganisms is therefore essential for cell growth (Schlegel, 1988). The enrichment of process air with carbon dioxide has proved to be beneficial in increasing the bio-oxidation rate at high solids concentrations in various cases (Torma *et al.*, 1972). An optimal carbon dioxide enrichment of approximately 1 % has been found, above which little further increase in the oxidation rate occurs.

Liu *et al.* (1988) studied the relative mass transfer rates of oxygen and carbon dioxide on *A. ferrooxidans*, and estimated that limitation by CO_2 would be encountered before oxygen limitation thereby supporting the trend to enrich air with CO_2. Nagpal *et al.* (1993) investigated the effect of carbon dioxide concentration on the bio-oxidation of a pyrite-arsenopyrite concentration at 16% solids. Carbon dioxide concentrations above 10 $mg.l^{-1}$ were found to inhibit bacterial growth, while 5 $mg.l^{-1}$ was found to be the optimal aqueous-phase concentration. Concentrations below this level resulted in a sharp decrease in bacterial growth rate.

4.2. HYPOTHESIS AND OBJECTIVES

The various factors that affect the performance of the mesophilic bioleaching cells as well as other microbial cells used in slurry reactors have been described in this chapter. These factors include:

- mechanical destruction

- inhibition of the microorganisms through the build-up of leach metabolites or by the introduction of toxic elements
- the cell concentration of the inoculum being too low with respect to the amount of ore present.

The conditions that the bioleaching and bio-oxidation reactions are subjected to led to more specific factors, namely:

- hydrodynamic forces caused by sparging, agitation and the impeller flow pattern
- effect of solid particles – particle size, pulp density and inhibitory effects of the particulate material (toxicity)
- mass transfer – oxygen limitation and availability of carbon dioxide.

These factors were considered when investigating the hypothesis and formulating the objectives of this thesis.

The hypothesis is as follows:

Archae involved in bioleaching are susceptible to damage in agitated aerated vessels, especially with increasing pulp density.

The objectives to investigate the hypothesis are:

1. To determine the effect of pulp density (at constant particle size) on metabolic activity on *Sulfolobus metallicus*.
2. To determine the effect of agitation intensity on metabolic activity.
3. To determine the mass transfer limitation of oxygen and carbon dioxide at increasing pulp density.
4. To determine the effect of the state of the inoculum used for the bioleaching on the bioleaching performance (rate and extent of leaching).

Other factors that needed to be checked were:

1. The extent of chemical leaching of pyrite at 68°C.
2. The partitioning of the *Sulfolobus metallicus* between the solid and liquid phase.

4.3. REFERENCES

Bailey, A.D. (1993), "An assessment of oxygen availability, iron build-up and the relative significance of free and attached bacteria, as factors affecting bio-oxidation of refractory gold-bearing sulphides at high solids concentrations", Thesis for Doctor of Philosophy, University of Cape Town

Bailey, A.D. and G.S. Hansford (1994), "Oxygen mass transfer limitation of batch bio-oxidation at high solids concentration", *Minerals Bioengineering*, **7**, 293-303

Bailey, A.D. and G.S. Hansford (1993), "A fluidised bed reactor as a tool for the investigation of oxygen availability on the bio-oxidation rate of sulphide minerals at high solids concentrations", *Minerals Engineering*, **6**, (4), 387-396

Bailey, J.E. and D.F. Ollis (1987), *Biochemical Engineering Fundamentals*, McGraw-Hill, Singapore, 488-494

Beyer, M., H.G. Ebner and J. Klein (1986), "Influence of pulp density and bioreactor design on microbial desulphurisation of coal", *Applied Microbiology and Biotechnology*, **24**, 342-346

Blancarte-Zurita, M.A., R.M.R. Branion and R.W. Lawrence (1986), "Particle size effects in the microbial leaching of sulphide concentrates by *Thiobacillus ferrooxidans*", *Biotechnology and Bioengineering*, **23**, 2761-2769

Chalmers, J.J. and F. Bavarian (1991), "Microscopic visualisation of insect cell-bubble interactions II: The film and bubble rupture", *Biotechnology Progress*, **7**, (2), 151-159

Cook, T.M. (1964), "Growth of *Thiobacillus thiooxidans* in shaken culture", *Journal of Bacteriology*, **88**, (3), 620-623

Croughan, M.S., E.S. Sayre and D.I.C. Wang (1989), "Viscous reduction of turbulent damage in animal cell culture", *Biotechnology and Bioengineering*, **33**, 862-872

Croughan, M.S., J.F.P. Hamel and D.I.C. Wang (1988), "Effects of microcarrier concentration in animal cell culture", *Biotechnology and Bioengineering*, **32**, 975-982

Croughan, M.S., J.F.P. Hamel and D.I.C. Wang (1987), "Hydrodynamic effects on animal cells grown in microcarrier cultures", *Biotechnology and Bioengineering*, **29**, 130-141

Dispirito, A.A., P.R. Duncan and O. Tuovinen (1981), "Inhibitory effects of particulate materials in growing cultures of *Thiobacillus ferrooxidans*", *Biotechnology and Bioengineering*, **23**, 2761-2769

Gormely, L.S. and R.M.R. Branion (1989), "Engineering design of microbiological leaching reactors", *Biohydrometallurgy '89*, Wyoming, USA, 499-515

Hackl, R.P., F.R. Wright and L.S. Gormley (1989), "Bioleacing of refractory gold ores – out of the lab and into the plant", *Biohydrometallurgy 1989*, Eds. J. Salley, R.G.L. McCready and P.L. Wichlacz

Hansford, G.S. and J.T. Chapman (1992), "Batch and continuous biooxidation kinetics of a refractory gold-bearing pyrite concentrate", *Minerals Engineering*, **5**, (6), 597-612

Hansford, G.S. and M. Drossou (1988), "A propogating pore model for the batch bioleach kinetics of refractory gold-bearing pyrite", *Biohydrometallurgy Proc. Int. Symp, 1987*, Eds. P.R. Norris and D.P. Kelly, 345-358

Hansford, G.S., C.D. Levy and J.W. De Kock (1976), "Rheological measurements on pulp from South African gold mines", *Journal of South African Institute of Mining and Metallurgy*, **76**, (8), 363-369

Hunter, J.B. and J.A. Asenjo (1988), "A structured mechanistic model of the kinetics of enzymatic lysis and disruption of yeast cells", *Biotechnology Bioengineering*, **31**, 929-930

Lee, J.C., S.S. Ali and P. Tasakorn (1982), "Influence of suspended solids on gas-liquid mass transfer in an agitated tank", *Proceedings of the 4th European Conference on Mixing*, Noordwijkerhout, Netherlands, Paper H4, 399-415

Liu, M.S., R.M.R. Branion and D.W. Duncan (1988), "The effects of ferrous iron, dissolved oxygen and inert solids concentrations on the growth of *Thiobacillus ferrooxidans*", *Canadian Journal of Chemical Engineering*, **66**, (3), 445-451

Mills, D.B., R. Bar and D.J. Kirwan (1987), "Effects of solids on oxygen transfer in agitated three-phase systems", *American Institute of Chemical Engineers' Journal*, **33**, (9), 1542-1549

Nagata, S. (1975), *Mixing: Principals and Applications*, Kodansha Ltd., Halstead Press, Japan

Nagpal, S., D. Dahlstrom and T. Oolman (1993), "Effect of carbon dioxide concentration on the bioleaching of a pyrite-arsenopyrite ore concentrate", *Biotechnology Bioengineering*, **41**, 459-464

Oguz, H., A. Brehm and W.D. Deckwer (1987), "Gas/liquid mass transfer in sparged agitated slurries", *Chemical Engineering Science*, **42**, (7), 1815-1822

Papoutsakis, E.T. (1991), "Fluid-mechanical damage of animal cells in bioreactors", *Trends in Biotechnology*, **9**, (12), 427-437

Pearce, S.J.A. (1993), "Disruption of micro-organisms due to agitation in slurries of fine particles", Thesis for Master of Science, University of Cape Town, South Africa

Pinches, A., R. Huberts, M. van Staden and R.M. Muhlbauer (1991), "Process options and parameters in the development and optimisation of bacterial oxidation processes for the preoxidation of refractory sulphide gold ores", *South African Institute of Mining and Metallurgy Colloqium on Bacterial Oxidation*, Johannesburg, South Africa, June, 1991

Rao, T.C. (1966), *Mineral Crushing and Grinding Circuits*, Ed. A.J. Lynch, Elsevier, Amsterdam, (1977), 98

Roy, P. and A.K. Mishra (1981), "Factors affecting oxidation of pyrite by *Thiobacillus ferrooxidans*", *Indian Journal of Experimental Biology*, **19**, 728-732

Rossi, G. (1999), "The design of bioreactors", *Biohydrometallurgy 1999*, Eds. R. Amils and A. Ballester

Schlegel, H.G. (1988), *General Microbiology*, 6th Edition, University Press, Cambridge, UK

Scholtz, N.J. (1998), "Quantifying solids suspension and its effect on microbial cell disruption in a slurry bioreactor", MSc, University of Cape Town

Torma, A.E., C.C. Walden, D.W. Duncan and R.M.R. Branion (1972), "The effect of carbon dioxide and particle surface area on the microbiological leaching of a zinc sulphide concentrate", *Biotechnology and Bioengineering*, **14**, 777-786

Torma, A.E., C.C. Walden, D.W. Duncan and R.M.R. Branion (1970), "Microbial leaching of zinc sulphide concentrate", *Biotechnology and Bioengineering*, **12**, 501-517

Tuovinen, O.H., S.I. Niemala, D.W. Duncan and R.M.R. Branion (1971), "Tolerance of *Thiobacillus ferrooxidans* to some metals", *Antoine van Leeuwenhoek*, **37**, 489-496

van Aswegen, P.C., M.W. Godfrey, D.M. Miller and A.K. Haines (1991), "Developments and innovations in bacterial oxidation of refractory ores", *Minerals Engineering*, **8**, (4), 191-199

van Staden, M. (1991), "Bacterial leaching of refractory gold-bearing ore and sulphide concentrates", Masters Diploma Thesis, Department of Metallurgy, Technikon Witwatersrand, South Africa

Yang, J.D., N.S. Wang, K.C. Chang and R.V. Calabrese (1990), "Hybridoma cell inactivation by air sparging in a mechanically agitated bioreactor", *Third International Conference on Bioreactor and Bioprocess Fluid Dynamics*, BHR Group Ltd., Cambridge, UK

CHAPTER 5

MATERIALS AND METHODS

This chapter describes the microorganisms used in this study and their maintenance. Furthermore, the apparatus set-up is illustrated and the experimental methodology explained.

5.1. MICROORGANISMS AND CULTURE MAINTENANCE

The thermophilic culture used in this research was *Sulfolobus metallicus (BC)* isolated from coal tips in Birch Coppice and provided by BHP-Billiton, South Africa. The culture was grown aerobically in a stirred tank reactor in a medium outlined in Table 5.1, and pyrite. The medium was made up to 2 m^3 using distilled water and the pH was adjusted to 2.5 using concentrated sulphuric acid.

Table 5.1: Composition of Medium (Nemati and Harrison, 2000)

Compound	Concentration (kg m^{-3})
$(NH_4)_2SO_4$	0.4
$MgSO_4.7H_2O$	0.5
KH_2PO_4	0.2
KCl	0.1

Of the 700 ml working volume of the stock culture, 200 ml was drawn daily and replaced with an equivalent volume of medium and 6.0 g pyrite. The stirrer speed was set at 350 rpm and the culture temperature was maintained at 68°C. The water lost due to evaporation was replaced with distilled water before drawing and feeding, to retain a constant liquid volume while preventing salts concentration through evaporation.

A culture of *Sulfolobus metallicus (BC)* was also maintained in a rotary shaker at 120 rpm and 68°C. This was termed the shake flask inoculum. The culture was incubated in 500 ml flasks, each containing 100 ml medium and 50 ml stock culture at a constant temperature of 68°C. This culture was subcultured every two weeks.

5.2. EXPERIMENTAL METHODOLOGY

All experiments performed were carried out with the medium described in Table 5.1 with pyrite at 68°C.

5.2.1. Bioleaching Experimental Set-up

The bioleaching experiments were carried out in a 1 litre stirred tank reactor of diameter 0.1 m with a working volume of 700 ml. The bioreactor vessels were jacketed and maintained at a temperature between 68°C and 70°C by a circulating water bath. Each reactor was equipped with:

- a four-pitch blade stainless steel impeller of diameter 0.058 m set at a clearance of 0.01 m from the reactor base
- a set of four 10 mm wide perspex baffles
- a condenser, and
- a ring air sparger with 4 holes along the base that fitted around the bottom of the reactor.

Compressed air (without any enrichment with oxygen or carbon dioxide, except in the experiments testing carbon dioxide limitation) was supplied at a rate of 2 l min^{-1}. The bioreactors were operated batchwise. For the experiment, each reactor was charged with 550 ml medium at pH 2.5, 150 ml of inoculum from the stirred tank reactor used for culture maintenance and the required amount of pyrite and silica to obtain a particular pulp density.

The pyrite was obtained from BHP-Billiton (Randburg, South Africa). The concentrate was wet sieved through a 75 and 38 μm mesh screen to obtain a 38-75 μm size fraction. Size analysis was performed on the fraction using a Malvern Particle Size Analyser. Detailed results of the size analysis are depicted in Appendix F. The composition of the ore was 42.2 % iron and 50.5 %

sulphur. The relative density of the pyrite was 5.0 kg m^{-3} (measured). The initial pyrite concentration used in each experiment was kept constant at 3% (w/v). Quartz was obtained from Consol (South Africa) and was wet sieved to obtain a 38-75 μm fraction. The silica acted as an inert solid material that allowed different solids loadings to be tested without changing the pyrite concentration. Consequently the dissolved metal ion concentration and ionic strength which increase with leaching did not increase with increasing solids loading. Hence changes in leaching performance can be attributed to the solids loading only, rather than to the combined effect of solids loading and dissolved solutes. The relative density of the silica was 2.6 kg m^{-3}. The difference in densities of the pyrite and silica may alter the flow pattern of the slurry suspension.

The initial concentration of biomass following inoculation was in the range of 2-4x10^8 cells ml^{-1}. A low agitation speed of approximately 285 rpm was initially applied, to provide mild hydrodynamic conditions for the adaption of the microorganisms and a rapid increase in microbial population (Nemati and Harrison, 2000). When the biomass concentration increased by 2-3x10^8 cell ml^{-1} to 4-7x10^8 cell ml^{-1}, the agitation rate was increased to approximately 560 rpm. Complete suspension of solids was observed visually. Under conditions of complete suspension, the solid particles do not stay on the vessel base for longer than 1 or 2 seconds. Samples were taken regularly from the reactor, the solids decanted and returned to the reactor, and the sample analysed for ferrous and ferric iron concentration, microbial cell concentration, pH and redox potential. The pH and redox potential were not measured online owing to the harsh environmental conditions due to the low pH, presence of pyrite particles and high temperature. As a result, discrete samples were taken for pH and redox potential measurements at 24 hourly intervals. The redox was measured against a Ag/AgCl probe. Distilled water was added to the reactor to maintain the set volume of 700 ml (marked on the side of the reactor). Jarosite precipitate was observed in the reactor and was withdrawn with the sample to be analysed. One part of the sample was treated with hydrochloric acid to dissolve the jarosite, while another sample was analysed for iron without the jarosite being dissolved. The iron results showed that the iron content of the sample with dissolved jarosite was similar to that with undissolved jarosite, indicating that the proportion of jarosite in the sample was minimal. Jarosite precipitate was observed to adhere to the reactor walls, so the iron content measured was lower than the actual quantity in the reactor. The samples used for microbial cell

counts were left to stand for 30 minutes to allow the jarosite precipitate to settle before the solution was prepared for cell counting.

5.2.2. Methodology

All of the leaching experiments employed the set-up described in Section 5.2.1. The adsorption experiments were carried out in the rotary shaker as described in Section 5.2.2.2.

5.2.2.1. Chemical Leach

The chemical leach experiment was carried out to determine the extent of chemical leaching at 68°C. This was determined by performing a leach experiment, as described in Section 5.2.1, where 150 ml of an aqueous solution containing 3.0 kg m^{-3} ferric iron replaced the 150 ml inoculum. This amount of ferric iron in the solution was the same as the amount as present in the reactor at the point where agitation was increased for complete suspension. As no cells were present, the chemical leach was started at a speed of 560 rpm. Samples were drawn regularly and analysed for ferrous and ferric iron concentration, pH and redox potential.

5.2.2.2. Adsorption

Adsorption experiments were carried out to establish whether the microorganisms adsorb onto the pyrite surface and also to gain a better understanding of the mechanism of cell damage. If adsorption was found, then the proposed method of biomass concentration determination of free cell counting, would require correction to be representative. The adsorption experiments were carried out in flasks on a rotary shaker at 120 rpm. The flasks were charged with 150 ml inoculum from the stirred tank reactor, 150 ml medium and 9.0 g of pyrite (3 % w/v). They were maintained at a temperature of 68°C. Three experiments, each with its own control, were performed.

Experiment 1

Two identically charged flasks containing microorganisms, media and pyrite were placed on the rotary shaker. After 1 hour, one flask was removed and the contents placed on a mesh sieve to

retain the pyrite. The pyrite was then placed in a flask with 300 ml fresh medium and placed back on the rotary shaker. The control flask was left on the rotary shaker with the original contents. Samples were analysed regularly for ferrous and ferric iron, microbial cell concentration and pH and redox measurements.

Experiment 2

This experiment was identical to experiment 1, except that the solution was left in contact with the pyrite for 24 h before the solution was decanted and replaced with fresh medium.

Experiment 3

This was similar to the second experiment, but the pyrite was replaced into 300 ml fresh medium containing 6.0 g $FeSO_4.7H_2O$. The control flask originally contained approximately 3.0 kg m^{-3} iron in the ferric form added with the inoculum. Ferrous iron was added rather than ferric iron as ferric iron chemically leaches pyrite and ferrous iron does not. In addition, according to the indirect microbial leaching mechanism, microorganisms convert ferrous iron to ferric iron, thus if any microorganisms were present, the ferrous should have been converted to ferric iron. Samples from both the experiment and control flasks were analysed regularly.

A second set of adsorption experiments were carried out by placing media, pyrite and microorganisms in a shake flask and monitoring the concentration of microbial cells in the suspension over time. A decrease in the number of cells in suspension over time within the doubling time of the cells, would suggest adsorption of the cells onto the solid surface, assuming normal growth was occurring.

5.2.2.3. Bioleaching Experiments Investigating the Effects of Pulp Density

The investigation into the effect of pulp density in the range of 3 to 27% (w/v) on leaching performance was achieved using a fixed pyrite concentration (3 % w/v) while varying quartz concentration from 0 to 24 % (w/v). The bioleaching experiments were performed as described in Section 5.2.1, with 21.0 g of pyrite and the required amount of quartz to give a specified pulp density.

5.2.2.4. Mass Transfer Recordings

The negative effect of increasing pulp density on bioleaching kinetics may be due to oxygen limitation. To verify this theory, the mass transfer coefficient, k_La was determined by measurements using a Mettler Toledo oxygen probe and the dynamic method of mass transfer determination at the various pulp densities. The mixture was sparged with nitrogen to remove all dissolved oxygen, and then sparged with air while measuring the dissolved oxygen concentration. This was done at approximately 67°C.

5.2.2.5. Bioleaching Experiments Investigating Carbon Dioxide Limitation

Carbon dioxide limitation may have an adverse effect on bioleaching kinetics and was investigated at pulp densities of 3 % pyrite (w/v) with no quartz present and at higher solids loading in the presence of 18 to 24% quartz. The bioleaching experiments were carried out as outlined in Section 5.2.1 with the addition of 1% (v/v) carbon dioxide to the compressed air using a high pressure flow of carbon dioxide, with the flowrate of the carbon dioxide measured on a rotameter, feeding into the air stream.

5.2.2.6. Bioleaching Experiments Investigating the Effect of Agitation Rate

To investigate the effect of agitation rate on bioleaching kinetics, experiments were carried out as described in Section 5.2.1, except that the agitation speed was increased from 560 rpm to 660 and 760 rpm. The pulp density used was 3 % pyrite and 15 % quartz (w/v) as an adverse effect on the bioleaching kinetics (observed from pulp density experiments) had not been observed at 560 rpm.

5.2.2.7. Bioleaching Experiments Investigating the State of the Inoculum

Inoculum grown in a stirred tank reactor and inoculum grown in a shake flask were compared in bioleaching experiments. The inoculum grown in the stirred tank had a higher concentration of microbial cells than that grown in the shake flask. The stirrer speed was increased to 560 rpm when each reactor had reached $3\text{-}4 \times 10^8$ cell ml^{-1}. The experiment was carried out as described in Section 5.2.1.

5.3. ANALYTICAL PROCEDURES

Liquid samples were drawn from the reactors at regular intervals, the solids decanted and returned to the reactor, and the sample analysed for ferrous and ferric iron concentration, microbial cell concentration, pH and redox potential. Distilled water was added to the reactor to maintain the 700 ml working volume (the required level marked on the reactor wall).

5.3.1. Ferrous Iron Concentration

The oxidation of ferrous iron was observed by determination of the ferrous iron concentration by titrating against 0.017 M potassium dichromate with a redox indicator of barium diphenylamine sulfonate (Vogel, 1989). Potassium dichromate is an advantageous oxidising agent as it can be obtained pure, is stable up to its fusion point, and aqueous solutions that are protected from evaporation are stable indefinitely. The titration is a redox reaction:

$$\underset{orange}{Cr_2O_7^{2-}} + 6Fe^{2+} + 14H^+ \Leftrightarrow \underset{green}{2Cr^{3+}} + 6Fe^{3+} + 7H_2O \qquad eqn.5.1$$

The green dichromate makes it difficult to ascertain the end point of the dichromate titration, and thus a redox indicator must be used to provide an unmistakable colour change.

Procedure

The total ferrous iron concentration (iron released by oxidation) was determined from the liquor and from dissolving the iron precipitate using hydrochloric acid. A known volume of sample, 2 ml in this case, was placed in a conical flask, and 2 ml of concentrated (32 %) HCl was added to the flask. The mixture was heated until just boiling and put aside to cool. Three drops of the barium diphenylamine sulfonate indicator was added and the mixture titrated against 0.017 M potassium dichromate. The expected colour change is from yellow to brown. The concentration of ferrous iron in the solution was then calculated using the following equation:

$$1 \text{ ml } 0.017 \text{ M } K_2Cr_2O_7 = 0.005585 \text{ g } Fe^{2+} \qquad eqn.5.2$$

The effective ferrous iron concentration in the liquor was determined by centrifuging samples containing suspended solids (iron precipitate) for 5 minutes at 5000 rpm. The supernatant of the sample that was free from precipitate was then analysed.

5.3.2. Total Iron and Ferric Iron Concentrations

To measure the total iron concentration, ferric iron was reduced to ferrous iron using stannous chloride as the reducing agent, followed by titration against $K_2Cr_2O_7$ in the presence of a barium diphenylamine sulfonate indicator (Vogel, 1989). The reduction of ferric iron by stannous chloride is as follows:

$$2Fe^{3+} + Sn^{2=} \Leftrightarrow 2Fe^{2+} + Sn^{4+} \qquad eqn.5.3$$

Procedure

To 2 ml of sample, 2 ml of concentrated HCl was added and then heated to boiling point to solubilise the iron-containing precipitate. A concentrated solution of stannous chloride was then added dropwise to the hot solution from a burette, until the yellow solution turned clear. The solution was then cooled under running water. Excess stannous chloride was removed by adding 4 ml of a saturated mercuric chloride solution. A white precipitate of mercuric chloride was obtained:

$$2HgCl_2 + Sn^{2+} \Leftrightarrow Hg_2Cl_2 + Sn^{4+} + 2Cl^- \qquad eqn.5.4$$

If a grey or black precipitate formed, too much stannous chloride had been added which would yield inaccurate results hence the procedure was repeated. The final solution was titrated against 0.017 M $K_2Cr_2O_7$ with barium diphenylamine sulfonate indicator, as described in Section 5.4.2. The expected colour change for the titration is from whitish to purple.

Solutions

Potassium dichromate: Potassium dichromate powder was heated in an oven at 140 to 150°C for 30 to 60 minutes, followed by cooling in a desiccator. The solution of 0.017 M $K_2Cr_2O_7$ was prepared by placing 4.9 g of the dry potassium dichromate in a 1 litre volumetric flask and filling to the mark with distilled water. The salt dissolved in the water.

Stannous chloride: The concentrated solution of stannous chloride was made by dissolving 30 g of analytical crystallised stannous chloride ($SnCl_2.2H_2O$) in 100 ml of concentrated hydrochloric acid and diluting to 200 ml with distilled water.

Mercuric chloride: A saturated solution of mercuric chloride was prepared by dissolving 10 g of mercuric chloride in 200 ml of distilled water.

5.3.3. Bacterial Concentration

The bacterial concentration was determined by direct counting of the free cells in solution using a Petroff-Hauser type cell counter (haemocytometer) of 0.02 mm depth and 1/400 mm^2 area. A drop of the sample was placed over the grid using a Pasteur pipette. A cover slip was placed over the central platform and gently pressed down, creating a uniform film over the grid. The total field consists of 16 large squares, each comprised of 16 small squares. The number of cells in each large square in the corners of the field were recorded, counting 64 small squares. A magnification of 1000X was used for the cell counts.

The concentration of microorganisms (cells ml^{-1}) was calculated using the following equation:

$$X = \frac{x \times \left(\frac{N}{n}\right)}{D \times A} \times \frac{1}{d} \times 10^3 \qquad \textit{eqn.5.5}$$

where:

X : bacterial concentration (cells ml^{-1})

x : number of cells in the large squares counted

N : total number of large squares (16)

n : number of large squares where cells were counted (4)

D : depth of the field (0.02 mm)

A : total area of the field (1 mm^2)

d : dilution ratio

5.4. SUMMARY

The objective of the experiments was to determine the effect of pulp density on the bioleaching performance. This was done using a fixed concentration of pyrite and varying the concentration of an inert to achieve pulp densities in the range of 3 to 27 % (w/v). Firstly, the extent of chemical leaching was determined by the chemical leach experiments, so as to quantify the extent of biological leaching. Thereafter the proposed method of biomass concentration determination was tested as the method proposed counting the free cells in solution. Adsorption of the cells had to be established as the method of concentration determination would require correction if the cells adsorbed onto the pyrite surface. Following this pulp density experiments were done. Pulp densities in the range of 3 – 27% (w/v) total solids loading was investigated. In all cases 3 % (w/v) pyrite was used. Possible causes of the effects observed in the pulp density experiments were then investigated. These included the effect of mass transfer and carbon dioxide limitations. Mass transfer recordings at each pulp density used were determined at 67°C. This was to ascertain if oxygen had become limiting at higher pulp densities. The limitation of carbon dioxide was tested by performing bioleaching experiments using air enriched with 1 % carbon dioxide. The effect of agitation on bioleaching performance was also determined. This was done by bioleaching experiments at agitation speeds of 560, 660 and 760 rpm. Finally, the effect of the state of the inoculum on bioleaching performance was established using inoculum from a stirred tank reactor, and inoculum from a shake flask.

5.5. REFERENCES

Nemati, M. and S.T.L. Harrison (2000), "Effect of solid loading on thermophilic bioleaching of sulphide minerals", *J. Chem. Technol. Biotechnol.* **75**, 526-532

Vogel, A.I. (1989), *Vogel's Textbook of Quantitative Chemical Analysis*, 5th ed., Longman Group Ltd., London, UK, 287-310

CHAPTER 6

RESULTS AND DISCUSSION: EFFECT OF THE PARTICULATE PHASE ON BIOLEACH PERFORMANCE

Chemical leaching experiments were first performed to assess the relative extent of chemical leaching at 68°C and thus the contribution of biological leaching to the overall leaching. This was done by carrying out a leach experiment without inoculum but in the presence of an aqueous ferric iron solution. The results of these experiments are shown in Section 6.2.

Adsorption experiments are reported in Section 6.3 to determine the location of the microbes relative to the concentrate thereby validating the assumption that the use of the free cell concentration was representative of the biomass concentration.

The effect of solids loading on bioleaching performance was determined by carrying out bioleaching experiments using solids loadings in the range of 3 to 27% w/v (Section 6.4). In each experiment, a constant pyrite loading of 3% (w/v) was used to ensure a constant energy source and limited variation in chemical environment. Total solids loading was varied by adding quartz (SiO) of a similar particle size distribution. Samples were withdrawn regularly from the reactor and analysed for ferrous and ferric iron concentration, sulphate concentration, microbial cell count, pH and redox potential. The effect of agitation speed and the state of the inoculum were also investigated (Sections 6.6 and 6.7).

Variation in particulate parameters has potential to alter suspension viscosity and mass transfer. The possible effects of oxygen and carbon dioxide limitations on the bioleach performance with increasing solids loading is presented in Section 6.5.

Reproducibility of the bioleaching experiments was examined and statistical analysis of the data performed. These results, in Section 6.1, provide a benchmark against which the significance of trends can be established.

6.1. REPRODUCIBILITY OF BIOLEACHING EXPERIMENTS

The reproducibility of the bioleaching experiments was determined by repeating experiments at 3% pyrite in the presence of 12, 15 21 and 24% silica. Figure 6.1 illustrates the reproducibility of the 3% pyrite plus 12% quartz in terms of the iron release concentration and the biomass concentration. An analysis of variance (ANOVA) was performed on the data collected for iron release and biomass concentrations at the various solids loading (Appendix A). The results indicate that no significant difference was observed between the two sets of data at each solids loading for both the iron release and the biomass concentration. In other words, the F-distribution coincided with confidence levels of less than 90% that translates to insignificant differences between the two sets of data.

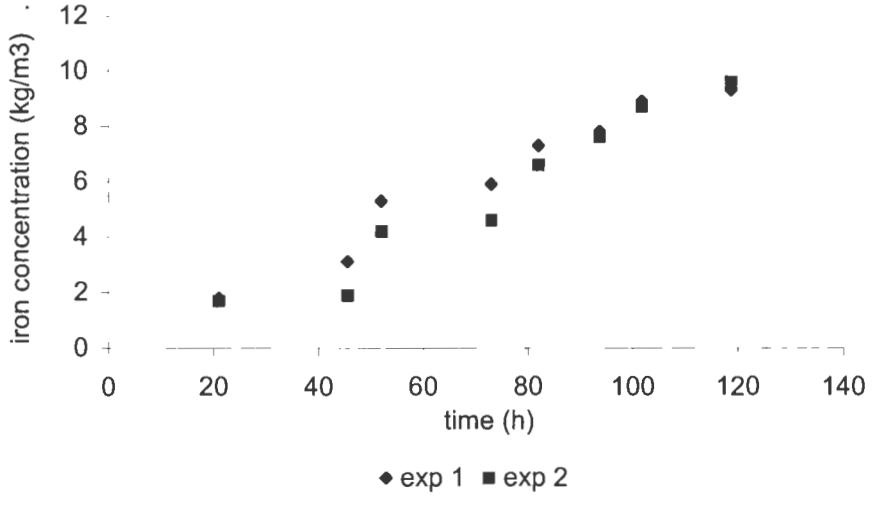

Figure 6.1 (a): Reproducibility of the bioleaching of 3% pyrite in the presence of 12% quartz by *Sulfolobus metallicus* in terms of iron release concentration

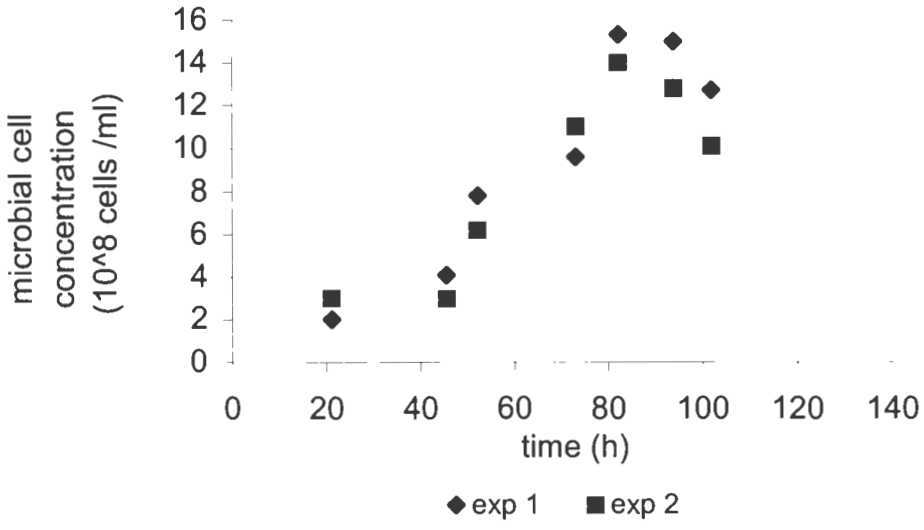

Figure 6.1 (b): Reproducibility of the bioleaching of 3% pyrite in the presence of 12% quartz by *Sulfolobus metallicus* in terms of microbial cell concentration

6.2. CHEMICAL LEACHING

The chemical leaching experiments were designed to determine the extent of chemical leaching at 68 to 70 °C. The experiments were carried out in a similar way to the bioleaching experiments, except that no inoculum of microorganisms was added. An aqueous solution containing 3 kg m^{-3} ferric iron, growth medium at a pH of 2.5 and 3 % (w/v) pyrite was placed in a 1l jacketed stirred tank reactor and maintained at 68°C. Compressed air was supplied at a rate of 2 l min^{-1} through a ring sparger. Two experiments were performed for the chemical leaching. The first experiment was carried out under the conditions described over 68 hours. The pH, redox potential, ferric and total iron concentrations and ferrous iron produced were monitored. The second experiment followed the same procedure, except that 9.0 g of ferric sulphate (2.5 g of ferric iron) was added to the reactor 48 hours after a decrease in ferrous iron production and a lowering of redox potential to determine whether further leaching would occur if the redox potential was increased. These experimental results are shown in Table 6.1.

Table 6.1: Chemical Leaching of Pyrite at 70°C under Bioleaching Conditions

EXPERIMENT 1

Time (hours)	pH	Redox Ag/AgCl	Iron Concentration [Fe] kg.m^{-3}			Fe^{2+} produced in Each time interval Kg m^{-3}
			Fe^{2+}	Fe^{3+}	Fe^{tot}	
0	1.83	492	0.42	2.93	3.35	
24.25	1.57	391	2.23	0.56	2.79	1.81
48.25	1.52	384	1.95	0.84	2.79	-0.28
68.50	1.52	382	2.23	0.56	2.79	0.28

EXPERIMENT 2

Time (hours)	pH	Redox Ag/AgCl	Iron Concentration [Fe] kg.m^{-3}			Fe^{2+} produced in Each time interval kg m^{-3}
			Fe^{2+}	Fe^{3+}	Fe^{tot}	
0	1.86	529	0.14	2.93	3.07	
24.00	1.45	395	2.23	0.56	2.79	2.09
48.00	1.5	383	2.79	0	2.79	0.56
		added 9.0 g of ferric sulphate (2.5g iron)				
49.00	1.48	451	3.63	1.68	5.31	
73.50	1.35	416	3.91	1.40	5.31	0.28
96.50	1.35	407	4.19	1.12	5.31	0.28
145.50	1.35	405	3.91	1.68	5.59	-0.28

The currently accepted mechanism for bioleaching is the indirect mechanism whereby the sulphide mineral is chemically leached by ferric iron and the role of the microorganisms is to regenerate the ferric iron and maintain a sufficiently high redox potential for the reaction to proceed (Hansford and Vargas, 2000). The ferric leach rate of pyrite decreases with decreasing redox potential concurring with the Butler –Volmer model and experimental data, with the redox potential only going as low as 625mV vs Ag/AgCl (Hansford and Vargas, 2000). Redox potentials as low as those observed in this experiment 529-382 mV) have not been used. The initial redox potentials used in these experiments were similar to those used in the bioleaching experiments where significant leaching took place (Section 6.4) and so these initial values are adequate for leaching to occur.

Chemical leaching is the chemical oxidation of a mineral sulphide by ferric iron. Thus as leaching occurs, the ferric iron concentration decreases, whilst the ferrous iron concentration increases. According to the chemical leach equation (*eqn.2.5*), 15 Fe^{2+} ions are produced for every 14 Fe^{3+}

ions consumed, and 1 pyrite molecule is oxidised. Thus the rate of ferrous iron production is 15 fold greater than the rate of pyrite oxidised.

$$FeS_2 + 14Fe^{3+} + 8H_2O \rightarrow 15Fe^{2+} + 2SO_4^{2-} + 16H^+ \qquad eqn.2.5$$

In both experiments, production of ferrous iron occurs. The average change in ferrous iron concentration with time is 0.026 kg m^{-3} h^{-1} in experiment 1 and 0.073 kg m^{-3} h^{-1} in experiment 2 before the addition of ferric iron. According to the chemical leach equation, this corresponds to an average iron leach rate of 0.0018 kg m^{-3} h^{-1} and 0.0048 kg m^{-3} h^{-1}, respectively. The average bioleaching rate for the same solids loading under similar conditions was 0.12 kg m^{-3} h^{-1} over a 117 h period. This indicates that bioleaching has a far greater contribution to leaching of pyrite than abiotic leaching. It also suggests that ferric iron cannot be regenerated under these conditions.

The rate of ferrous iron production was 0.075 kg m^{-3} h^{-1} at a redox potential of between 492 and 391 mV in experiment 1. The production of ferrous iron below 391 mV was negligible. In experiment 2, the rate of ferrous iron production was 0.087 kg m^{-3} h^{-1} at a redox potential of between 529 and 395 mV. This rate decreased to 0.058 kg m^{-3} h^{-1} at a redox potential of between 395 and 383 mV. An increase in redox potential to 451 mV did not induce ferrous iron production. Thus it appears that low redox potential has an adverse effect on ferric leaching. This is in accordance with experimental data that shows that ferric leaching is a function of redox potential (Hansford and Vargas, 2000). A high ferric iron concentration cannot be maintained abiotically with the ferric iron and pyrite concentration in this system and thus abiotic leaching is negligible.

6.3. PARTITIONING OF *SULFOLOBUS* BETWEEN CONCENTRATE SURFACE AND LIQUID PHASE

A set of adsorption experiments was conducted to determine the extent to which the microorganisms attached to the pyrite. This was important for two reasons – firstly, to confirm the applicability of the proposed method of biomass determination (microscopic counting of free cells) to the thermophilic bioleaching system; and secondly, to determine the mechanism of cell damage. The cell size is much less than the eddy size, whereas the solids are approximately the same size as the eddies and so if the cells move independently to the solids the mechanism of cell damage may be determined. The experiments were performed by placing cells, growth medium and pyrite into Erlenmeyer flasks on a rotary shaker maintained at a temperature of 68°C. In the first experiment, the entire suspension was left in the flask for an hour, after which the pyrite was separated from solution and rinsed using a mesh sieve. The pyrite was then placed back into the flask with fresh medium and bioleaching activity monitored. In the second experiment, the same procedure was followed, but the pyrite was rinsed following a 24 hour contact period. The third experiment was conducted in the same way as the second with the pyrite being rinsed after a 24 hour contact period, but the pyrite was returned into growth medium containing ferrous iron. A control was used in each of the experiments whereby the entire suspension of biomass, growth media and pyrite was left undisturbed in the flasks and leaching progress monitored.

The results of the adsorption experiments are given in Table 6.2 in terms of iron release after the pyrite was separated from the microbial cell suspension and at the corresponding times for the controls. In experiment 1, no iron was leached from the ore after 44 hours, whereas the concentration of iron released in the control was 1.12 ± 0.04 kg m^{-3} after 24 hours and 0.84 ± 0.04 kg m^{-3} after 44 hours. The decrease in iron concentration was most likely due to iron precipitation on the reactor wall. Observation of the solution from experiment 1 revealed that the concentration of free cells in solution was less than 6.6×10^7 cells ml^{-1}. The concentration of free cells in solution in the control remained approximately constant at $6.3 \times 10^8 \pm 6.6 \times 10^7$ cells ml^{-1} throughout the experiment. A decrease of 0.26 ± 0.04 kg m^{-3} in the iron released corresponded to the constant biomass concentration.

Table 6.2 Adsorption of *Sulfolobus metallicus* to pyrite – the experiment indicates the iron release results obtained when the pyrite, growth media and inoculum suspension was washed leaving the pyrite with fresh medium, while the control indicates the results obtained with the suspension intact. The biomass concentration of free cells in the experiments after washing was less than $6.6x10^7$ cells ml^{-1}.

Experiment 1 Time (hours)	Experiment Total Iron in Solution (kgm^{-3})	Control Total Iron in Solution (kgm^{-3})	Control Planktonic Biomass Concentration (10^8 cells ml^{-1})
0	0.00	0.00	6.5
24	0.00	1.12	6.9
44	0.00	0.84	5.7

Experiment 2 Time (hours)	Experiment Total Iron in Solution (kgm^{-3})	Control Total Iron in Solution (kgm^{-3})	Control Planktonic Biomass Concentration (10^8cells ml^{-1})
0	0.00	0.00	5.7
24	0.00	1.96	5.4
48	0.14	3.07	5.5
74	0.28	3.35	7.0
97	0.28	4.47	5.9

Experiment 3 Time (hours)	Experiment Total Iron Released (kgm^{-3})	Control Total Iron Released (kgm^{-3})	Control Planktonic Biomass Concentration (10^8cells ml^{-1})
0	0.00	0.00	7.9
23	0.00	1.12	5.7
47	0.00	1.40	6.8
73	0.00	2.23	7.5
96	0.00	3.35	9.2

In the second experiment, no iron was leached in the first 24 hours. After 48 hours, 0.14 ± 0.04 kg m^{-3} was leached. The concentration increased to 0.28 ± 0.04 kg m^{-3} after 73 hours. This iron concentration remained constant for a further 23 hours. In the control, the iron release increased over the 96 hour period, from an initial value of 0 to 4.45 ± 0.04 kg m^{-3}. The ferric iron concentration increased over the 96 hours. The free cell concentration observed in the experiment was less than $6.6x10^7$ cells ml^{-1}, while the concentration of free cells in the control remained above $5.4x10^8$ cells ml^{-1}.

No iron was released in 96 hours in the third experiment. In the control, the iron released increased throughout that period and a final concentration of 3.4 ± 0.04 kg m^{-3} is leached. Observation of the solution from the experiment revealed a free cell concentration of less than $6.6x10^{7}$ cells ml^{-1}, whilst the biomass concentration of free cells in the control ranged from $5.7x10^{8}$ to $9.2x10^{8}$ cells ml^{-1}.

In the first experiment where the cells were in contact with the pyrite for only an hour, no leaching occurred throughout a 44 hour time period. The initial inoculum and the environmental conditions were adequate for leaching of the pyrite as leaching occurred in the control (1.12 ± 0.04 kg m^{-3} of iron was leached in 24 hours). This 1 h contact period may have not been sufficient for attachment of the cells to the pyrite.

The time period of contact between the cells and the pyrite was increased to 24 hours. During this contact period, 0.84 ± 0.04 kg m^{-3} of iron was leached. The initial free cell concentration remained approximately constant at $5.7x10^{8}$ cells ml^{-1} during this time period. The free cells and solution were then removed and the pyrite was placed with fresh medium in the flask. The total amount of iron leached from the pyrite in the experiment was very little (0.28 ± 0.04 kg m^{-3}) compared to that released in the control (4.47 ± 0.04 kg m^{-3}) over the same time period. In this experiment, only medium was added to the pyrite after the free cell suspension was removed. The medium did not contain any iron, hindering the leaching of the pyrite by any possible microorganisms present.

In the third experiment, 4.20 kg m^{-3} of ferrous iron was added to the pyrite after the free cell suspension had been removed. Ferrous iron was added to provide a ready substrate to microbes present. This was preferred to ferric iron because ferric iron is capable of chemically leaching pyrite. Thus if any microorganisms were present, conversion of the ferrous iron to ferric iron could occur with subsequent leaching of the pyrite by ferric iron according to *equation 2.3*. This, however, does not occur, as indicated by the negligible iron released.

The controls in each of the experiments clarify the suitability of conditions for leaching. The presence of iron added with the inoculum was accounted for in the third experiment. Very little, if any leaching occurred in the experiments, while at least 1.12 ± 0.04 kg m^{-3} of iron was leached in

the controls. The concentration of free cells in the experiments was less than $6.6x10^7$ cells ml^{-1}, while that in the controls was at least $5.0x10^8$ cells ml^{-1}. These results suggest that very little or no leaching occurs if the concentration of free cells in suspension is low.

A second set of adsorption experiments were carried out by placing growth medium in a shake flask with inoculum and 3%(w/v) pyrite and observing the cell concentration in the free solution with time. The result of this experiment is in Table 6.3.

Table 6.3: Adsorption experiments showing the change in free cell concentration with time

Experiment 1		Experiment 2	
Time (h)	**Microbial cell Concentration 10^8 cells ml^{-1}**	**Time (h)**	**Microbial cell Concentration 10^8 cells ml^{-1}**
0.0	8.2	0.0	4.5
1.0	6.7	0.25	4.0
2.0	6.4	4.0	4.8
3.0	5.9	27.0	5.0
4.0	6.9	48.0	5.0
24.0	7.1		
48.0	6.1		
72.0	5.4		

Observation of the trend in biomass concentration of free cells in suspension with both short and long time intervals, illustrates a decrease of 25% in experiment 1 and a fairly constant biomass concentration in experiment 2, within the experimental error of counting of $6.6x10^7$ cells ml^{-1}. The doubling time for inoculum maintained in a stirred tank is 63 h ($\mu = 0.032\ h^{-1}$). As this inoculum was obtained from a stirred tank and then placed in a shake flask where the mass transfer conditions are lower (no sparging with air and no agitation), a longer doubling time would be expected. The microbial cell concentration in experiment 2 would not be expected to increase while that in experiment 1 may increase or remain the same. If the microbial cells partitioned themselves on the concentrate surface, a significant decrease in microbial cells would be observed in both experiments. The results obtained indicate that the microbial cells remain predominantly in

the liquid phase. Thus the method of free cell counting may be taken as representative of the biomass concentration.

The fact that the cells are not attached to the solid particles indicates that the cells will not be subjected to velocity gradients caused by fluid eddies passing across the cell surface. The cells are much smaller than the fluid eddies, and so may be entrained in the eddies, but will not be subjected to shear from the eddy movement.

6.4. EFFECT OF SOLIDS LOADING ON BIOLEACHING / BIOOXIDATION PERFORMANCE

In order to assess the effect of solids loading on bioleaching/biooxidation without introducing substantial change to the physiological environment, bioleaching experiments were conducted in the presence of 3% (w/v) pyrite supplemented with 0 to 24%(w/v) quartz. In Section 6.4.1, the leaching performance of each experiment is reported. In Section 6.4.2, the results are compared as a function of solids loading. Section 6.4.3 discusses the findings in terms of current knowledge presented in the literature and conclusions are drawn in Section 6.4.4.

6.4.1. Bioleaching Performance as a Function of Solids Loading

The results of bioleaching of pyrite at 3% (w/v) solids loading pyrite in the presence of 0 to 24% (w/v) silica are presented in Figures 6.2 through 6.6, while the detailed data is presented in Appendix B. The microbial cell number in suspension, pH and redox potential profiles are also given. Figures 6.2 to 6.4 indicate that the trends in microbial growth (microbial cell count) and bioleaching (total iron released) are similar for the solid loading of 3% pyrite in addition to 0, 6 and 15% quartz. The bioleaching rates at each of these solids loadings remained approximately constant (0.099 kg Fe m^{-3} h^{-1}) until a maximum iron concentration was measured. A constant iron concentration or a decrease in iron concentration was then observed. No initial lag phase in

microbial growth or bioleaching was observed on complete suspension of the solid phase. The total duration of the exponential phase varied between 70 and 110 hours. In the experiment with 3% pyrite the biomass concentration increased exponentially from the start of the experiment to a maximum cell concentration of $17x10^8$ cells ml^{-1} at 70 h. The stationary phase continued to 120 h, followed by a decrease in biomass concentration. The bioleaching rate in terms of the concentration of total iron released remained constant for 117 hours, thus indicating the ability of the cells to maintain a constant bioleaching rate while changing from exponential to stationary growth phase. The result suggests that the non-growing cells can maintain activity regarding the oxidation of pyrite. A sharp decrease in biomass concentration at 120 h corresponded to an exhaustion of the energy source, namely Fe^{2+} generated from pyrite.

With the addition of 6 and 15% quartz, the exponential growth phase of the cells extended for a longer period of time, varying from 90 hours in the presence of 6% quartz to 120 hours in the presence of 15% quartz. The maximum planktonic cell numbers observed in these experiments were 18 and $16x10^8$ cells ml^{-1}, respectively. A sharp decrease in cell number in the presence of 3% pyrite and 6% quartz was observed as the iron oxidation ends at 125 h, while a constant stationary phase cell number was observed in the presence of 3% pyrite and 15% quartz. The bioleaching rates remained constant throughout the initial 125 h period of both experiments. These constant bioleach rates corresponded to a shift in growth phase from exponential to stationary. This indicated the ability of the biomass to maintain bioleach activity on growth phase transition, and the ability of the stationary phase cells to maintain the activity of the growing cells.

The initial pH for the bioleaching of 3% pyrite in the presence of 0 to 15% quartz was in the range of 1.5 to 1.7. The pH decreased steadily during the bioleach. The lowest pHs of 0.8 to 1.0 were obtained towards the end of the experiments (118h, 122h and 120h, respectively). A decrease in pH from 1.1 to 0.9 in the presence of 3% pyrite corresponded to a shift in growth phase of the biomass from exponential to stationary. The changes in pH in the presence of 6 and 15% quartz did not affect the biomass concentration. The total iron in solution at the minimal pH values represented 95-98% of the iron available in the pyrite fraction added. The initial redox potentials of 475 to 547 mV for these solids loading increased gradually to a final redox potential in the range of 639 to 650mV, relative to a Ag/AgCl electrode.

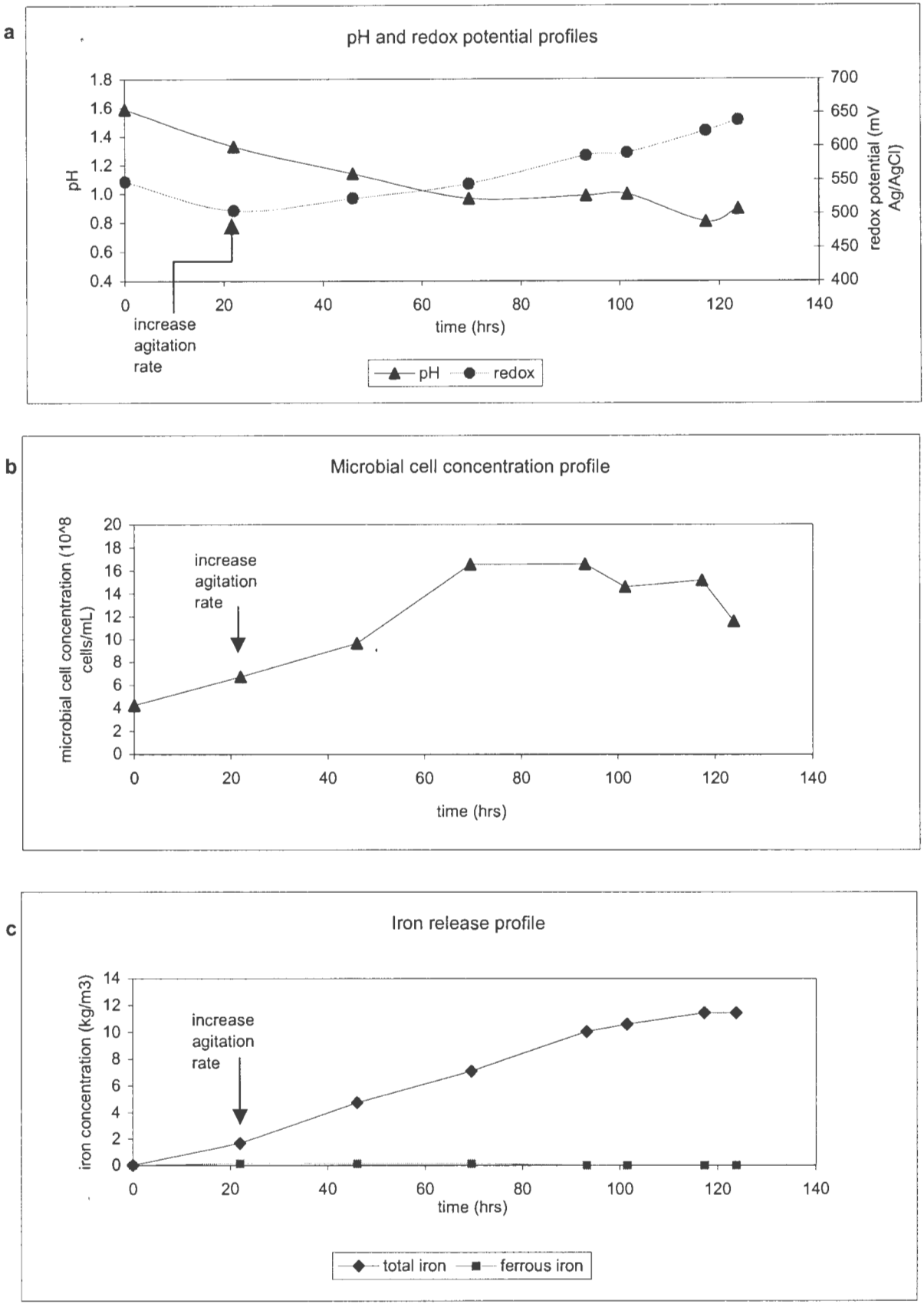

Figure 6.2: Bioleaching profiles of *Sulfolobus metallicus* at 68 C in the presence of 3% pyrite as a function of time: a) pH and redox profiles; b) microbial cell count in solution; c) iron release and ferrous iron concentration

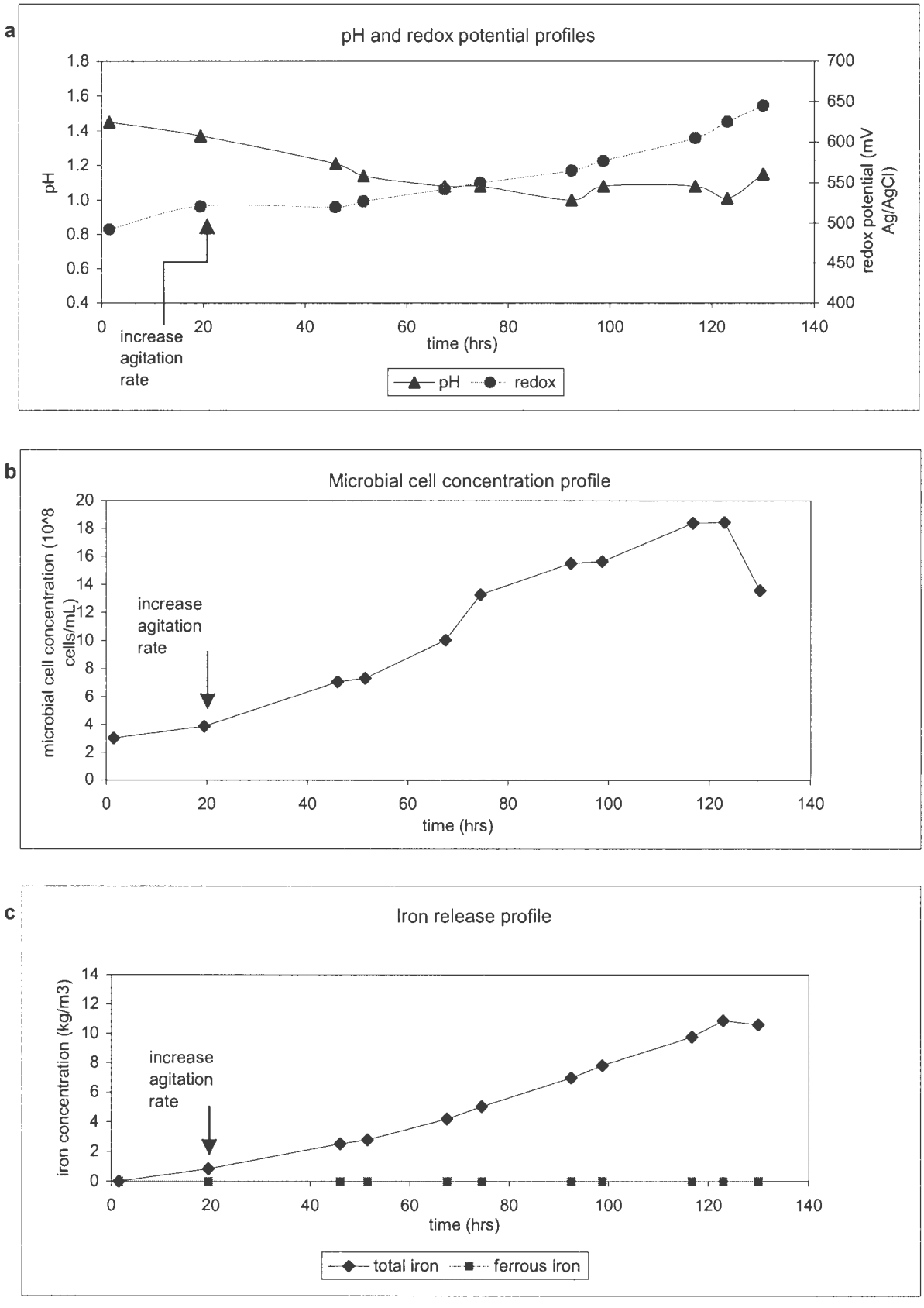

Figure 6.3: Bioleaching profiles of *Sulfolobus metallicus* at 68 C in the presence of 3% pyrite with 6% quartz as a function of time: a) pH and redox profiles; b) microbial cell count in solution; c) iron release and ferrous iron concentration

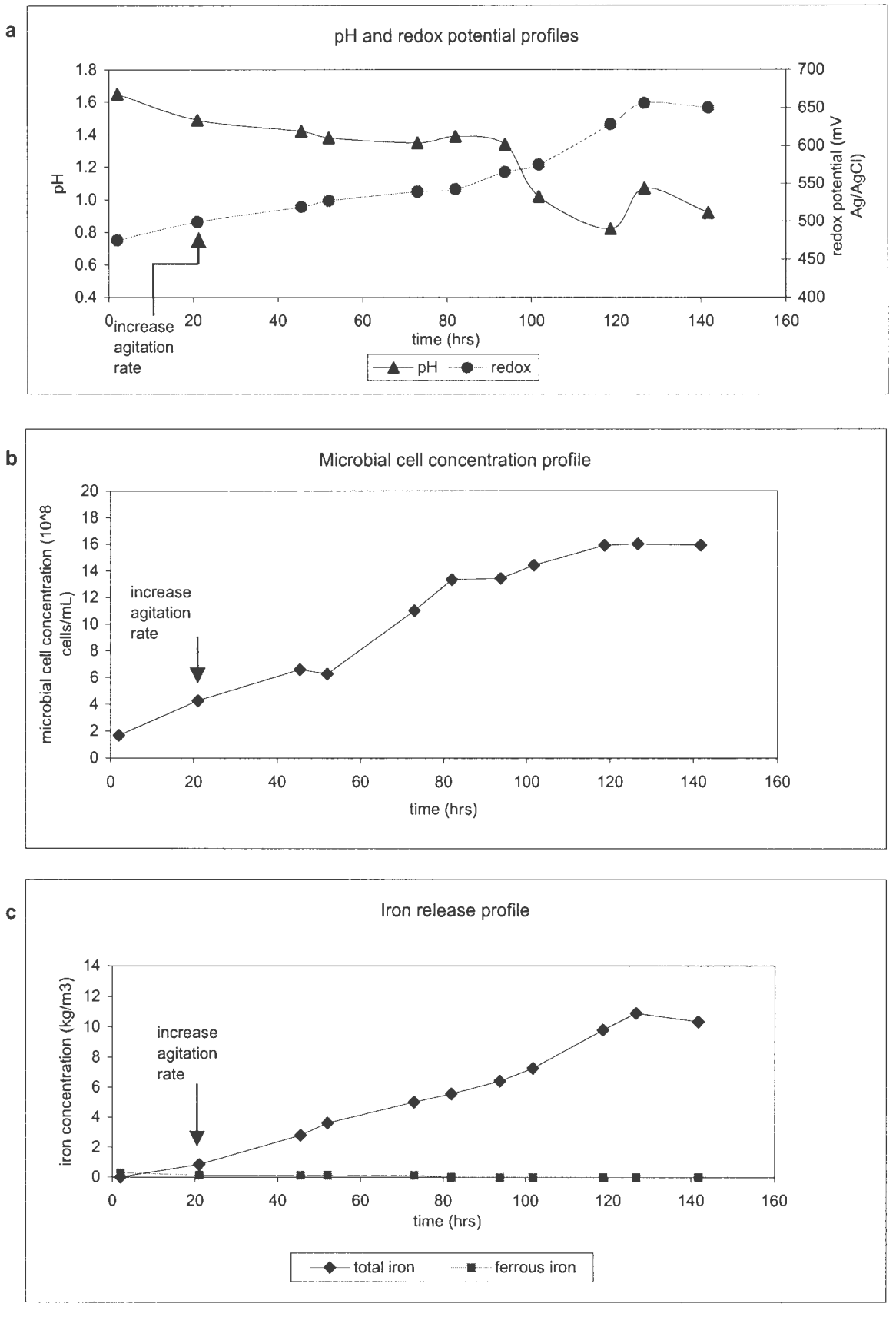

Figure 6.4: Bioleaching profiles of *Sulfolobus metallicus* at 68 C in the presence of 3% pyrite with 15% quartz as a function of time: a) pH and redox profiles; b) microbial cell count in solution; c) iron release and ferrous iron concentration

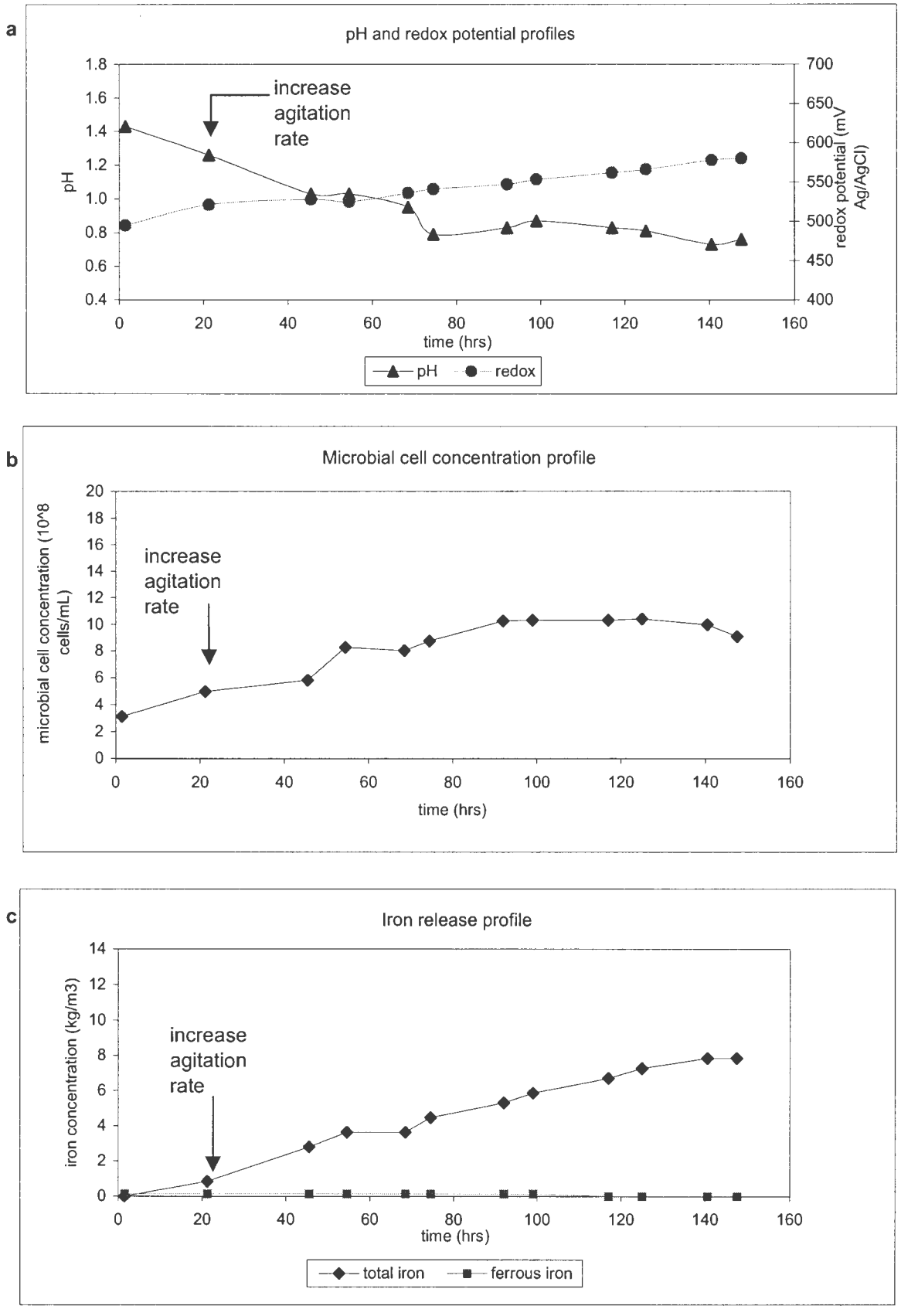

Figure 6.5: Bioleaching profiles of *Sulfolobus metallicus* at 68 C in the presence of 3% pyrite with 21% quartz as a function of time: a) pH and redox profiles; b) microbial cell count in solution; c) iron release and ferrous iron concentration

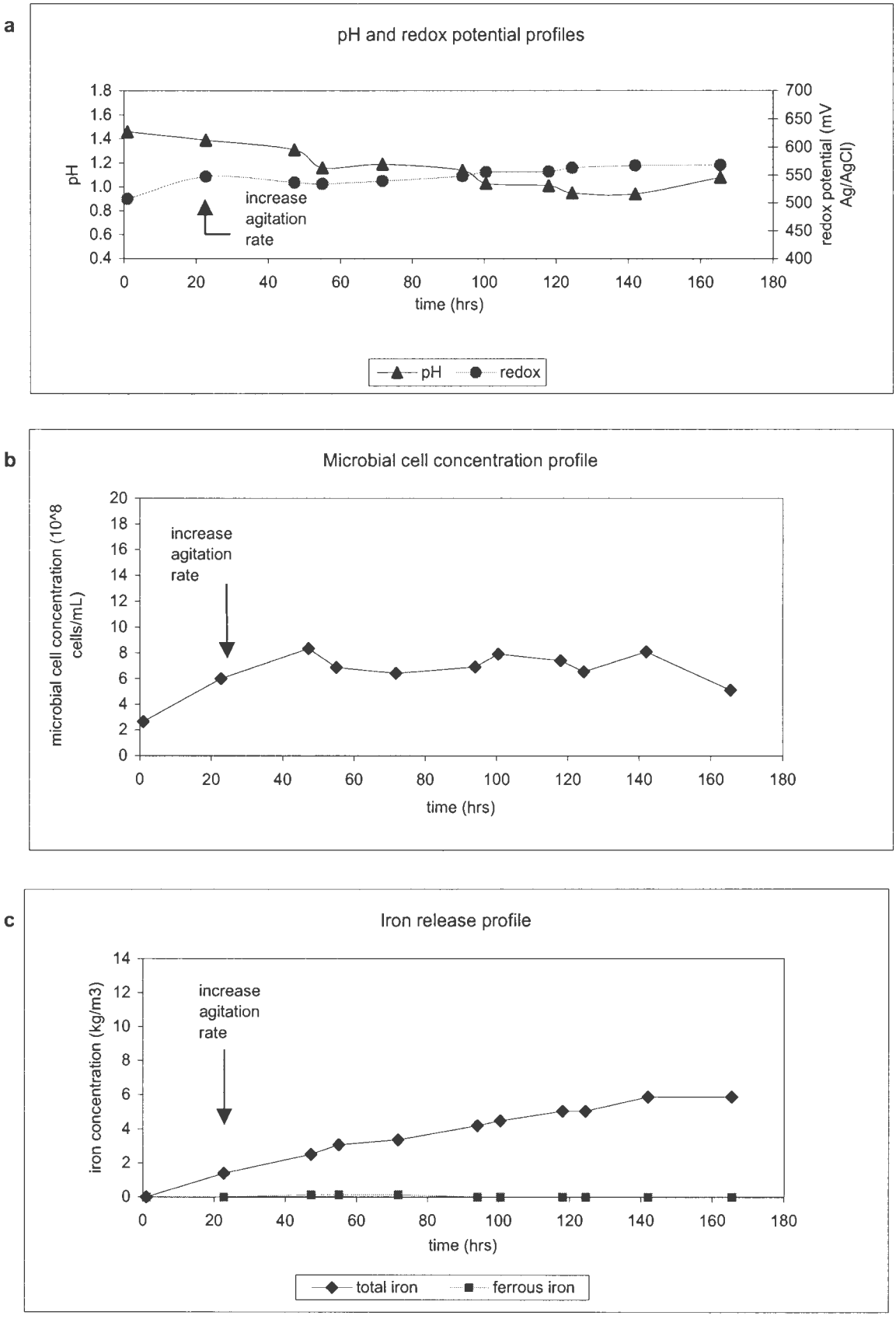

Figure 6.6: Bioleaching profiles of *Sulfolobus metallicus* at 68 C in the presence of 3% pyrite with 24% quartz as a function of time: a) pH and redox profiles; b) microbial cell count in solution; c) iron release and ferrous iron concentration

The trend in microbial growth and bioleaching in the presence of 3% pyrite in addition to 21% quartz differed from those at lower solid loading. The bioleaching rate in terms of total iron release was fairly constant across 140 h, but lower than that obtained in the presence of 0 to 15% quartz. The microbial cell number increased exponentially over 90 h, followed by a stationary phase at a maximum cell number of $10x10^8$ cells ml^{-1} from 90 to 140 hours and a death phase from 140 to 148 hours. The corresponding constant bioleaching rate suggests that the oxidation of pyrite proceeded by catalytic activity of growing cells, followed by maintenance of this activity by non-growing cells. The initial pH of 1.4 decreased to 0.8 in 75 hours and remained approximately constant throughout the rest of the experiment. The low pH did not affect the bioleach rate. The total iron released was all in solution at this pH. The redox potential increased gradually from a value of 495 to 578mV.

Using a solid loading of 3% pyrite plus 24% silica, the constant bioleaching rate observed was further reduced. The biomass profile displayed a fairly constant cell concentration, varying between 6 and $8x10^8$ cells ml^{-1} in the period after the agitation rate has been increased to 550 rpm to fully suspend the solids (23 – 142 hours). This was followed by a decrease in biomass concentration corresponding to the cessation of iron release. The stationary phase of the biomass coincided with a constant bioleach rate. This suggested that the activity of the cells in terms of pyrite oxidation was maintained over the 40 to 140 hour period. The pH of the experiment decreased from 1.5 to 0.9 through the experiment. All iron released remained in solution at this pH, i.e. no iron precipitated. The redox potential increased rapidly by 40mV in the first 24 hour period at an agitation rate of 280 rpm before the solids have been fully suspended. This was followed by a small increase from 547 to 568mV during the remainder of the experiment.

In order to assess the effect of solids loading on the growth and leaching performance of *Sulfolobus metallicus* in the absence of changing physiological conditions, Section 6.4.2 gives a comparison of the bioleaching performance using 3% pyrite supplemented with 0 to 24% quartz (increased in 3% intervals).

6.4.2. Effect of Solids Loading on Bioleach Performance – Iron Release and Microbial Cell Concentration

6.4.2.1. Iron Release at Various Solids Loading

The total iron release as a function of time at the various solids loadings are given in Figure 6.7. The average linear leach rates for each experiment, as well as the corresponding correlation coefficient, R^2, are given in Table 6.4. The extent of pyrite solubilisation, calculated from the total iron concentration in the suspension (iron in solution and precipitate), and the iron content in the mineral concentrate, are presented with the time required to achieve these values. Figure 6.7 shows that a solids loading of 3% (w/v) pyrite exhibits the best bioleaching performance in terms of bioleach rate and extent of solubilisation. A bioleach rate of 0.113 kg iron m^{-3} h^{-1} (R^2 = 1.0) and an extent of solubilisation of 91% was achieved in 117 hours. The addition of quartz in the range of 6 to 15% (w/v) decreased the bioleach performance similarly. The bioleach rates over this range of solids loading is similar at an average of 0.095 kg iron m^{-3} h^{-1} (R^2 = 0.98) and an extent of solubilisation of approximately 86% was observed in 123 - 127 hours. The addition of 21% quartz reduced the bioleach rate further to 0.057 kg iron m^{-3} h^{-1} (R^2 = 0.98) and an extent of solubilisation of pyrite of 62% after 148 hours. The bioleach rate and extent of solubilisation of pyrite obtained after 148 hours using 3% pyrite and 24% quartz was 0.035 kg iron m^{-3} h^{-1} (R^2 = 0.99) and 46% respectively.

Table 6.4: Average pyrite leach rates and extent of pyrite solubilisation at the various solids loading

Solids Loading (w/v)	Average Leach Rate kg Fe m^{-3} h^{-1}	R^2	Extent of Solubilisation %	Time h
3% pyrite	0.113	1.00	91	117
3% pyrite, 6% quartz	0.099	0.98	86	123
3% pyrite, 12% quartz	0.094	0.99	80	127
3% pyrite, 15% quartz	0.091	0.98	86	127
3% pyrite, 18% quartz	0.062	0.98	86	166
3% pyrite, 21% quartz	0.057	0.98	62	148
3% pyrite, 24% quartz	0.035	0.92	46	148

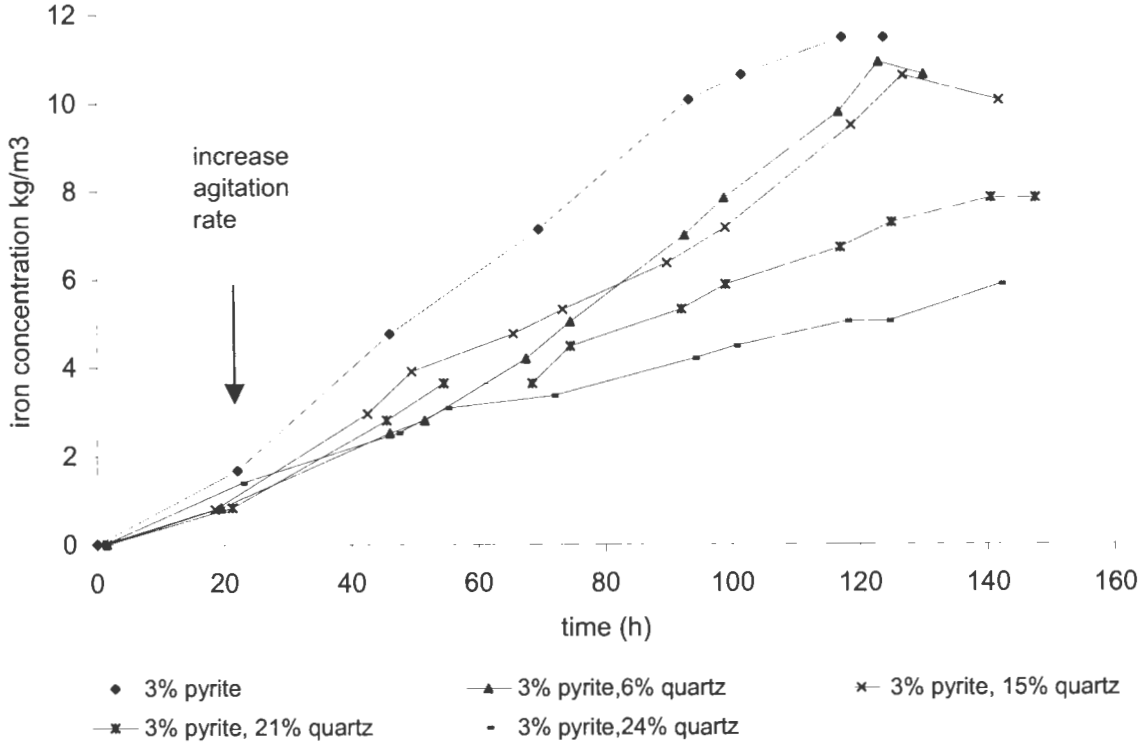

Figure 6.7: Total iron release as a function of time at various solids loading

The results of this set of experiments indicates that 3% pyrite exhibits the best bioleaching performance in terms of iron release and pyrite dissolution. The addition of 6 to 15% quartz to the 3% pyrite decreased the bioleach performance by 18% in terms of leach rate, but is similar throughout this range of solids loading. This suggests that the depression was due to the presence of quartz rather than the degree of solids loading. The addition of 21% quartz and 24% quartz progressively worsen the bioleach performance and the extent of pyrite dissolution is lower and requires a longer time period to achieve.

6.4.2.2. Comparison of Free Cell Concentration Profiles at Various Solids Loading

Profiles of the free cell concentration for each solids loading is given as a function of time in Figure 6.8. Specific growth rates, yields and maximum microbial cell concentration are given in Table 6.5 as a function of solids loading. The specific growth rates reported were calculated from the time of increase of agitation speed to approximately 70 hours into the experiment. The growth rates for solids loading of 3% pyrite in the presence of 0 to 15% quartz were similar with an average

value of 0.018 h^{-1} (R^2 = 0.98). An analysis of variation was performed on this data and the results indicated that there was no significant difference between the free cell concentration data sets at these different solids loadings. In the presence of 21% quartz, the growth rate decreased to 0.011 h^{-1} (R^2 = 0.97). The microbial cell concentration was constant at 3% pyrite in the presence of 24% quartz.

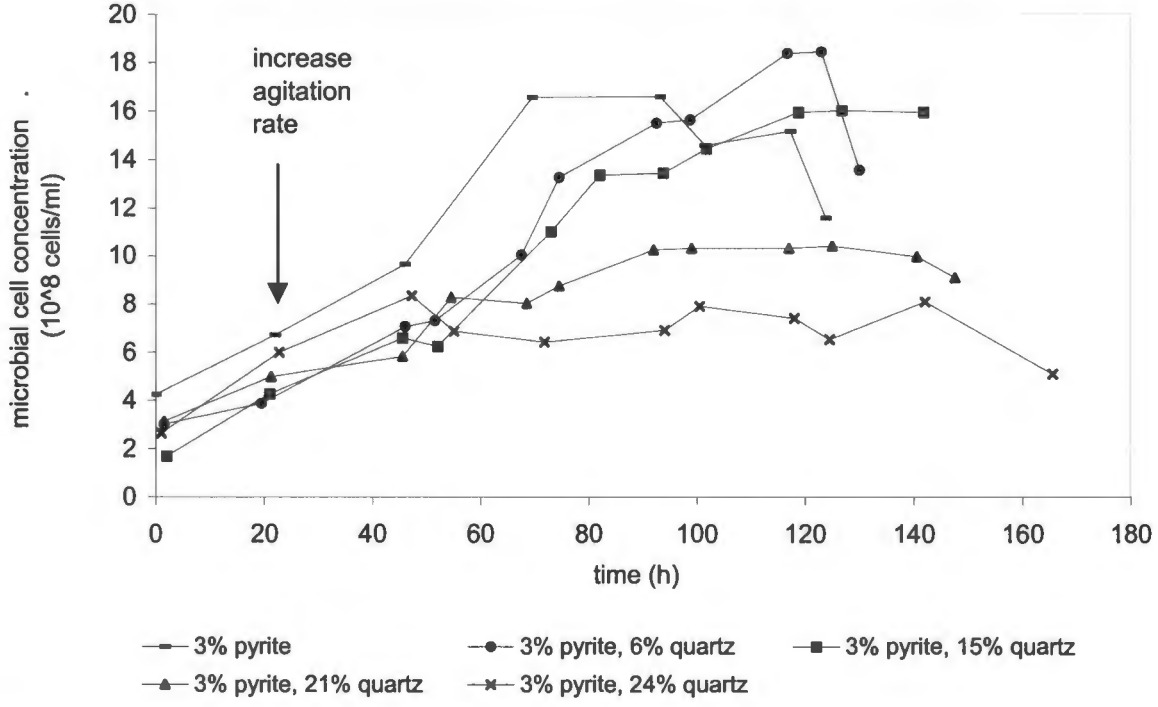

Figure 6.8: Microbial cell concentration profiles for various solids loading

Table 6.5: Microbial cell data for various solids loading

Solids Loading (w/v)	Specific Growth Rates (20-70 h) rate h^{-1}	R^2	Yield $_{X/Fe}$ 70 h 10^{14}cellskg^{-1}Fe	X_{max} 10^8cells ml^{-1}	Time at X_{max} h
3% pyrite	0.019	0.99	1.81	17	68
3%pyrite, 6% quartz	0.020	0.99	1.84	18	115
3%pyrite, 15% quartz	0.016	0.96	1.61	16	120
3%pyrite, 21% quartz	0.011	0.97	1.09	10	92
3%pyrite, 24% quartz	0	-	0.22	8	45

The yields in terms of microbial cells produced per kg iron oxidised between the increase of agitation speed and 70 hours is similar for 3% pyrite in the presence of 0 to 6% quartz at $1.8x10^{14}$ cells kg^{-1} Fe. The yield is slightly lower in the presence of 15% quartz with a value of $1.6x10^{14}$ cells kg^{-1} Fe, and decreases further to $1.1x10^{14}$ cells kg^{-1} Fe in the presence of 21% quartz. In the presence of 24% quartz, during which time a slight fluctuation in microbial cell concentration was observed, the yield was $0.22x10^{14}$ cells kg^{-1} Fe. Thus a decrease in yield was detected with an increase in solids loading, until a sharp decrease occurs in the presence of 24% quartz.

After 70 hours, the microbial cell concentration remained constant for a period of 50 hours in the case of 3% pyrite and increased for 50 hours each in the case of 3% pyrite in the presence of 6 and 15% quartz, and 20 hours in the presence of 21% quartz. The maximum microbial cell concentrations for each of the experiments across the solids loading range is approximately $17x10^{8}$ cells ml^{-1} for 3% pyrite in the presence of 0-15% quartz, $10x10^{8}$ cells ml^{-1} in the presence of 3% pyrite with 21% quartz and $8 x10^{8}$ cells ml^{-1} in the presence of 3% pyrite and 24% quartz.

The specific activity of the cells (rate of iron released per unit microbial cell number) from the increase of agitation rate (20 hours) to the end of the experiments was determined and is shown in Figure 6.9. The specific activity decreases during the period of exponential growth (20 to 70 hours) across all solids loading values except with 24% quartz. In the presence of 24% quartz a growth rate of zero was observed, the specific activity remained constant and was approximately equal to the lowest specific activity in any experiment. The specific activities in the 20 to 70 hour period in the presence of 6 and 15% quartz are the highest. In the presence of 21% quartz, the specific activity is reduced. After 70 hours, when the exponential growth phase has either reached a stationary phase in the case of 3% pyrite in the absence of quartz, or a lower growth rate in the case of 6, 15 and 21% quartz, the activities for each solids loading reached a constant value. These specific activities are very similar across all experiments.

Thus the exponential growth rates across the solids loading range were similar over the range of 0 to 15% quartz. A decrease in growth rate was observed in the presence of 21% quartz, while in the

presence of 24% quartz no growth rate was observed. The yields in the presence of 0 and 6% quartz were similar, and started to decrease in the presence of 15% quartz. A larger decrease was observed in the presence of 21% quartz, while in the presence of 24% quartz the yield decreased by a factor of 10. The activity of the cells decreased with time until 70 h. This 70 h period corresponded to the exponential growth phase. The solids loading using 24% quartz showed a constant specific activity that coincided with the zero growth rate of microbial cells. From 70 h onwards, the specific activities at the various solids loading levelled off and were similar across the range of solids loading.

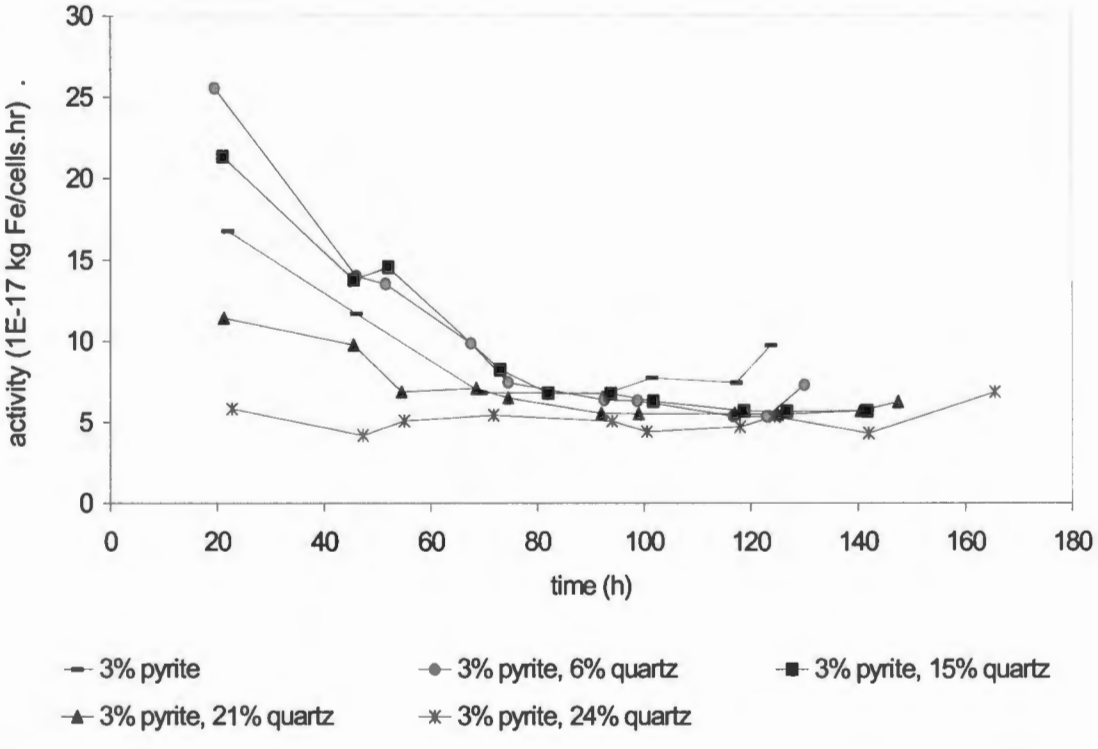

Figure 6.9: Microbial cell activity in terms of specific pyrite oxidation rate as a function of solids loading and duration of experiment

6.4.2.3. pH and Redox Potential

The pH profiles of the bioleach experiments, depicted in Figure 6.10, are similar across the range of solids loading investigated. The pH decreases gradually with time from approximately 1.6 to

0.8. This suggests that the stress caused by the higher solids loading, observed in terms of the iron release, is not reflected in the pH values.

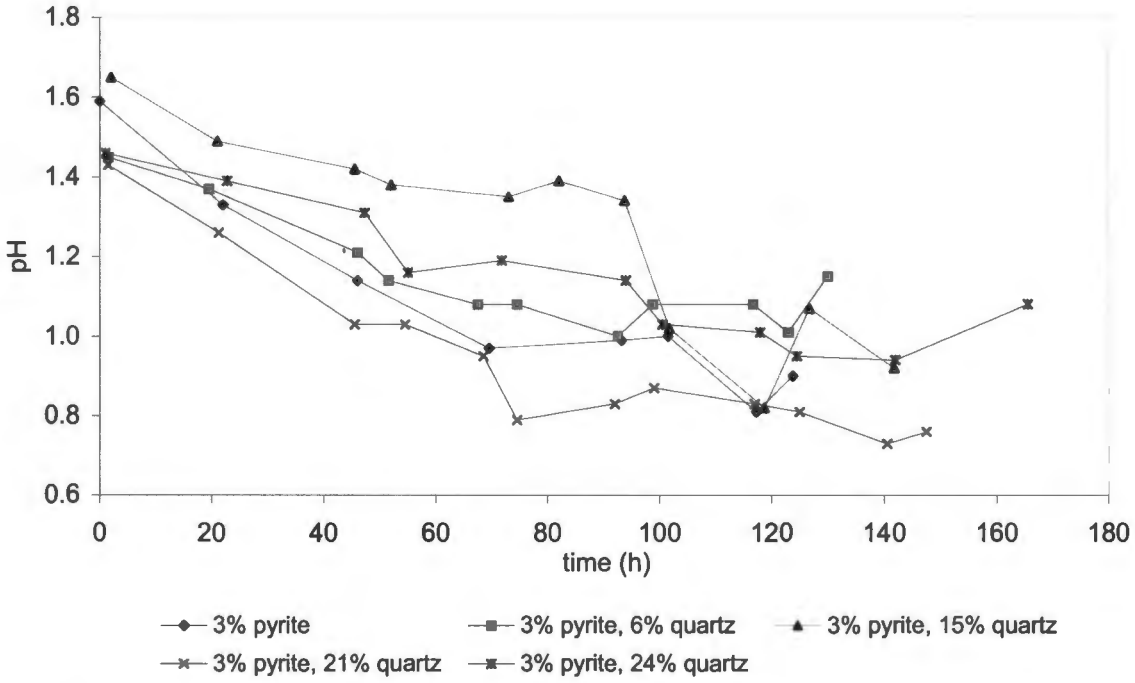

Figure 6.10: pH profiles for various solids loading

The profiles of redox potential increased from an initial range of 470 to 500 mV to a final range of 550 to 650 mV. The redox potential profiles, depicted in Figure 6.11, were similar for the solids loading of 3% pyrite in the presence of 0, 6 and 15% quartz, with the maximum redox potential observed being 650 mV. An increase of solids loading to 21% quartz, resulted in a decrease of the maximum redox potential to 600 mV. In the presence of 24% quartz, the maximum redox potential decreased further to 550 mV. As the redox potential gives an indication of the ferric to ferrous iron ratio (according to the Nernst equation), a lower redox potential suggests a lower ferric iron concentration as compared to the ferrous iron concentration. The indirect bioleaching mechanism proposes that the ferric iron attacks the mineral sulphide releasing ferrous iron, while the microorganisms convert the ferrous iron generated to ferric iron. In the experiments with low solids loading, the redox potentials were high, implying that the microorganisms were efficient in

converting the ferrous iron to ferric iron. At the higher solids loading, the redox potential decreased, suggesting that the ferric iron decreased, the ferrous iron increased, or both occurred. As a decrease in total iron released is observed with increasing solids loading, bioleaching must be decreasing with increasing solids loading. Thus the ferrous iron concentration released is expected to decrease. The results showed that the ferrous iron concentration remained the same, implying that the microorganisms were efficiently converting the ferrous iron present to ferric iron. This is confirmed by the fact that the activity across the solids loading range is similar from 70 hours onwards (period of stationary phase for the microorganisms). The ferric iron concentration must therefore have decreased. This is as expected since the ferrous iron being released from the oxidised pyrite decreased. Thus the decrease of redox potential with increasing solids loading was due to the decreased ferrous iron released from the reduction in pyrite oxidation.

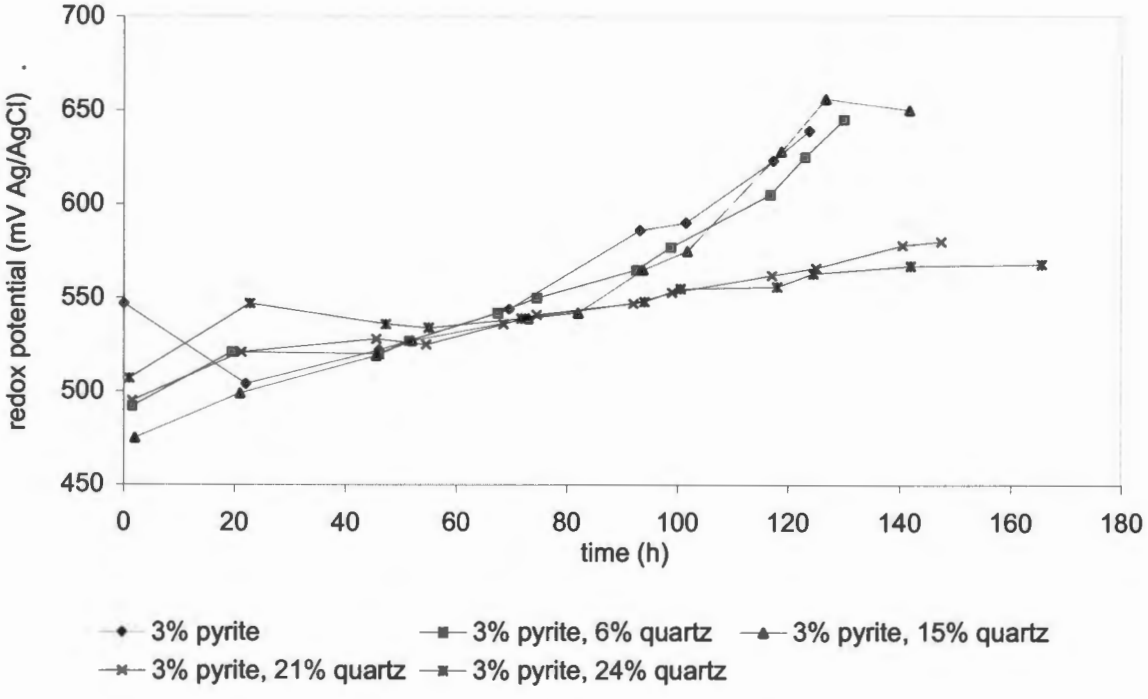

Figure 6.11: Redox potential profiles for various solids loading

6.4.3. Comparison of Current Research with Literature

In this study, the work of Nemati and Harrison (2000) is extended by using a small fixed quantity of leachable pyrite and varying the inert quartz content to vary the solids loading. The implications of the extension to the current system, compared to that of Nemati and Harrison, is that:

i. Variation in physicochemical conditions owing to the release of inhibitory metal and sulphate ions, as well as variation in pH and redox potential, is minimised by the presence of a constant leachable mineral phase while varying solids loading.
ii. The density of the quartz is less than that of pyrite.

The system used in Nemati and Harrison's study differed from that used in this work in the following ways:

i. The solids loading comprised pyrite only.
ii. The inoculum was prepared in a shake flask rather than the stirred tank reactor used in this study.
iii. No baffles were used in Nemati and Harrison's reactor, thus the mass transfer conditions may have been different.

The mass transfer coefficient, k_La, was measured with growth media and 3% pyrite in the experimental apparatus of Nemati and Harrison and the experimental apparatus used in the current system. It was found that the value for k_La at 20°C in the previous study was $1.4x10^{-3}$ s^{-1} ($\sigma = 0$) while that in the current study was $2.0x10^{-3}$ s^{-1} ($\sigma = 8.9e\text{-}5$). Thus the mass transfer conditions in the current set-up were better than those in the previous work.

The results from Nemati and Harrison's work indicated that an increase in solids loading above 12% resulted in a decrease in bioleach performance in terms of iron release. At 18% (w/v) pyrite, the system failed and no bioleaching was observed. To facilitate comparison between the study reported here and the work of Nemati and Harrison, an experiment using 18% (w/v) pyrite was performed in the current system. The inoculum state and mass transfer differed as discussed previously and quantified in Section 6.4.3.4. A comparison of these results at 18% pyrite is given

in Section 6.4.3.2. This is preceded by a comparison of the two systems using 3% pyrite to give an indication of the difference in performance when the system is not stressed.

A comparison of the 18% (w/v) pyrite system and 18% (w/v) pyrite/silica system is described in Section 6.4.3.3. These experiments were performed in the current study using the same experimental system. The apparatus for mass transfer is similar, although the actual mass transfer conditions may be different due to the difference in solids loading material.

6.4.3.1. Bioleaching Performance at a Solids Loading of 3% (w/v) Pyrite: Comparison with Nemati and Harrison (2000)

The extent and rates of bioleaching for the 3% pyrite systems in the current work and those reported by Nemati and Harrison are similar. The iron release and microbial cell concentration profiles are shown in Figure 6.12. The key parameters of these experiments are tabulated in Table 6.6. The extent and rate of bioleaching reported by Nemati and Harrison were 100% and 0.098 kg m^{-3} ($R^2 = 0.99$) respectively, while those determined for the current work was 91% and 0.12 kg m^{-3} ($R^2 = 1.0$). The results indicate that a greater extent of bioleaching although at a slower rate was observed in the work done by Nemati and Harrison (2000) than in the current work. The initial lower cell number in Nemati and Harrison's work could account for the slower leaching rate.

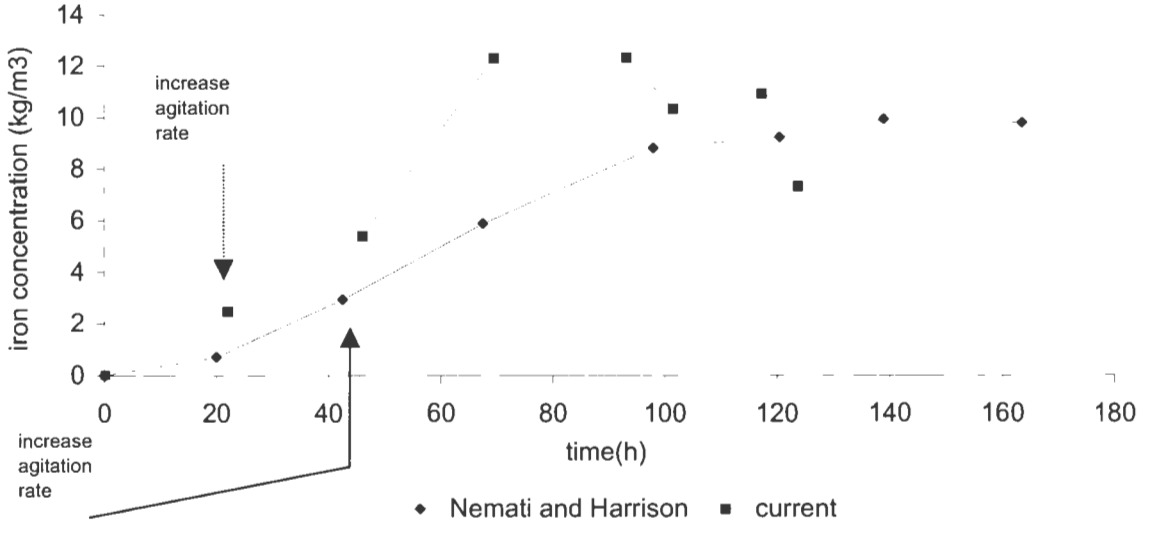

Figure 6.12 (a): Comparison of iron release profiles for 3% pyrite reported by Nemati and Harrison (2000) and in the current system

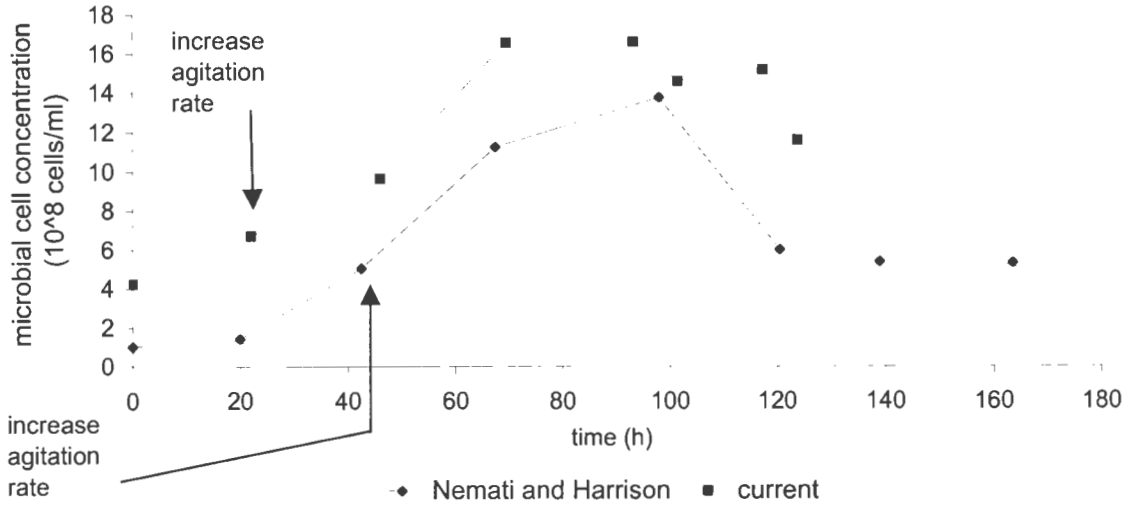

Figure 6.12 (b): Comparison of microbial cell concentration profiles for 3% pyrite reported by Nemati and Harrison (2000) and in the current system

Table 6.6: Comparison of bioleaching performance of Nemati and Harrison (2000) and the current work

Parameter	Nemati and Harrison	Current Work
Initial microbial cell concentration (cells ml^{-1})	$1x10^8$	$3x10^8$
Time at 285 rpm (h)	40	23
Microbial cell concentration at increase of agitation (cells ml^{-1})	$5x10^8$	$6x10^8$
Specific growth rate at 285 rpm (h^{-1})	0.04	0.03
Specific growth rate at 560 rpm (h^{-1})	0.009	0.02
Iron release rate at 560 rpm (kg Fe m^{-3} h^{-1})	0.098	0.12
Time at 560 rpm (h)	110	95
Maximum iron released (kg Fe m^{-3})	12.5	11.4
Maximum microbial cell concentration (cells ml^{-1})	$14x10^8$	$17x10^8$
Percentage Iron released (%)	100	91

Thus for the conditions imposing little or no stress on the experiments, the two systems perform similarly. The smaller inoculum prepared in shake flask culture used in the work of Nemati and Harrison took a longer time to increase the cell number, while that in the current work increased cell number rapidly.

6.4.3.2. Bioleaching Performance at a Solids Loading of 18% (w/v) Pyrite: Comparison with Nemati and Harrison (2000)

The iron release and microbial cell concentration profiles for the 18% pyrite experiments of Nemati and Harrison and from the current work are shown in Figure 6.13. The microbial cell concentration on inoculation of the 18% pyrite experiment conducted in this study was $3.3x10^8$ cells ml^{-1}. This concentration increased to $4.2x10^8$ cells ml^{-1} in the first 22 hours at an agitation speed of 285 rpm. The iron release during this period was 1.1 kg m^{-3}. On increase of agitation rate to 560 rpm, the microbial cell concentration decreased to $1.8x10^8$ cells ml^{-1} while the concentration of iron released increased to 2.8 kg m^{-3}. The iron release rate was constant from incubation at the agitation speed of 285 rpm until 24 hours after the speed was increased at a value of 0.055 kg m^{-3} h^{-1}(R^2 = 1.0). This rate was maintained even though the microbial cell concentration decreased. The microbial cell concentration continued to decrease throughout the remainder of the experiment (93 hours in total) at a cell death rate of 0.036 h^{-1} (R_2 = 1.0). Inspection of the cells under a microscope revealed a decrease in cell size over the course of the experiment. The total iron concentration in the supernatant and precipitate remained constant indicating that no further pyrite was dissolved. The extent of bioleaching was 22%. The pH decreased gradually from 1.6 to 1.2, while the redox potential decreased from 516 to 412 mV.

In the 18% (w/v) pyrite experiment performed by Nemati and Harrison (2000), the initial microbial cell concentration decreased from $3.0x10^7$ cells ml^{-1} to $2.0x10^6$ cells ml^{-1}, and after 5 days of operation, 150 cm^3 of reaction liquid was replaced with the same volume of inoculum. The addition of inoculum led to an increase in the microbial cell concentration and an exponential growth phase after 24 hours. The concentration of iron release before the agitation rate was increased was 5.6 kg m^{-3} (310 hours). When the microbial cell concentration reached $3.5x10^8$ cells ml^{-1}, the agitation speed was increased to 500 rpm to fully suspend the solid particles. This led to a decrease in microbial cell concentration to $7.5x10^7$ cells ml^{-1}. The cell death rate was 0.0075 h^{-1} (R^2=0.99). Examination of the samples under a microscope revealed smaller cells than noted earlier in the experiment. The experiment was continued for 10 days (520 hours total experiment time). The total iron concentration in supernatant and precipitate did not change from the time the speed was increased to the end of the experiment. The extent of bioleaching was 11%. The pH decreased

from 2.0 to 1.3. The redox potential decreased from 400 to 355 mV, increased to 450 mV with the cells in exponential growth phase, and decreased to 410 mV when the microbial cell concentration decreased.

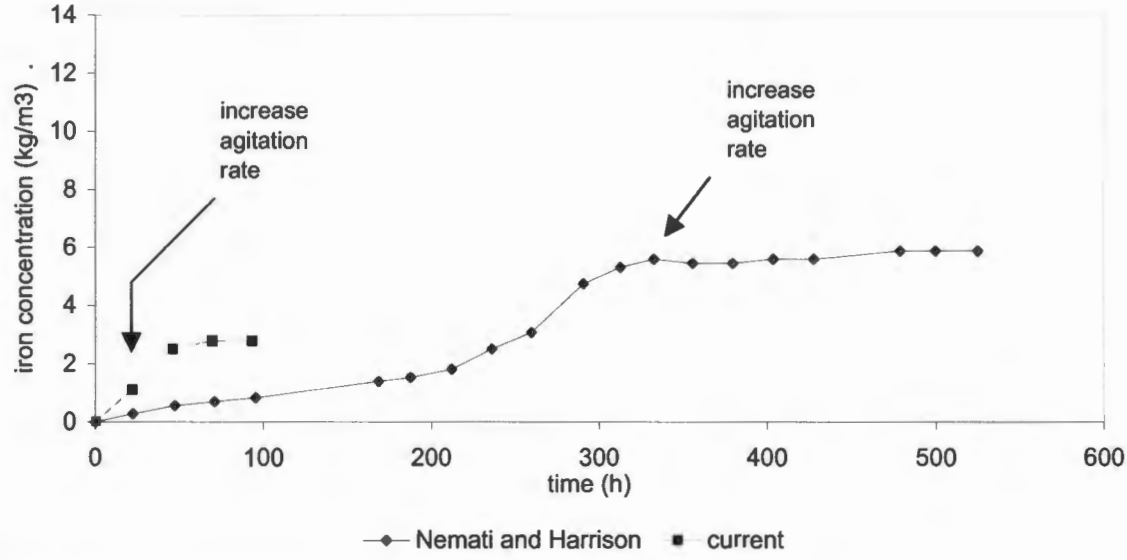

Figure 6.13: Comparison of iron release profiles for 18% pyrite from the literature and in the current system

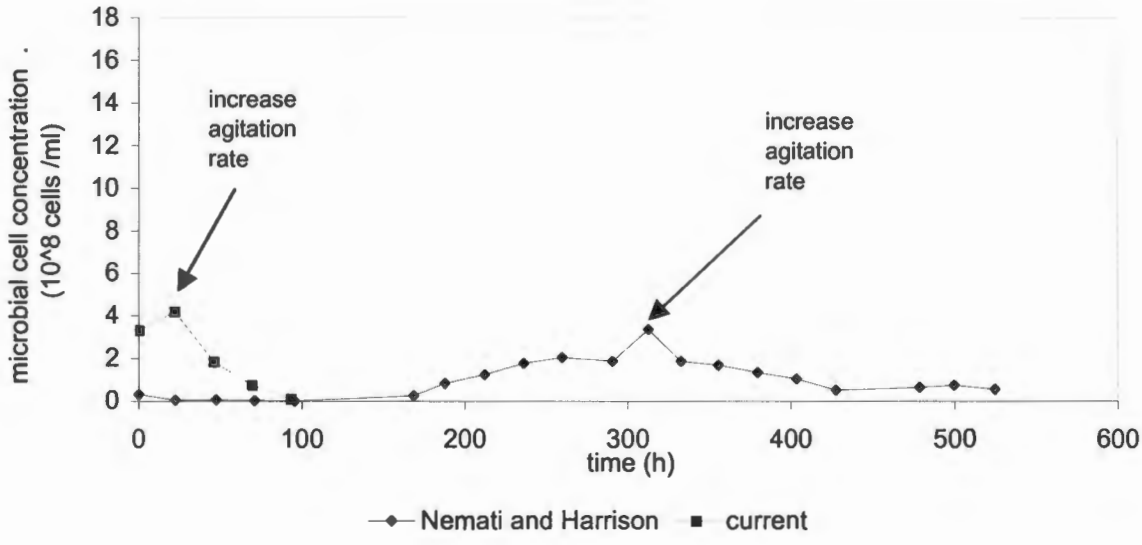

Figure 6.13 (b): Comparison of microbial cell concentration profiles for 18% pyrite from the literature and in the current system

It is clear from these results that both systems failed at a solids loading of 18% pyrite (w/v). The higher cell concentration in the more active inoculum and increased mass transfer in the current work resulted in a higher biomass concentration in a shorter period of time under conditions of incomplete suspension (N = 285 rpm). Pyrite dissolution occurred in the first 24 hours after the agitation speed had been increased. No bioleaching was observed by Nemati and Harrison after the agitation speed had been increased. The biomass concentration for both systems decreased rapidly after the agitation speed was increased. The specific cell death rates for the current work and that of Nemati and Harrison were 0.036 h^{-1} ($R^2 = 1.0$) and 0.0075 h^{-1} ($R^2 = 0.99$), respectively.

6.4.3.3. Comparison of the Bioleaching Performance using Pyrite only and a Pyrite/quartz system at 18% Solids Loading: Current Study

The iron release and biomass concentration profiles for both the 18% (w/v) pyrite and 3% (w/v) pyrite/ 15% (w/v) quartz systems are depicted in Figure 6.14. The initial cell concentration for pyrite with 15% quartz system was $1.7x10^8$ cells ml^{-1} while that for 18% pyrite was $3.3x10^8$ cells ml^{-1}. The growth rates of the cells in the first 22 hours of the experiments (285 rpm) was 0.049 h^{-1} ($R^2 = 1.0$) for the pyrite/quartz system and 0.011 h^{-1} ($R^2 = 1.0$) in the pyrite system. The cell concentration in each of the experiments at 22 hours was $4.2x10^8$ cells ml^{-1}. The concentration of iron released in this period is similar in both systems, with 0.8 kg m^{-3} in the pyrite/quartz system and 1.1 kg m^{-3} in the pyrite system.

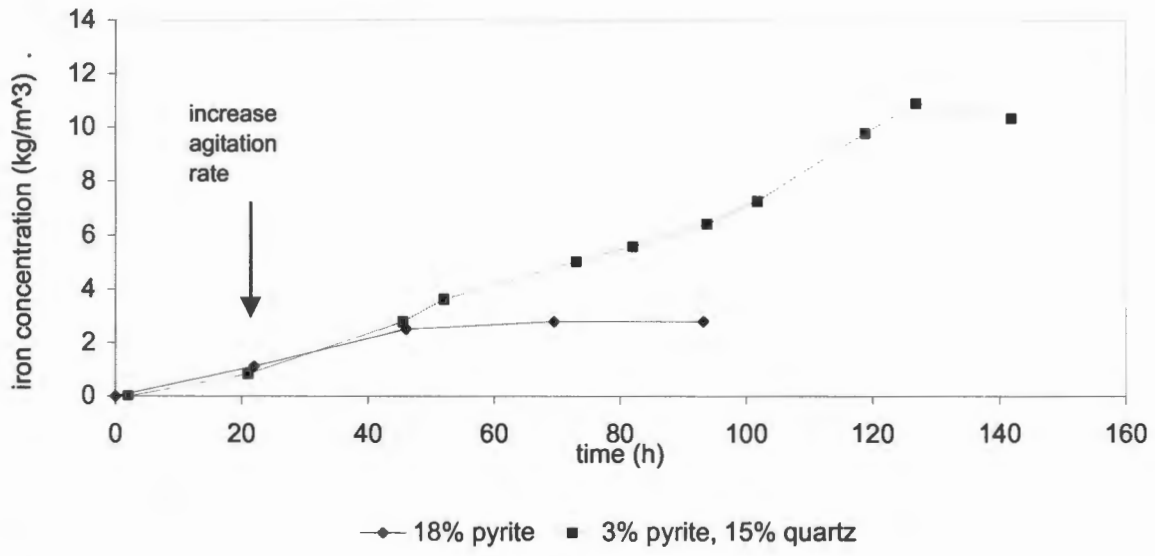

Figure 6.14(a): Comparison of iron release profiles for 18% pyrite and pyrite/quartz from the current system

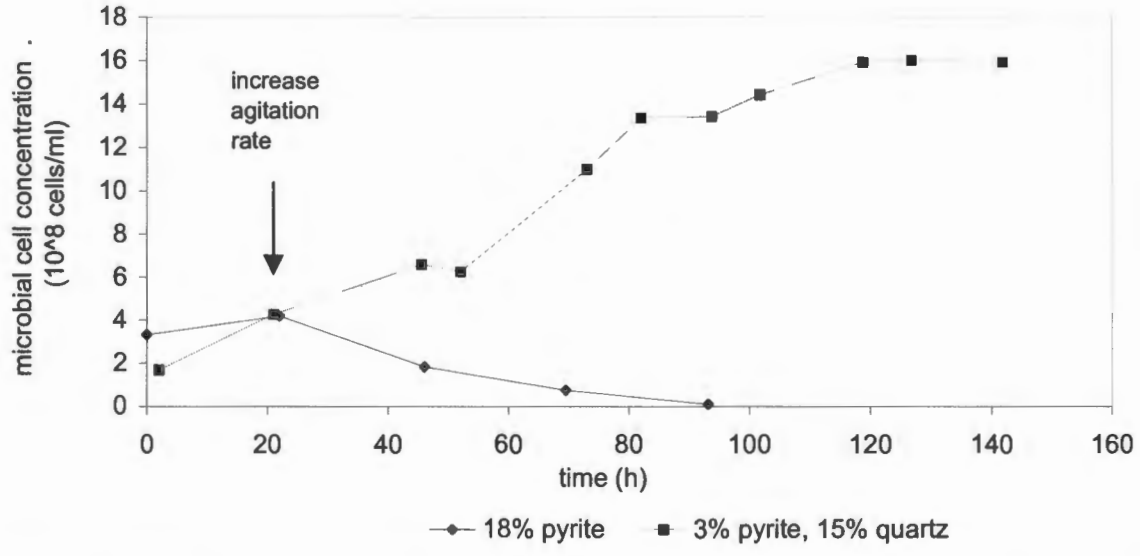

Figure 6.14(b): Comparison of microbial cell concentration profiles for 18% pyrite and pyrite/quartz from the current system

The cell concentration after the agitation rate was elevated to 560 rpm increased at a rate of 0.016 h^{-1} for the pyrite/quartz system for 118 hours to a maximum cell concentration of $16x10^8$ cells ml^{-1}. For the pyrite system, the cell concentration decreased after the speed was increased. Inspection of

these cells under the microscope revealed that the cells were much smaller than those observed with the pyrite/quartz system. The cell concentration continued to decrease at a rate of 0.0075 h^{-1} to a concentration of less than $6.6x10^7$ cells ml^{-1} 94 hours after the start of the experiment. The bioleach rate for the pyrite/silica system remained constant at 0.092 kg Fe m^{-3} h^{-1} throughout the experiment. The extent of pyrite solubilisation was 86%. The pyrite system leached for 24 hours after the speed had been increased at a rate of 0.058 kg Fe m^{-3} h^{-1}, after which leaching ceased. The extent of pyrite solubilisation was 22%. These results are shown in Table 6.7.

Table 6.7: Comparison of bioleach performance using 18% pyrite only and 3% pyrite with 15% quartz

Solids Loading	**Initial X** cells/ml	**Initial μ** h^{-1}	**X at ↑ of N** cells/ml	**[Fe] at ↑ of N** kg m^{-3}	**μ after ↑ of N** h^{-1}	**Time of X ↑** h	**Final X** cells/ml	**Leach Rate** $kgm^{-3}h^{-1}$	**Extent of Fe solubilisation** %
3% pyrite, 15%quartz	$1.7x10^8$	0.049	$4.2x10^8$	0.8	0.016	118	$16x10^8$	0.092	86
18% pyrite	$3.3x10^8$	0.011	$4.2x10^8$	1.1	-0.0075	0	$0.66x10^8$	0.058	22

X is the cell concentration
μ is the cell growth rate
N is the agitation rate (rpm)

The use of quartz in place of pyrite to vary the solids loading in the pyrite/quartz systems minimises potential variation of the physicochemical conditions in the reactor as less metal and sulphate ions are released. In addition, the variation in pH and redox potential is minimised. The maximum iron concentration attained in the pyrite/quartz system was 10.9 kg m^{-3}, while that in the pyrite system was 2.5 kg m^{-3}. The higher iron concentration in the pyrite/quartz system was due to the higher bioleaching that occured in the pyrite/quartz system. The pyrite system failed before a substantial iron concentration had been released. The corresponding pH in the pyrite system exhibited a minimum of 1.2, while that in the pyrite/quartz system decreased as low as 0.8 whilst bioleaching still occurred. The redox potential decreased from 516 to 412 mV in the pyrite system, whereas the redox increased from 475 to 650 mV in the pyrite/quartz system. The variations in the physicochemical conditions are not a dominant factor in the performance between the pyrite and pyrite/quartz systems as the iron concentration in the pyrite system was low and the low pH observed in the pyrite/quartz system did not cease bioleaching. The decrease of redox potential in

the pyrite system illustrated the inability of the microorganisms to convert ferrous iron to ferric iron.

Since the pyrite is denser than the quartz (specific gravity of 5.0 compared with 2.6 kg m^{-3}), the solids loading on a volume fraction basis corresponding to the weight percentage of 18% is less for the pyrite system than the pyrite/silica system. The volumetric loading for the 18% (w/v) pyrite is 3.6% (v/v), while that for the 3% pyrite and 15% quartz (w/v) is 6.4% (v/v). As the size of the particles is the same, a larger volume percentage leads to a larger quantity of particles. If cell damage is a function of the frequency of collisions between particles and cells, the larger solids loading on a volume basis is expected to increase cell damage and thus decrease bioleaching. The pyrite/quartz system, however, exhibits better bioleaching performance than the pyrite system despite the higher volume percentage of solids. This suggests that the frequency of collisions between particles and cells is not the dominant factor controlling cell damage under the conditions of these experiments.

The difference in densities of the pyrite and silica will also affect the momentum of the particles, and thus the collision momentum between the particles and the cells. The momentum is a function of particle size, particle density and the agitation speed, and is calculated as the product of the particle mass and the impeller tip speed. Since the particle sizes and agitation speeds are similar for the two systems, the momentum will vary with particle density. The system consisting of pyrite only will therefore have a higher particle momentum, and this will lead to microorganism-particle collisions with higher momentum. This higher particle collision momentum may be a contributing factor in the failure of the pyrite only bioleach system. The pyrite/quartz system which has a lower particle collision momentum does not fail. Harrison *et al.* (2002) have previously illustrated the importance of collision momentum on cell damage in a yeast slurry bioreactor system.

Measurement of the mass transfer coefficients in the pyrite and pyrite/quartz systems revealed that the former system had a mass transfer coefficient of 8.0×10^{-3} s^{-1} while the latter was 4.0×10^{-3} s^{-1} (measured at 67°C for a baffled system). The oxygen demand for the pyrite system is higher than that for the pyrite/quartz system (1 kg of oxygen is required to oxidise 1 kg of pyrite). The higher mass transfer coefficient of the pyrite system may be adequate to meet the higher oxygen demand

of the pyrite system. However, the limited mass transfer work performed in this study is not conclusive as to the oxygen limitations.

6.4.3.4. Comparison of Bioleach Performance at Various Solids Loadings for Pyrite and Pyrite/quartz system

The bioleach performance for the pyrite and pyrite/quartz system at various solids loading is shown in Figure 6.15. As described previously, the systems perform similarly at 3% pyrite where there is little stress on the microorganisms. The pyrite system fails at 18% solids loading, while the pyrite/quartz system still exhibits bioleaching at 3% pyrite in the presence of 24% quartz while failing at 3% pyrite in the presence of 27% quartz. The differences in the two systems include:

- Physicochemical differences in terms of toxicity, pH and redox potential due to the use of an inert material to make up solids loading.
- Density differences between the pyrite and pyrite/silica system due to the different density of quartz as compared to pyrite. This affects the volume fraction of solids present and the particle momentum.
- Mass transfer differences from the conditions of the experiments and the different materials used.
- State of the inoculum. The pyrite system used an inoculum grown in a shake flask, while the inoculum used in the pyrite/quartz system was grown in a stirred tank reactor and thus had a higher cell count and was better accustomed to the conditions imposed by the stirred tank reactors used in both experiments.

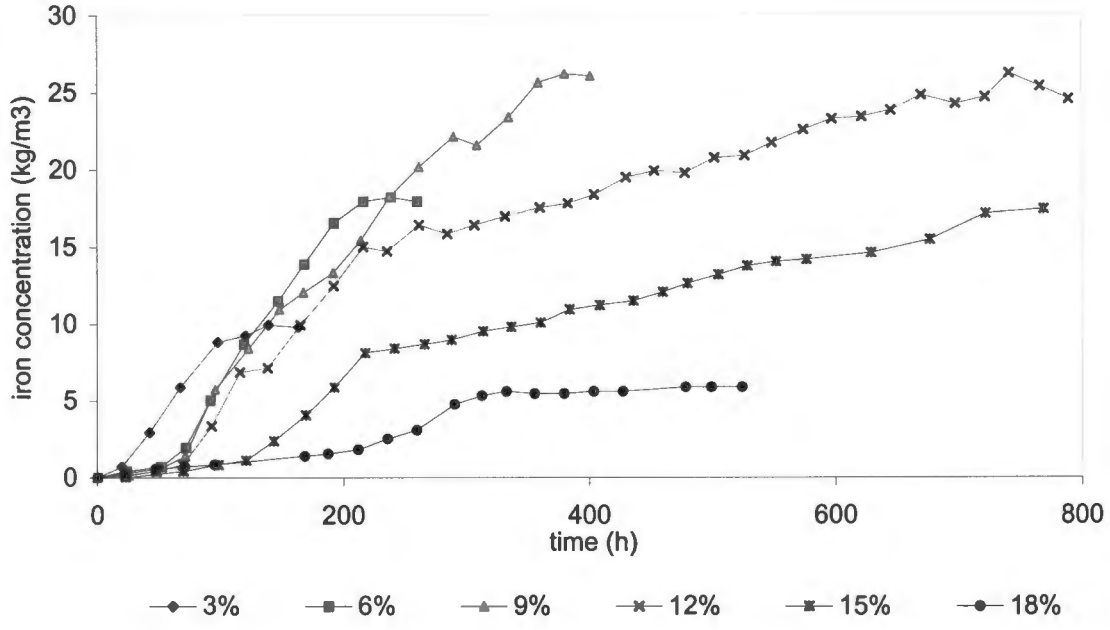

Figure 6.15(a): Bioleaching performance as a function of solids loading - pyrite system with respective solids loading of pyrite

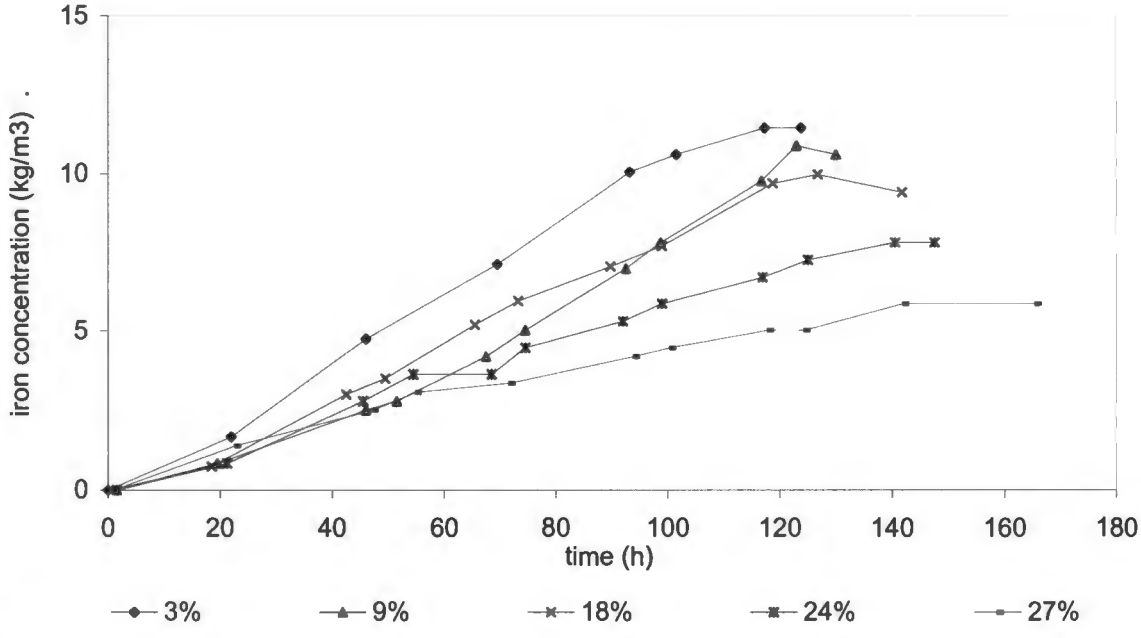

Figure 6.15(b): Bioleaching performance as a function of solids loading - pyrite/quartz system with 3% pyrite in the presence of the respective amounts of quartz

In the pyrite system, the agitation rate was increased once the biomass had achieved exponential growth rate and the microbial cell concentration was approximately 3-4x10^8 cells ml^{-1}. The lag phase of the biomass increased with increasing solids loading. In the pyrite/silica system, as no lag phase was observed, the agitation rate was increased when the microbial cell concentration reached 4-7x10^8 cells ml^{-1}. This occurred after approximately 24 hours for each of the solids loading.

The mass transfer conditions and the state of the inoculum did not alter the bioleach performance at low solids loading (3% w/v). At higher solids loading when the bioleaching system is under greater stress, inhibition limitations and density differences of the two systems may be of greater significance.

The higher pyrite quantity in the pyrite system, resulted in higher iron concentrations due to the larger quantity of pyrite dissolved, and lower pH values. At 9, 12 and 15% pyrite, the concentration of dissolved iron was approximately 27 kg m^{-3} in each of the reactors at the end of the experiment. The extent of pyrite solubilisation at each solids loading is 88, 88 and 70%, respectively. For the pyrite/quartz system, the quantity of pyrite is constant at 3% yielding a maximum iron concentration in solution of 11 kg m^{-3}. The pH of the 9, 12 and 15% pyrite experiments decreased as low as 0.6, while the values in the pyrite/quartz system only decreased to 0.8. Thus the inhibitory environment at higher solids loading was higher in the pyrite system, with a potential adverse effect on the cells. At 18% pyrite where the system failed completely, the iron concentration in solution was 6 kg m^{-3} and the pH value decreased to 1.3. This suggests that some other factor besides higher iron concentration and lower pH values, is prevalent in affecting the bioleach performance as only a small quantity of pyrite is dissolved at this solids loading, resulting in a low iron concentration and the corresponding pH is relatively high.

The different density of the pyrite and quartz affected the volume fraction of solids present, as mentioned previously. The system consisting of pyrite only failed at a solids loading of 18% (w/v) that corresponded to a volumetric loading of 3.6%. The pyrite/quartz system still exhibited bioleaching at 3% pyrite in the presence of 24% quartz (w/v), which corresponded to a volumetric

loading of 9.9%. Since the particles are of similar size, the higher volume percentage corresponds to a larger quantity of particles. If cell damage is caused predominantly by the collisions between cells and particles, severe damage and little bioleaching would be observed in systems with higher quantities of particles. However, bioleaching is observed at volume percentages of 9.9% pyrite/quartz, while 3.6% (v/v) pyrite exhibits no bioleaching. This indicates that cell damage due to the frequency of collisions between cells and particles is not the dominant factor in the bioleaching performance of these systems.

A difference in particle momentum also results from the difference in density of the pyrite and quartz. The momentum of the d_{50} particles throughout the pyrite experiments is 3.21×10^{-9} kg m s^{-1}, while that of the quartz particles at d_{50} is 4.20×10^{-10} kg m s^{-1}. The range of particle sizes in both the pyrite and pyrite/quartz system did result in a large range of particle momentum across each experiment, the range of momentum being larger than that across the different experiments. The range of particle momentum was higher for the pyrite system than the pyrite/silica system, however. The higher particle collision momentum could therefore be responsible for the pyrite system failing at a lower solids loading than the pyrite/quartz system. Although the latter had more frequent collisions, the particle collision momentum was lower. There may be a critical particle momentum for damaging collisions.

Differences in mass transfer could cause the different performance of the two systems. The unbaffled reactors used in the pyrite system resulted in different mass transfer conditions. A volumetric mass transfer coefficient, k_La, of 1.4×10^{-3} s^{-1} ($\sigma = 0$) was determined for the unbaffled system and 2.0×10^{-3} s^{-1} ($\sigma = 8.9 \times 10^{-5}$) in the current baffled system at 3% solids loading and 20°C. At low solids loading, this difference did not affect the bioleaching performance, as discussed in Section 6.4.3.1. At higher solids loading, the difference in conditions may be more significant as the maximum oxygen demand of the pyrite system increases with increasing solids loading, while the maximum oxygen demand remains constant in the pyrite/quartz system due to the constant pyrite concentration throughout the solids loading. The oxygen transfer potential, which is affected by the mass transfer coefficient (k_La), the saturated dissolved oxygen concentration and the critical dissolved oxygen concentration, is only affected by the k_La value as the saturated and critical dissolved oxygen concentrations are both similar in these systems. The k_La values measured are

similar across the solids loading range of the pyrite/quartz system (Table 6.8). The oxygen transfer potential for the unbaffled pyrite system is therefore lower than that for the pyrite/quartz system at low solids loading. The increase in oxygen demand with solids loading in the pyrite system, while the oxygen transfer potential remains constant, could lead to the oxygen demand being greater than the oxygen transfer potential, and thus a limitation in oxygen that affects the bioleaching.

The inoculum used in the pyrite system was maintained in a shake flask on a rotary shaker, whereas that used in the pyrite/quartz system was maintained in a stirred tank reactor. The implications of the states of the different inoculum on the bioleaching performance is discussed in Section 6.8.

6.4.4. Concluding Remarks

While the performance of the bioleach system is similar at low solids concentration in the presence of either pyrite only or pyrite and quartz, at high solids concentration performance in the presence of 3% pyrite and quartz was better than at an equivalent high solids loading generated by pyrite only (Nemati and Harrison, 2000). Further differences in the systems include:

- chemical differences in terms of metal and sulphate ions in solution, ionic strength, pH and redox potential;
- density differences between the pyrite and quartz that affect the volume fraction present and the particle momentum;
- mass transfer differences generated from the experimental set-up and the different materials used; and
- the state of the inoculum.

Analysis of these differences showed that the physicochemical differences were not a contributing factor to the lower performance at high solids loading in the pyrite system. At 18% (w/v) pyrite, the system failed at low iron concentration and relatively high pH, indicating that some other factor had caused the system failure.

The density difference between the pyrite and quartz results in a higher volume percentage of silica present for a given weight percentage and a greater frequency of collisions in the pyrite/quartz system than in the pyrite system at a particular solids loading. The frequency of collisions, however, is not a dominant factor in the bioleach performance. The density also affects the particle momentum in the different systems. The particle momentum in the pyrite system is greater than that in the pyrite/quartz system. The higher particle collision momentum, although with lower frequency of collisions, may be responsible for the failure of the pyrite system at a lower solids loading than the pyrite/quartz system that has a higher frequency of collisions but at lower particle momentum. Particle momentum has been seen to influence yeast cell damage (Harrison *et al.*, 2002).

The oxygen demand in the pyrite system is higher than that in the pyrite/quartz system. The mass transfer coefficient for the pyrite system is higher than that for the pyrite/quartz system, but it is inconclusive from this study as to whether the higher mass transfer coefficient in the pyrite system is adequate to cope with the higher oxygen demand of that system. Mass transfer differences in the two systems can therefore not be deduced as a reason for the different bioleaching performances of the two systems.

6.5. THE EFFECT OF OXYGEN AND CARBON DIOXIDE SUPPLY

6.5.1. Gas Liquid Mass Transfer in the Slurry System

The effect of pulp density on bioleaching kinetics may be reflected by its effect on gas-liquid mass transfer, thereby restricting the supply of oxygen and carbon dioxide to the microorganisms. If oxygen limitation is a factor in the system, the oxygen demand will be greater than the oxygen transfer potential. As the pyrite concentration is constant throughout the range of solids loadings investigated, the oxygen demand in terms of pyrite solubilisation remains unchanged. The oxygen transfer potential is dependent on the mass transfer coefficient and the maximum possible driving force of the dissolved oxygen (difference between saturated dissolved oxygen concentration and

critical dissolved oxygen concentration). The saturated dissolved oxygen concentration is dependent on the oxygen concentration in the gas sparged (air) and on the operating temperature and pressure in the reactor. The critical dissolved oxygen concentration is dependent on the microorganisms present. Both the saturated and critical dissolved oxygen concentrations are therefore similar across the range of solids loading tested. Thus the oxygen transfer potential in this system is solely dependent on the mass transfer coefficient. To quantify this effect, the mass transfer coefficient, k_La, for oxygen transfer were determined using a dynamic method at the various pulp densities. The mixture was sparged with nitrogen to remove all dissolved oxygen, and then sparged with air at 2 l min^{-1} while measuring the dissolved oxygen concentration. These measurements were performed at ± 67°C.

The mass transfer coefficients measured at the various solids loading are shown in Table 6.8. The mass transfer coefficients determined across the solids loading range of 0 to 24% (w/v) quartz in the presence of 3% pyrite are similar, ranging from $7.3x10^{-3}$ to $4.0x10^{-3}$ s^{-1}. While the magnitude of the variation exceeds the standard deviations of measurement found, no clear trend in mass transfer coefficient as a function of solids loading was found, the minimum k_La being found in the silica loading range of 6 to 18%. Hence variation in mass transfer does not correlate to reduced leaching performance in the presence of increasing solids loading. Both the oxygen demand and the oxygen transfer potential are similar over the range of solids loading investigated, and thus oxygen limitation is not a factor affecting bioleaching over the range of solids loading in this system.

Table 6.8: Mass transfer coefficient measurements at various solids loading

Solids Loading	**k_La (10^{-3}) s^{-1}**	**Standard deviation**
3% pyrite	7.3	$1.2x10^{-4}$
3% pyrite, 3% quartz	6.7	$1.2x10^{-4}$
3% pyrite, 6% quartz	4.0	0
3% pyrite, 15% quartz	4.0	0
3% pyrite, 18% quartz	4.0	$2.0x10^{-4}$
3% pyrite, 21% quartz	6.0	0
3% pyrite, 24% quartz	6.0	0

6.5.2. The Effect of Carbon Dioxide Limitation

The effect of carbon dioxide limitation on the bioleach performance was investigated by carrying out bioleach experiments with and without the addition of 1% CO_2 to the air supply. The limitation of CO_2 to the system may be a hindrance to the physiological status of the microbes. The solids loadings used in the experiments were 3% pyrite in the presence of 0 and 18-24% quartz. The bioleach performance in terms of iron release, the microbial cell growth, pH and redox potential were measured throughout the experiments.

Growth and bioleach profiles as a function of time in the presence of CO_2 enrichment and on sparging with air are compared in Figure 6.16 (data in Appendix C). The percentage depression for the iron release and microbial cell concentration for the experiments in the absence of CO_2 relative to those with CO_2 enrichment is summarized in Table 6.9. The results indicate that both the bioleach performance and microbial cell growth were similar for the experiments with and without CO_2 at solids loading of 3% pyrite in the presence of 0 and 18% quartz. This suggests that CO_2 is not limiting at these solids loadings. At solids loading of 3% pyrite in the presence of 21% quartz, the percentage depression of the iron release with respect to that in the presence of 1% CO_2 in the absence of CO_2 is 18%. The iron release rate at this solids loading in the absence of CO_2 is depressed by 32%. The maximum microbial cell concentration is depressed by 31%. CO_2 is thus becoming limiting at this solids loading. Using a solids loading of 3% pyrite in the presence 24% quartz, the percentage depression for the experiments without CO_2 addition is 51% for the concentration of iron released and 71% for the maximum microbial cell concentration. The depression in the iron release rate in the absence of CO_2 is 49% in the presence of 24% quartz.

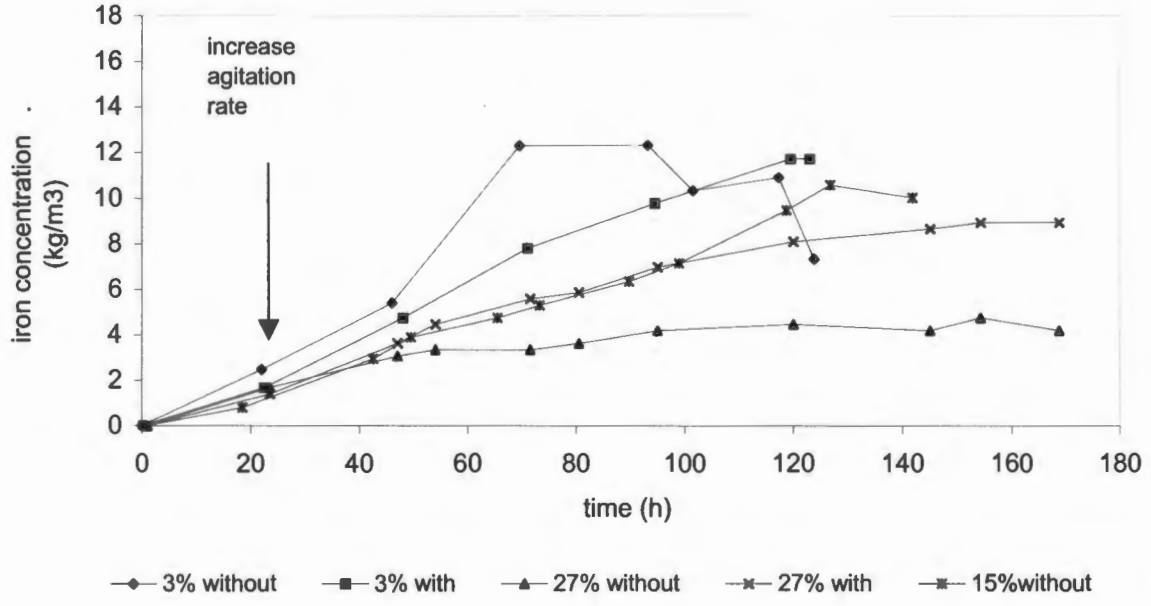

Figure 6.16: Iron release profiles with and without 1% CO_2 enriched air at various solids loading

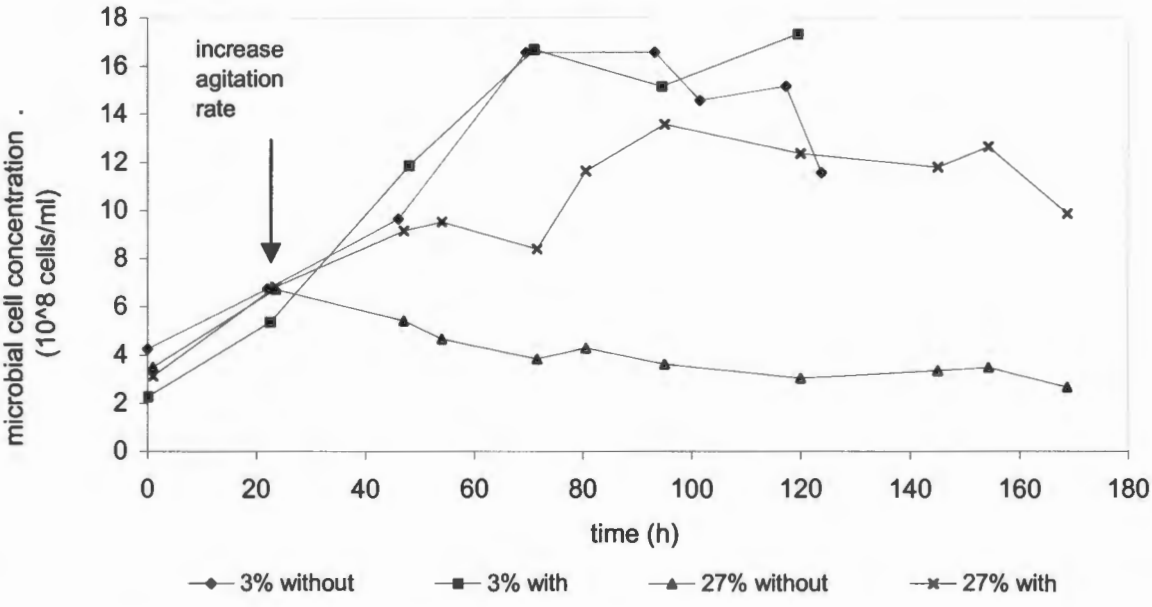

Figure 6.16(b): Microbial cell concentration profiles with and without 1% CO_2 enriched air at various solids loading

Table 6.9: Percentage depression in the absence of CO_2 enrichment relative to enrichment with 1% CO_2

Solids Loading (w/v)	Iron Release %	Iron Release Rate kg m^{-3} h^{-1}	Biomass Concentration %
3% pyrite	0	0	0
3% pyrite, 18% quartz	0	0	0
3% pyrite, 21% quartz	18	32	31
3% pyrite, 24% quartz	51	49	71

In the presence of 21% quartz, the iron release rate and microbial cell concentration is depressed by similar amounts. At 24% quartz the microbial cell concentration is depressed more than the iron release rate. Thus at higher solids loading, the decrease in microbial cell concentration is greater in the absence of CO_2, suggesting that CO_2 limitation influences the physiological status of the microbes, which in turn affects the leach rate.

The recovery in leaching performance obtained with the addition of CO_2 at 3% pyrite in the presence of 24% quartz as compared to lower solids loading where limitation is not found, is illustrated in Figure 6.16. The rate and extent of iron release and the microbial cell concentration is significantly improved with the addition of CO_2, but is not as high as that obtained for the solids loading of 3% pyrite in the presence of 15% quartz. The rate and extent of iron release is 0.092 kg m^{-3} h^{-1} (R^2 = 0.97) and 86% using 3% pyrite in the presence of 15% quartz. The rate and extent with 3% pyrite in the presence of 24% quartz with the addition of CO_2 is 0.055 kg m^{-3} h^{-1} (R^2 = 0.95) and 71%. This indicates that CO_2 limitation is a cause for reduced bioleaching performance at high solids loading. However, other factors also affect bioleach performance at high solids loading, hence recovery obtained with the addition of CO_2 is not complete.

6.6. THE EFFECT OF AGITATION SPEED ON THE BIOLEACHING PERFORMANCE

The effect of agitation speed on the bioleach performance was investigated by increasing the agitation speed in the range above the critical impeller speed used to ensure fully suspended solids. A critical impeller speed of 560 rpm was observed visually, i.e. the speed at which the solid particles were observed not to remain on the vessel base for longer than 1 or 2 s. The agitation rates investigated were 560, 660 and 760 rpm, corresponding to impeller tip speeds of 1.67, 1.97 and 2.27 m s^{-1}, respectively. The solids concentration used for the investigation was 3% pyrite in the presence of 15% quartz. An initial agitation rate of 285 rpm (less than the critical impeller speed) was used on inoculation of each experiment, with the agitation rate being increased after approximately 20 hours (microbiological count of 4-7x10^8 cells ml^{-1}). Bioleach experiments were executed and the iron release, microbial cell concentration, pH and redox potential monitored.

Iron release and microbial cell formation as a function of time across these agitation rates is shown in Figure 6.17 (data in Appendix D). These profiles indicate that the highest iron release rate is obtained at 660 rpm (tip speed of 1.97 m s^{-1}), while the system fails at 760 rpm (tip speed of 2.27 m s^{-1}). The iron release rates for the experiments at 560 and 660 rpm are significantly different at 0.091 and 0.096 kg m^{-3} h^{-1}, respectively, according to an analysis of variance. The extent of iron release is 86% at 560 rpm and 90% at 660rpm. Pyrite dissolution at 760 rpm was limited to 13% generated at 285 rpm with no further increase following 100h incubation at 760 rpm.

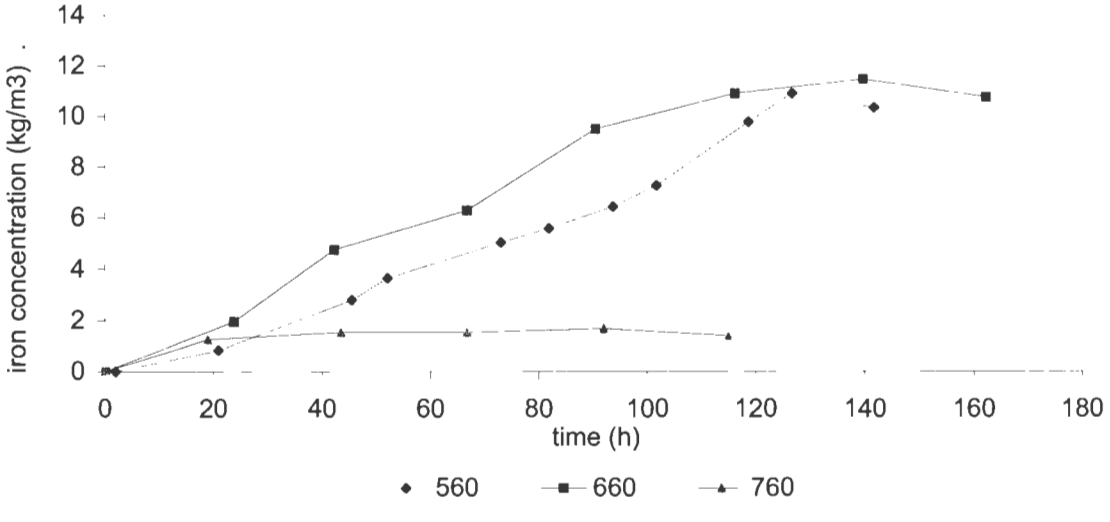

Figure 6.17(a): Iron release profiles for various agitation rates (rpm)

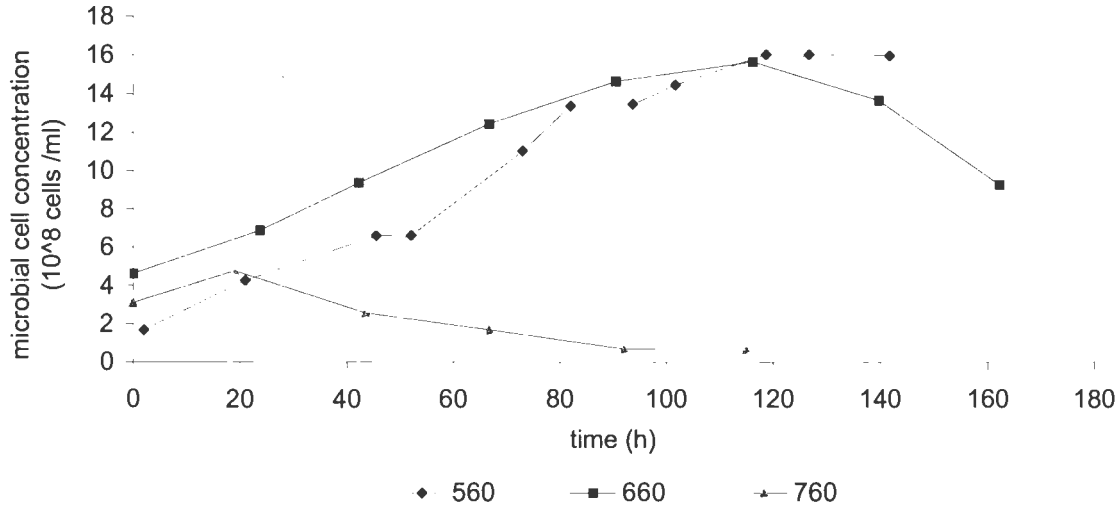

Figure 6.17(b): Microbial cell concentration profiles for various agitation rates (rpm)

The specific microbial cell growth rates at 560 and 660 rpm are similar at 0.014 h^{-1} and 0.011 h^{-1}, respectively. At 760 rpm, the microbial cell concentration increases to $4.8x10^8$ cells ml^{-1} within the first 20 h whereafter it decreases to less than $0.66x10^8$ cells ml^{-1} at a specific cell death rate of 0.026 h^{-1} with no further leaching.

Since the initial microbial cell concentration for the experiment at a speed of 560 rpm was lower than that at 660 rpm ($1.7x10^8$ cells ml^{-1} and $4.6x10^8$ cells ml^{-1} respectively), the specific activity of the microorganisms (iron release per hour per microbial cell) as a function of time is given in Figure 6.18 to provide a true reflection of the bioleach performance. The activity of the cells at 560 rpm is higher than that at 660 rpm. At 660 rpm, the mass transfer may be greater, and an increase in growth rate with agitation speed may be expected. Instead, a lower growth rate is observed which may be due to increased damage on increased energy dissipation at the higher speed i.e. the contribution of an increasing cell death rate. The overall result is that the activity of the cells is lower at the higher speed. At 760 rpm, the rate of damage to the cells exceeds their growth rate such that the system fails.

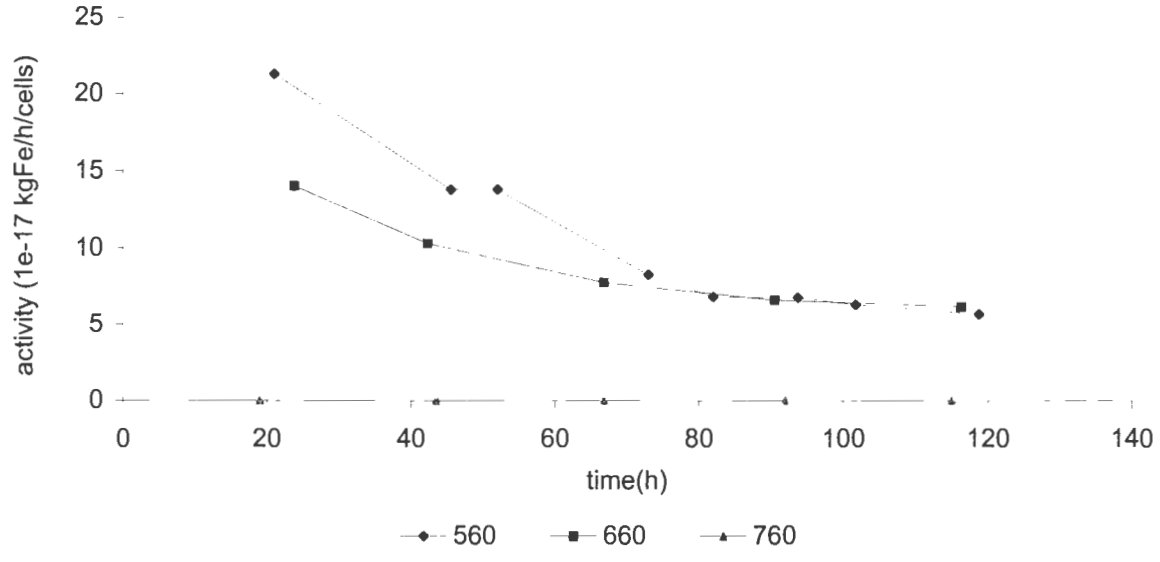

Figure 6.18: Activity of microbial cells (iron release per hour per cell) at various agitation rates (rpm)

The agitation rate affects the particle momentum, which in turn affects the collision momentum and cell damage. Particle density and size also affect the particle momentum, but are held constant in this set of experiments, hence the particle momentum varies with the variation in agitation speed. The particle momentum was calculated as the product of the particle mass and impeller tip speed. The tip speed represents the maximum fluid velocity in the active impeller zone and thereby maximum potential particle velocity. The particle momentum calculated for the d_{50} particle size at 560, 660 and 760 rpm is 5.94×10^{-10} kg m s^{-1}, 7.01×10^{-10} kg m s^{-1} and 8.08×10^{-10} kg m s^{-1}, respectively. The range of particle momentum at each agitation rate varies greatly (exponential -8 to -12) due to the range of particle sizes used in the experiment (Figure 6.19). Thus the range of particle momentum within each agitation rate is greater than that across the agitation rates. The particle momentum can therefore not be compared across the agitation rates.

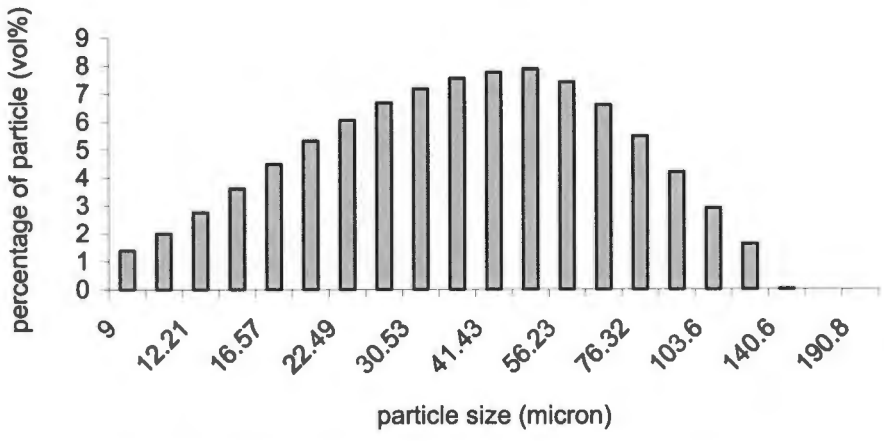

Figure 6.19: Particle size distribution of quartz fraction used

6.7. THE EFFECT OF INOCULUM STATE ON THE BIOLEACH PERFORMANCE

The effect of the physiological state of the inoculum on the bioleach performance was investigated by carrying out bioleach runs with inoculum grown in a shake flask and inoculum grown in a stirred tank reactor. The initial concentration of the shake flask inoculum was much lower than that of the stirred tank ($2.78x10^7$ cells ml^{-1} as compared to $2.33x10^8$ cells ml^{-1}). The physiological activity of the microbes from the shake flask is expected to be lower than those from the stirred tank based on the lower cell concentration, the less frequent reculturing time interval (once every 2 weeks for the shake flask, and daily for the stirred tank) and the oxygen limitation within the shake flasks. Solids loading of 3% pyrite and 15% quartz was used in the investigation. The experiments were inoculated at a low agitation rate of 285 rpm. This was increased to 560 rpm to fully suspend the solids after the microbial cell concentration achieved a concentration of $4\text{-}5x10^8$ cells ml^{-1}. Samples were withdrawn regularly and analysed for ferric and ferrous iron concentration, microbial cell concentration, pH and redox potential.

The effect of inoculum state on bioleach performance in terms of iron release and microbial cell concentration is shown in Figure 6.20 (data in Appendix E). The zero time point in Figure 6.20 corresponds to the increase of the agitation rate to 560 rpm, thus representing the period of completely suspended solids. The initial microbial cell concentration following inoculation (21% by volume) from the shake flask was 2.8×10^7 cells ml^{-1}. This increased to 5.6×10^8 cells ml^{-1} in 120 hours on agitation at 285 rpm at a specific growth rate of 0.036 h^{-1} ($R^2 = 0.97$), at which time the agitation rate was increased. The concentration of iron released during this time was 3.4 ± 0.04 kg Fe m^{-3} at a rate of 0.028 kg Fe m^{-3} h^{-1}. The initial microbial cell concentration following inoculation (21% by volume) from the stirred tank was 2.3×10^8 cells ml^{-1}. This concentration increased to 4.4×10^8 cells ml^{-1} in 24 hours at a growth rate of 0.027 h^{-1}, at which time the agitation rate was increased from 285 to 560 rpm. The concentration of iron released during this time was 1.7 ± 0.04 kg Fe m^{-3} at a rate of 0.071 kg Fe m^{-3} h^{-1}.

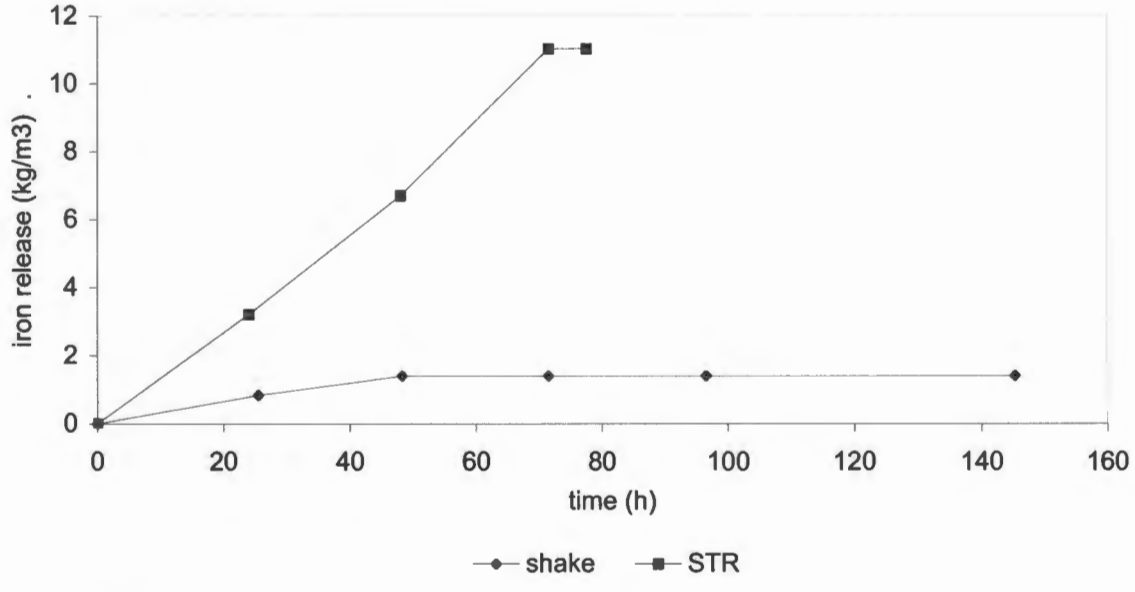

Figure 6.20(a): Comparison of iron release profiles for 3% pyrite in the presence of 15% quartz using shake flask (shake) and stirred tank (STR) inoculum after increase of agitation rate. The zero time point is at the increased agitation rate of 560 rpm

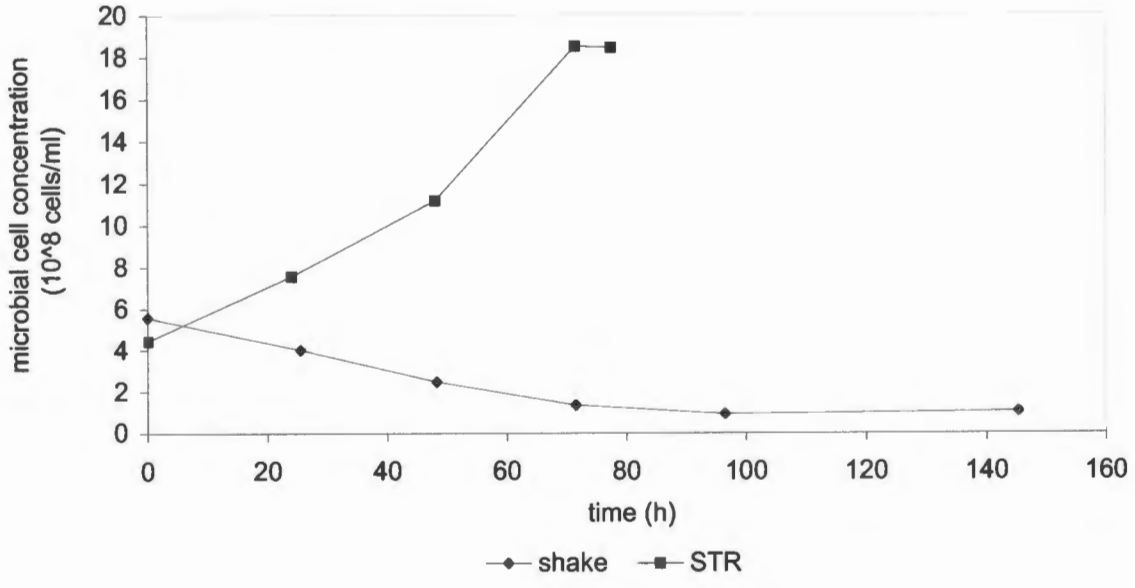

Figure 6.20(b): Comparison of microbial cell concentration profiles for 3% pyrite in the presence of 15% quartz using shake flask (shake) and stirred tank (STR) inoculum after increase of agitation rate. The zero time point is at the increased agitation rate of 560 rpm

After the increase in agitation speed, the concentration of iron released using the shake flask inoculum was 1.4±0.04 kg Fe m^{-3} in the first 50 hours (0.028 kg Fe m^{-3} h^{-1}). Thereafter, no iron was released for 100 hours. The corresponding microbial cell concentration showed a decrease from $5.6x10^8$ cells ml^{-1} to $1.0x10^8$ cells ml^{-1}, the death rate (k_D) value being 0.020 h^{-1} (R^2 = 0.99). The iron release rate using the stirred tank inoculum was 0.15 kg Fe m^{-3} h^{-1} (R^2 = 0.99), with a maximum concentration of released iron of 12.7±0.04 kg Fe m^{-3}. Complete solubilisation of pyrite was observed in 72 hours. The specific growth rate of the microbial cell using the stirred tank inoculum was 0.021 h^{-1} (R^2 = 0.99) and the highest biomass concentration observed was $18.5x10^8$ cells ml^{-1}. This data is summarised in Table 6.10.

Table 6.10: The effect of inoculum state on the bioleach performance

Parameter	Shake flask	Stirred tank
Initial microbial cell concentration (cells ml^{-1})	$2.8x10^{7}$	$2.3x10^{8}$
Time at 285 rpm (h)	120	24
Microbial cell concentration at increase of agitation (cells ml^{-1})	$5.6x10^{8}$	$4.4x10^{8}$
Specific growth rate at 285 rpm (h^{-1})	0.036	0.027
Iron release rate at 285 rpm (kg Fe m^{-3} h^{-1})	0.028	0.071
Specific growth rate at 560 rpm (h^{-1})	-0.020	0.021
Iron release rate at 560 rpm (kg Fe m^{-3} h^{-1})	0.028 (in 1st 50 h)	0.15
Time at 560 rpm (h)	150	72
Maximum iron released (kg Fe m^{-3})	1.4	12.7
Maximum microbial cell concentration (cells ml^{-1})	$5.6x10^{8}$	$18.5x10^{8}$
Specific Iron release at maximum microbial cell concentration (kg Fe cell $^{-1}$ h^{-1})	$5.0x10^{-10}$	$8.1x10^{-10}$
pH range during experiment	1.8-1.2	1.6-0.9
Redox potential range during experiment (mV Ag/AgC/)	446-513	513-606
Percentage Iron released (%)	38	100

The pH profiles of the bioleach experiments inoculated with shake flask and stirred tank inoculum are depicted in Figure 6.19. The pH of the experiment using the shake flask inoculum was initially 1.8. This decreased to a value of 1.2 while the iron release concentration and the biomass concentration increased before full suspension of the solids. Thereafter, a constant pH value was observed. The redox potential increased from 446 to 513 mV, corresponding to the increasing iron release and increase in biomass concentration, but decreased to 473 mV after the increase of agitation rate. The pH of the experiment using the stirred tank inoculum displayed a pH value that decreased steadily from 1.6 to 0.9 throughout. The redox potential increased from 513 to 606 mV.

The extent of iron release using the shake flask inoculum was 38% in 150 hours while that using the stirred tank inoculum was 100% in 72 hours. The inoculum state thus has a significant effect on the bioleach performance. Although the shake flask inoculum, which had a lower cell number, was kept at a low agitation rate to increase the cell number and obtain equivalent microbial cell

concentrations in both experiments, the microbial cells could not tolerate the high agitation rate. The microbial cell concentration decreased, and subsequently no iron was solubilised. This is also reflected in the constant pH value and the decrease in redox potential with increase in agitation rate.

The microbial cells from the shake flask is able to tolerate low agitation rates as observed by the concentration of iron released (3.4 ± 0.04 kg Fe m^{-3}) and the microbial cell growth rate ($0.036\ h^{-1}$) at 285 rpm. In addition, the ferrous iron concentration remains constant at 0.28 ± 0.04 kg Fe m^{-3} at low agitation rate indicating the ability of the microbial cells to convert the ferrous iron present to ferric iron, thus maintaining a low ferrous iron concentration and observing an increase in redox potential. The increase of agitation rate results in an increase of ferrous iron concentration to a value of 1.4 ± 0.04 kg Fe m^{-3}, indicating the inability of the microbial cells to convert the ferrous iron present to ferric iron (reduced microbial activity), and thus the redox potential decreases.

These results indicate the difference of inoculum states on bioleach performance, with inoculum from the stirred tank showing a significantly better performance in terms of extent and rate of pyrite dissolution than the inoculum from the shake flask.

6.8. CONCLUSION

The results of the various experiments have been presented and discussed in this Chapter. The implications of these results are discussed in Chapter 7.

6.9. REFERENCES

Hansford, G.S. and T. Vargas (2000), "Chemical and electrochemical basis of bioleaching processes", *Hydrometallurgy*, **59**, 135-145

Harrison, S.T.L., N.J. Scholtz-Brown and S.A.J. Pearce (2002), "The effect of inert particulate parameters on microbial cell disruption in a slurry bioreactor", *Journal of Chemical Technology and Biotechnology*, accepted for press

Nemati, M. and S.T.L. Harrison (2000), "Effect of solid loading on thermophilic bioleaching of sulphide minerals", *Journal of Chemical Technology and Biotechnology*, 75, 526-532

CHAPTER 7

CONCLUSION

The aim of this thesis was to determine the effect of the solid particulate fraction on the thermophilic bioleaching of pyrite using *Sulfolobus metallicus*. Similar investigations were carried out by Nemati and Harrison (2000) using a pyrite system. Nemati and Harrison reported no effect of solids loading of 3 to 9%(w/v) on leaching performance, reduced performance at 12 to 15% loading and system failure at 18% loading. In this study a constant mineral concentration was used with a varying inert solid fraction to obtain different solids concentrations, and to minimize physicochemical variation in the system, and thereby gain better understanding of the solids effects. A range of experiments were performed in addition to preliminary investigations to determine the extent of chemical leaching at high temperature and the extent of adsorption of the microbes to the sulphide mineral. The effect of solid concentration, including mass transfer limitation, effect of agitation rate and effect of inoculum state were investigated. The overall findings of the study are consolidated in this chapter, summarized in Section 7.7 with ensuing recommendations made in Section 7.8.

7.1. CHEMICAL LEACHING

Thermophilic bioleaching is thought to be advantageous over mesophilic bioleaching due to possible increased leaching in terms of rate and extent (Konishi *et al.* 1995, Le Roux and Wakerley 1987). The increase in chemical leaching with increasing temperature may have been a predominant factor in the increase in leaching with little contribution from the microorganisms. The rate and extent of chemical leaching at 68-

70°C was thus investigated by carrying out experiments similar to the bioleaching experiments, except in the absence of the microorganisms. Similar initial redox potentials were also used. The results showed that the redox potential dropped from values of 492 and 529 mV to 382 and 383 mV, at rates of ferrous iron production of 0.075 kg m^{-3} and 0.087 kg m^{-3} with the extent of leaching being less than 30%. In one of the experiments, the redox potential was increased from 383 mV to 451 mV, which did not induce ferric leaching. The microorganisms are required to maintain a sufficiently high redox potential, such that ferric leaching occurs. At 68-70°C therefore, little chemical leaching occurs in the absence of microorganisms, illustrating that the increased rate and extent of leaching is due to microbiological leaching.

7.2. PARTITIONING OF *SULFOLOBUS* BETWEEN CONCENTRATE SURFACE AND LIQUID PHASE

This set of experiments was performed to achieve better understanding of the mechanism of cell damage as free cells in suspension are exposed to different conditions than cells attached to the solid particulates, and to validate the microbial cell concentration determination by counting of microbial cells. To confirm the applicability of this method, the extent to which the microorganisms attach to the pyrite had to be determined. This was done in two ways. Firstly following a contact time between the pyrite and microorganisms, the solution was removed, the pyrite placed in fresh medium and its leaching monitored. This was done while maintaining a control to ensure that the conditions were fit for leaching. Secondly, the free cell concentration was monitored while the microorganisms were in contact with the pyrite. The contact times in the first set of experiments were 1 h and 24 h. In one of the 24 h experiments, ferrous iron was added with the fresh medium as the presence of any microorganisms would result in the conversion of the ferrous iron to ferric iron to facilitate leaching. Ferric iron was not added as chemical leaching may have occurred. The results of these experiments showed that the conditions were suitable for leaching as notable leaching

occurred in the controls, but negligible leaching occurred in the experiments. This suggests that the microorganisms were present free in solution and were thus removed with the solution leaving no inoculum on the pyrite phase. The second set of experiments revealed a constant or slightly decreasing (25%) microbial cell concentration in free solution with time. The slow growth rate of these cells implies that over the period tested (48 and 72 hr) a significant increase in microbial cell concentration due to growth would not occur, and thus the majority of cells remain in solution. Both sets of experiments therefore suggest that the cells do not attach to the pyrite and so the proposed method of counting microbial cells is applicable.

The fact that the cells are not attached to the solid surface implies that the cells are not subjected to a velocity gradient caused by the movement of fluid eddies passing across the cell surface. The cells are smaller than the eddies and since they are not attached to the solid surface, will be entrained in the eddies, but not damaged by shear forces generated by the velocity gradient of the eddies.

7.3. EFFECT OF SOLID CONCENTRATION ON BIOLEACHING PERFORMANCE

The effect of solids loading on the growth and leaching performance of *Sulfolobus metallicus* was investigated in the absence of changing physicochemical conditions using 3% pyrite supplemented with 0 to 24% quartz (increased in 3% intervals). This was in contrast to previous work by Nemati and Harrison (2000) who used a system of pyrite only and varied this to obtain different solids concentrations. In the pyrite/quartz system, a bioleach rate of 0.113 kg m^{-3} h^{-1} (R^2 = 1.00) was observed with an extent of leaching of 91% using 3% pyrite. Addition of quartz in the range of 6 to 15% (w/v) decreased the bioleach rate to an average of 0.095 kg m^{-3} h^{-1} (R^2 = 0.98) and the extent of leaching to 86%. The addition of 21% quartz further reduced the bioleach rate to 0.057 kg m^{-3} h^{-1} (R^2 = 0.98) and the extent to 62%. The bioleach rate and extent of pyrite

solubilisation using 24% quartz was 0.035 kg m^{-3} h^{-1} (R^2 = 0.99) and 46%, respectively. These results are depicted in Figure 7.1. Thus bioleaching performance is optimal at 3% pyrite and remains essentially constant up to 18% total solids concentration. Thereafter, the bioleaching performance is progressively impaired with higher solids concentrations.

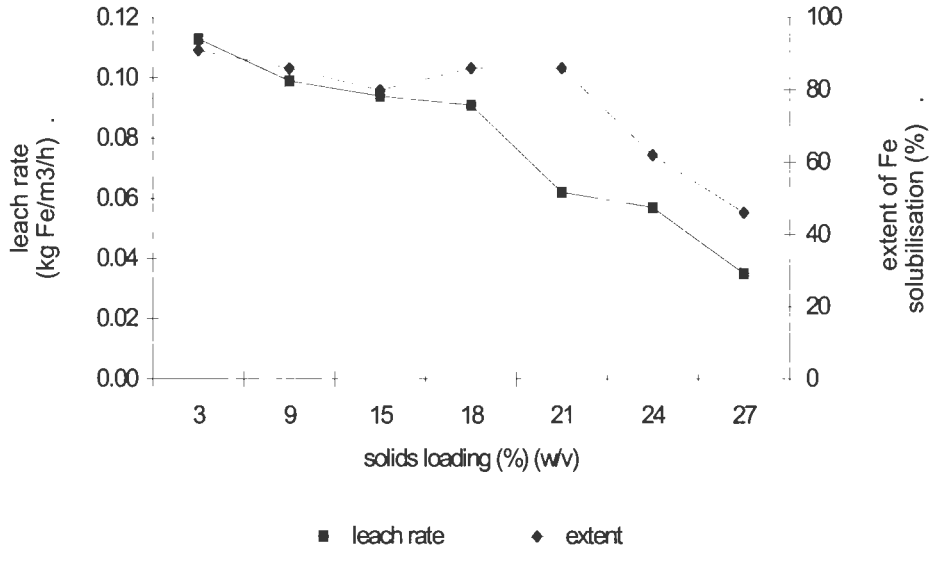

Figure 7.1: Bioleach rate and extent of iron solubilisation as a function of total solids loading (comprised of 3% pyrite, the remainder quartz)

The microbial cell concentration profiles for the experiments in the presence of 0 to 15% quartz exhibited similar growth rates ranging from 0.016 to 0.020 h^{-1} (R^2 = 0.95 – 1.00) for the first 50 h of the experiment. Thereafter the growth rate remained constant in the presence of 3% pyrite and increased in the presence of 3% pyrite with 6-15% quartz. In the presence of 21% quartz, a maximum growth rate of 0.011 h^{-1} was observed, followed by a stationary phase after 95 hours. The specific growth rate in the presence of 24% quartz exhibited no growth throughout the experiment. The yields in terms of microbial cells produced per kg iron oxidized in the presence of 0 and 6% quartz are similar. The yield is lower in the presence of 15% quartz. A further decrease

is observed with 21% quartz, and by a factor of 10 in the presence of 24% quartz. This is illustrated in Figure 7.2. The reduced yield suggests that the microorganisms are becoming less efficient at utilizing the iron for growth. This may be attributed to the increased maintenance energy requirement to sustain the biomass phase under the adverse conditions of high solids loading.

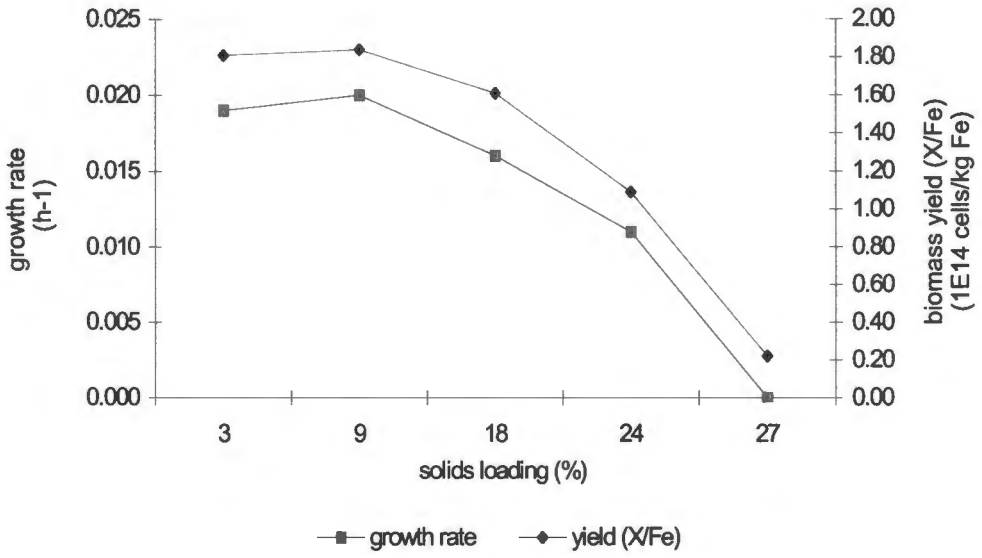

Figure 7.2: Microbial growth rate and biomass yield ($Y_{X/Fe}$) in terms of microbial cells produced per kg iron oxidized as a function of total solids loading (comprised of 3% pyrite, the remainder quartz)

During the exponential growth phase, higher specific activity (rate of iron released per microbial cell) is observed at lower solids loading, i.e. 0-15% quartz exhibited higher activity than 21% quartz, and 24% quartz exhibited the lowest activity. This is shown in Figure 7.3. The similarity in activity across the solids loading range during the stationary phase suggests the efficiency of the microorganisms in converting ferrous iron present to ferric iron at the various solids loading is similar in the absence of microbial growth. However, the microbial cell concentration decreases with solids loading. Hence the decrease in pyrite oxidation with solids loading in the stationary phase corresponds to a

lower microbial cell concentration as opposed to lower microorganism activity. In the exponential growth phase, both reduced specific activity and a decreased biomass concentration contribute to the decreased leaching performance.

The pH profiles across the range of solids loading are similar. The profiles for redox potential are similar for solids loading of 3% pyrite in the presence of 0 to 15% quartz. A decrease in the maximum redox potential is observed in the presence of 21% quartz and a further decrease with 24% quartz, owing to the reduced conversion of ferrous to ferric iron.

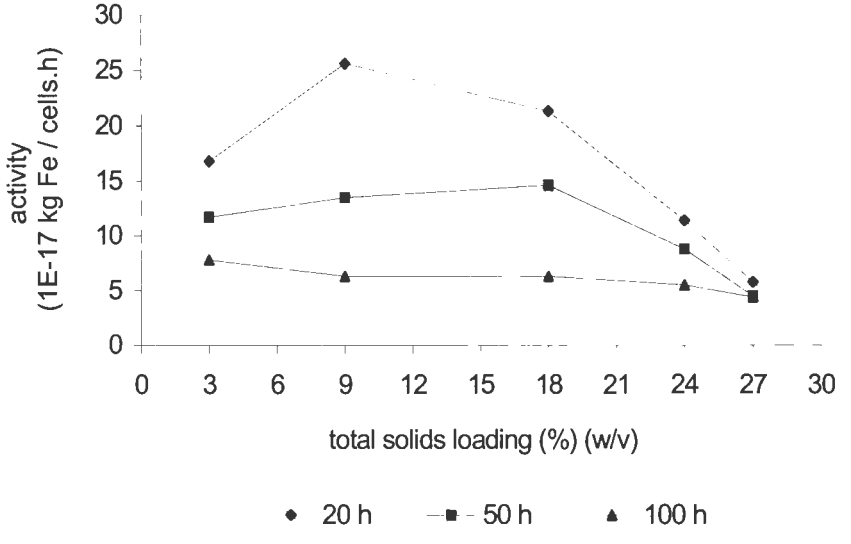

Figure 7.3: Microbial cell activity in terms of specific pyrite oxidation rate as a function of solids loading and duration of experiment

7.3.1. Interactions Between Solids Loading and Physicochemical Conditions and their Effect on Bioleaching

A comparison of the pyrite/quartz system used in this study and pyrite system investigated by Nemati and Harrison (2000) was made to gain a better understanding of the effect of solid concentration on the thermophilic bioleaching of pyrite using *Sulfolobus metallicus*. The pyrite/quartz system did not result in the variation in

physicochemical conditions with varying solids concentration observed in the pyrite system. In the pyrite/quartz system, the physicochemical conditions owing to the release of inhibitory metal ions and sulphates, as well as change in pH and redox potential is minimized by the presence of a constant mineral phase while varying solids loading. The implication of using quartz to vary solids loading is that the density of the quartz is less than that of the pyrite, and so mass transfer and momentum of the systems may be different. The differences in Nemati and Harrison's work compared to the current system were:

- The solids loading comprised only pyrite.
- The inoculum cultured in a shake flask was less active and had a lower cell concentration than that from a stirred tank used in the current system.
- No baffles were used in Nemati and Harrison's experimental set-up, thus the mass transfer conditions may have been different.

The mass transfer coefficients (k_La) of the two systems were measured and it was found that k_La in the current set-up exceeded that of Nemati and Harrison ($2.0x10^{-3}$ s^{-1} as opposed to $1.4 x10^{-3}$ s^{-1}).

To ascertain the difference in bioleach performance due to the differences in inoculum and mass transfer, comparisons of the 3% pyrite experiments (experiments A and C), and 18% pyrite experiments (experiments B and D) using the two different systems were made. At 3% pyrite, where little or no stress was imposed on the system, the two systems performed similarly, although the less active shake flask inoculum (experiment C) exhibited a long lag phase whereas no lag phase was observed using an inoculum for a stirred tank reactor (experiment A). When 18% pyrite was used, both systems failed, but differences were observed. The increase with cell concentration in the more active inoculum and the higher mass transfer in the current work (experiment B) resulted in higher microbial cell concentration in a shorter period with pyrite dissolution within the first 24 h after the increase of agitation rate. No bioleaching was observed in the experiment of Nemati and Harrison (experiment D) or in the experiment performed in the current work after the increase of agitation rate. The experiment descriptors are given in Table 7.1.

Table 7.1: Bioleaching experiments performed at different solids loading, under different conditions by different operators

Descriptor	Experiment	Operator
A	3% pyrite, baffled system	Sissing (2002)
B	18% pyrite, baffled system	Sissing (2002)
C	3% pyrite, unbaffled system	Nemati and Harrison (2000)
D	18% pyrite, unbaffled system	Nemati and Harrison (2000)

The higher inhibition that is observed in the pyrite system due to the greater release of iron and sulphates and reduction in pH is postulated to contribute to the failure of the bioleach system at higher solids loading (Nemati and Harrison, 2000). However, the experiment performed using 18% pyrite failed at low iron concentration and relatively high pH, suggesting that system failure is not due only to inhibition from these sources, and that hydrodynamic stress may also be implicated.

A comparison of the overall performance of the pyrite/quartz system and the pyrite system revealed that the pyrite system failed at a lower solids concentration than the pyrite/quartz system. As the quartz is less dense than the pyrite and the solids loading is calculated on a weight per volume basis, the pyrite/quartz system represents a higher loading on a volume basis i.e. contains more particles than the equivalent pyrite system. As the pyrite/quartz system contained a greater amount of particles, the frequency of collisions was greater in this system. However, the pyrite system failed at a lower solid concentration than the pyrite/quartz system, suggesting that the frequency of collisions is not a dominant factor in the failure of the system. The particle collision momentum in the pyrite system was greater than that in the pyrite/quartz system due to the density of the pyrite being greater than that of quartz. Thus the higher particle collision momentum, although with lower frequency of collisions, may play a part in the failure of the pyrite system at a lower solids concentration than the pyrite/quartz system. This is consistent with the data of Pearce (1993) for cell damage in a yeast-silica system.

The mass transfer coefficients for the pyrite/quartz and pyrite systems were measured in similar systems (i.e. with baffles) to determine the effect of mass transfer conditions on the two systems. The k_La value for the pyrite/quartz system was lower than that for the pyrite system ($4.0x10^{-3}$ s^{-1} for the pyrite/quartz system and $8.0x10^{-3}$ s^{-1} for the pyrite system). Since the experimental set-ups were similar, both the saturated and critical dissolved oxygen concentrations were similar for the two systems. Oxygen transfer potential (OTP) is dependent on k_La, saturated and critical dissolved oxygen concentrations, hence the OTP will be similar for the two systems. The oxygen demand in the pyrite system, however, is greater than in the pyrite/quartz system (1 kg O_2 required to oxidize 1kg pyrite). Since the mass transfer coefficient in the pyrite system is greater than that in the pyrite/quartz system, the greater oxygen demand may be compensated for, but it is not conclusive from this study.

The state of the inoculum, was different in the two systems, with that used for the pyrite system less active and at a lower concentration than that from the stirred tank. However, similar bioleaching performance resulted. At 3% pyrite, similar rates and extents were observed with both inocula, while at 18% pyrite system failure occurred. Thus the inoculum state did not appear to be a major factor in the failure of the pyrite system at a lower solids loading than the pyrite/quartz system.

The pyrite system fails at a lower solids loading (18% pyrite) than the pyrite/quartz system (27%, comprised of 3% pyrite and 24% quartz). The most probable cause for the failure at the lower solids loading for the pyrite system is the higher particle collision momentum although with lower collision frequency. The increased inhibition due to the physicochemical variations in the pyrite system does not appear to play a major role in the system failure at this loading.

7.4. MASS TRANSFER

The effect of solids loading on bioleaching kinetics may be due to the effect of the gas-liquid mass transfer, restricting the supply of oxygen and carbon dioxide to the microorganisms. An attempt to verify this theory was made by determining the mass transfer coefficient and saturation concentration for oxygen transfer using a dynamic method at various solids loading. The mass transfer coefficients measured at the various solids loading are similar across the range from 0 to 24% (w/v) quartz in the presence of 3% pyrite, ranging from 7.3×10^{-3} to 4.0×10^{-3} s^{-1}. If oxygen is a limiting factor, oxygen demand will be greater than the oxygen transfer potential (OTP). As the pyrite concentration remained constant, oxygen demand in terms of pyrite solubilisation remained constant. OTP, which is dependent on k_La, saturated and critical dissolved oxygen concentrations, only varied with k_La as the dissolved oxygen concentrations would remain unchanged due to the similar conditions of the experiments. As k_La did not vary with solids loading, OTP would not vary. Since both oxygen demand and OTP are similar over the range of solids loadings, oxygen limitation is not a factor affecting bioleaching over the range investigated.

To investigate the carbon dioxide limitation, bioleach experiments were performed with the addition of 1% CO_2 to the air supply. Carbon dioxide limitation may affect the physiological status of the microbes. The results indicated that on increasing solids loading up to 3% pyrite in the presence of 18% quartz, no change is observed in the bioleach performance with the addition of CO_2 and thus it is not limiting under these conditions. At 21% quartz, a depression of 32% in the iron release rate and 31% in the maximum microbial cell concentration is observed in the absence of CO_2. At 24% quartz, the depression in iron release rate is 49% and 71% depression is observed in the maximum microbial cell concentration. These results are shown in Table 6.8. The larger depression in microbial cell concentration at the higher solids loading suggests that CO_2 limitation impacts the physiological status of the microbes. Results clearly show that lower microbe concentration results in reduced leaching. Comparison of the leach rate and extent in the presence of 15% quartz (whereby fairly good leaching is observed and

where CO_2 limitation is not a factor) with that at 24% quartz with CO_2 present, reveals rates of 0.092 kg m^{-3} h^{-1} with an extent of 86% at 15% quartz, and 0.055 kg m^{-3} h^{-1} with an extent of 71% at 24% quartz.

It appears that increased CO2 leads to increased physiological health of the microbes which increases the ability of the microbes to handle stress. The addition of CO_2 on leaching at the solids loading of 24% quartz does not exhibit as high a rate and extent of leaching as that in the presence of 15% quartz. Therefore, although CO_2 limitation is a major factor in bioleach performance, it is not the only factor.

Table 6.8: Percentage depression in the absence of CO_2 enrichment relative to enrichment with 1% CO_2

Solids Loading (w/v)	Extent of Iron Release %	Bioleach Rate kg m^{-3} h^{-1}	Microbial Cell Concentration %
3% pyrite	0	0	0
3% pyrite, 18% quartz	0	0	0
3% pyrite, 21% quartz	18	32	31
3% pyrite, 24% quartz	51	49	71

7.5. EFFECT OF AGITATION RATE

The effect of agitation rate on the bioleach performance was investigated by increasing the agitation rate in the range above the critical impeller speed used to ensure fully suspended solids. The agitation rates investigated were 560, 660 and 760 rpm which corresponded to tip speeds of 1.67, 1.97 and 2.27 m s^{-1} respectively, with a solids loading of 3% pyrite and 15% quartz. The system failed at an agitation rate of 760 rpm (tip speed 2.27 m s^{-1}), where the rate of damage to the cells exceeded their growth rate. The rate of iron release and the extent of pyrite solubilisation was higher at 660 rpm than at 560 rpm due to the higher initial microbial cell concentration at 660 rpm. The growth rate of the

microorganisms was slightly lower at the higher agitation rate. The activity of the microorganisms at 560 rpm was higher than that at 660 rpm, suggesting an adverse effect of higher agitation rate on the microorganisms. This may be due to increased damage on increased energy dissipation at the higher agitation rate. A specific cell death rate of 0.026 h^{-1} was observed at an agitation rate of 760 rpm. These results are depicted in Figure 7.4.

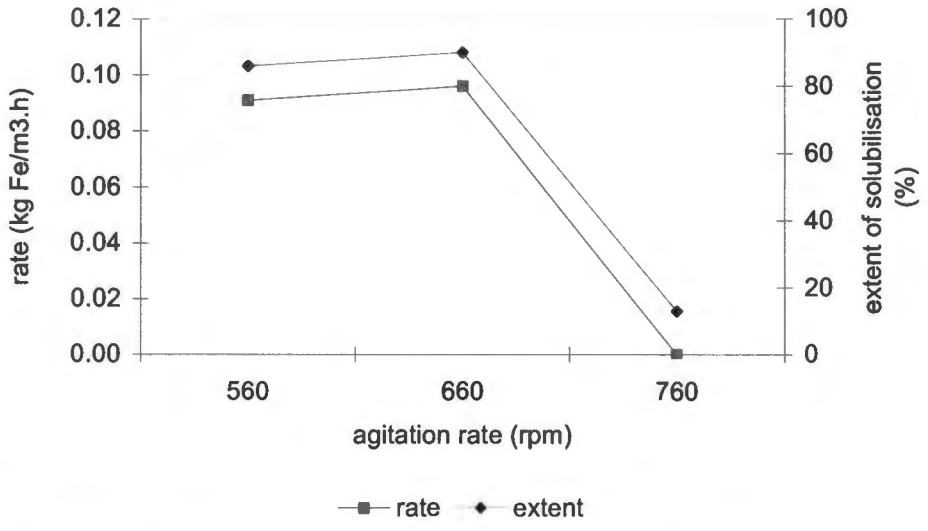

Figure 7.4(a): Rate of iron release and extent of pyrite dissolution at various agitation rates

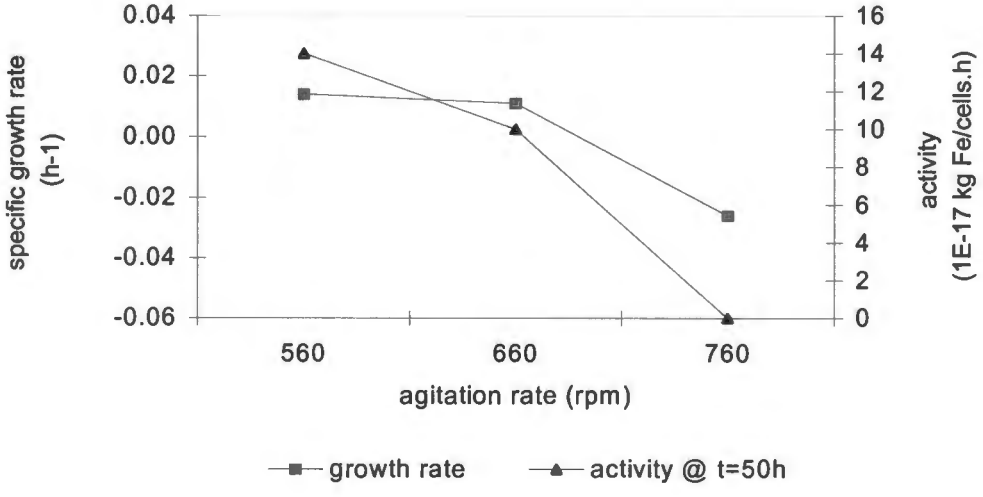

Figure 7.4(b): Specific growth rate and microbial activity at various agitation rates

7.6. EFFECT OF INOCULUM STATE

The physiological state of the inoculum on the bioleach performance was investigated by carrying out bioleach runs with inoculum grown in a shake flask and inoculum grown in a stirred tank reactor. The metabolic activity of the microbes from the shake flask was lower than that from the stirred tank as illustrated by the lower cell concentration and the reculturing time of 2 weeks in comparison to daily for the stirred tank inoculum. The microbes in the shake flask may have been oxygen limited. A solids loading of 3% pyrite with 15% quartz was used in the experiments. A long lag time was observed with the shake flask inoculum, followed by a period of iron release at a rate of 0.028 kg m^{-3} h^{-1}. The iron release then ceased, corresponding to a decrease in biomass concentration. The experiment using the stirred tank inoculum exhibited no lag phase and an iron release rate of 0.15 kg m^{-3} h^{-1} with complete pyrite solubilisation. Thus the difference in physiological status of the inoculum resulted in significant difference in bioleach performance, with microbes recultured in a stirred tank exhibiting significantly better bioleach performance in terms of rate and extent of pyrite dissolution.

7.7. SUMMARY OF KEY FINDINGS

The key findings of this study in terms of solids loading in the pyrite/quartz system are summarized as follows:

- The extent of leaching is limited to less than 30% in the absence of microorganisms. To be substantial, chemical leaching is strongly dependent on the presence of suitable microorganisms at 68°C to regenerate ferric irons. In the absence of suitable microorganisms, the effect of chemical leaching is limited by the available ferric irons.
- *Sulfolobus metallicus* cells do not associate significantly with the concentrate surface in the agitated slurry reactor but stay in suspension in the liquid phase. This was

determined by the observation of negligible leaching when the cells in suspension were removed from the reactor.

- The best bioleaching performance was observed in the presence of 3% (w/v) pyrite. Similar results were obtained for bioleaching up to 18% (w/v) total solids (3% pyrite in the presence of varying quartz concentration). Bioleaching was progressively impaired with increasing solids loading above 18% (w/v) total solids.
- Similar growth rates for *Sulfolobus metallicus* were observed in the presence of 3 to 18% (w/v) total solids loading (3% pyrite and the remainder comprised of quartz). The growth rate decreased by 39% in the presence of 24% total solids loading, and no growth rate was observed in the presence of 27% total solids loading.
- The yield in terms of microbial cells produced per kg iron oxidized remained constant at 1.6-1.9x10^{14} cells kg Fe^{-1} at solids loading of 3 to 18% (w/v) total solids loading (comprised of 3% pyrite and the remainder quartz). The biomass yield decreased with increased solids loading above 18% total solids loading. This decrease suggests that the microorganisms are becoming less efficient at utilizing the iron substrate or required a higher maintenance energy to withstand the hydrodynamic stress generated.

On comparing the studies of the effect of solid loading on bioleach performance using the pyrite and pyrite/quartz systems, the key findings are summarized as follows:

- The pyrite bioleaching system failed at 18% (w/v) total solids loading, while the pyrite/quartz system still exhibited iron solubilisation at 27% (w/v) total solids loading (3% pyrite and 24% quartz).
- Failure of the pyrite system at 18% solids loading is not due to inhibition from high iron concentration and low pH as the system failed before these were generated. Hence hydrodynamic stress may be implicated.
- Higher particle collision momentum, even though at a lower frequency of collisions, may have contributed to the failure of the pyrite system at a lower total solids loading than the pyrite/quartz system.

The influence of mass transfer on the bioleaching system investigated may be summarized as follows:

- Oxygen transfer potential was not significantly influenced in the bioleaching process over the range of solids loading investigated.
- Carbon dioxide is a major factor affecting bioleaching performance. By reducing CO_2 limitation under conditions of severe hydrodynamic stress, bioleach performance approaches that under the less stressed environment. However, performance is not restored completely, indicating that CO_2 limitation is not the only factor affecting reduced performance at high solids loading.

The effect of agitation rate on the bioleaching performance was as follows:

- The rate of iron release and extent of pyrite solubilisation was slightly higher at 660 rpm (tip speed of 1.97 m s^{-1}) than at 560 rpm (tip speed of 1.67 m s^{-1}). This was due to a higher initial microbial cell concentration for the 660 rpm experiment than the 560 rpm experiment. The growth rate of the microorganisms was lower at 660 rpm than at 560 rpm. At 760 rpm (tip speed of 2.27 m s^{-1}), the bioleach system failed, and a specific cell death rate of 0.026 h^{-1} was observed.
- An increase in agitation rate from 560 rpm to 660 rpm resulted in a marginally lower activity of the microorganisms.

The effect of the different inoculum states on bioleach performance is summarized as follows:

- The difference in inoculum state resulted in significant differences in bioleach performance. Microbes maintained in a stirred tank exhibited significantly better performance with an iron release rate of 0.15 kg m^{-3} h^{-1} at 560 rpm, while inoculum maintained in a shake flask achieved an iron release rate of 0.028 kg m^{-3} h^{-1}.

7.8. RECOMMENDATIONS FOR FURTHER STUDY

7.8.1. Improved Experimental Conditions in the Laboratory

- Baffled systems should be used as the mass transfer coefficient of an unbaffled system is half that of a baffled system.
- As carbon dioxide was found to be a limiting factor in bioleaching performance, air should be enriched with CO_2 (air enrichment with 1% CO_2 has been shown to significantly improve bioleach performance).
- An agitation rate of 560 rpm appears optimal as it resulted in complete suspension of 27% solids and exhibited the highest activity of the microorganisms. An agitation rate of 660 rpm resulted in lower activity of the microorganisms, while 760 rpm resulted in a failed bioleaching system.
- Inoculum maintained in a stirred tank reactor should be used as better bioleaching performance is exhibited by this inoculum as compared to that maintained in a shake flask.

7.8.2. Implementing Findings at a Commercial Scale

Based on the consolidated study, it may be concluded that:

- Decreased performance is associated with decreased microbial cell number or growth.
- Exponential phase: cell activity decreased with increased hydrodynamic stress due to increased solids loading or increased agitation rate.
  Stationary phase: cell activity is constant.
- Physiologically healthy cells are postulated to be more resilient.
- Physicochemical environment may compound stress damage – hydrodynamic stress is implicated.

Maximum physiological health of the microorganisms is postulated to result in maximum resistance to stress by the microorganisms. This was based on the results of the mass transfer limitation of CO_2 and the state of the inoculum experiments. This was proved at laboratory scale and should investigated further on a large scale. Determining key factors in maximizing physiological status of the microorganisms would prove to be beneficial in developing a system that could utilize extreme thermophiles in bioleaching.

7.9. REFERENCES

Konishi, Y., S. Yoshida and S. Asai (1995), "Bioleaching of pyrite by acidophilic thermophile *Acidianus brierleyi*", *Biotechnology and Bioengineering*, **48**, 592-600

Le Roux, N., W. and D.S. Wakerley (1987), "Leaching of Chalcopyrite ($CuFeS_2$) at 70°C using *Sulfolobus*", in *Biohydrometallurgy '87,* Eds. P.R. Norris and D.P. Kelly, *Science and Technology Letters*, Surrey, United Kingdom, 305-317

Nemati, M. and S.T.L. Harrison (2000), "Effect of solid loading on thermophilic bioleaching of sulphide minerals", *Journal of Chemical Technology and Biotechnology,* **75**, 526-532

Pearce, S.J.A. (1993), "Disruption of micro-organisms due to agitation in slurries of fine particles", Thesis for Master of Science, University of Cape Town, South Africa

APPENDIX A: Analysis of Variance (ANOVA)

To determine whether several means are significantly different from one another, as a group, an analysis of variance (ANOVA), which is a statistical technique, can be used. In this technique, an F-distribution is used to assess the significance of the variances due to the means. It partitions the total data variance into its components and makes comparisons between them. The one-way ANOVA allows the comparison between the variance associated with replicate measurements or observations (the *within-sample variance*) and the variance associated with different samples (*between-sample variance*) each of which has a sum of squared errors associated with it. For a set of k samples and N observations, the following table can be set up:

Sample number	**Observations**	**Total**	**Mean**	**Number of observations**
1	$x11x12x13.....x1N_1$	S_1	x_1	N_1
2	$x21x22x23.....x2N_2$	S_2	x_2	N_2
3	$x13x32x33.....x3N_2$	S_3	x_3	N_3
.				
.				
.				
K	$xk1xk2xk3.....xkN_2$	S_k	x_k	N_k
Σ		S		N_{total}

The procedure used is as follows:

1. Correction for mean (C) = S^2/ N_{total}
2. Total sum of squares (SS_{total}) = $((x11)^2 + (x12)^2 + \ldots + (xkn_k)^2) - C$
3. Sum of squares between samples (Ssbetween) = $(S_1^2/ n_1 + S_2^2/ n_2 + \ldots + S_k^2/ n_k) - C$
4. Sum of squares within samples (SS_{within}) = $SS_{total} - SS_{between}$
5. Mean square for each component (MS) = SS/degrees of freedom

A calculation table is set up as follows:

Source of variation	**Sum of squares**	**Degrees of freedom**	**Mean square**	**F**
Between samples	$SS_{between}$	k-1	$M_{between}$	$M_{between} / M_{within}$
Within samples	SS_{within}	$N_{total} - k$	M_{within}	-
Total	SS_{total}	$N_{total} - 1$	-	-

The *between-sample* mean square ($M_{between}$) results from real differences between the samples and the *within-sample* mean square (M_{within}) is due to the testing or analytical procedure (i.e. indeterminate error). The null hypothesis $M_{between} = M_{within}$ is tested against the alternative hypothesis $M_{between} > M_{within}$. If F, which equals $M_{between} / M_{within}$ exceeds the value of F with (k-1) and $N_{total} - k$ degrees of freedom for the desired confidence level, the null hypothesis is rejected and the alternative hypothesis accepted i.e. the differences between the means of the different samples can be regarded as significant at that level of confidence.

APPENDIX B – Experimental Results for Bioleach Experiments at Various Solids Loading

3% pyrite

Time	pH	Redox	Iron Concentration kgFe/m^3				Iron release		Total count
		Eh	Suspension		Supernatant		kgFe/m^3		
hours		Ag/AgCl	Fe^{2+}	Fe^{tot}	Fe^{2+}	Fe^{tot}	Fe^{tot}	Fe^{2+}	cells/ml
0	1.59	547	0.14	1.95	0.14	1.95	0.00	0.00	4.25E+08
22	1.33	504	0.28	3.63	0.28	3.35	1.68	0.14	6.73E+08
46	1.14	522	0.28	6.70	0.28	6.14	4.75	0.14	9.66E+08
70	0.97	544	0.28	9.08	0.28	8.38	7.12	0.14	1.66E+09
93	0.99	586	0.14	12.01	0.14	12.01	10.05	0.00	1.66E+09
102	1.00	590	0.14	12.57	0.14	12.29	10.61	0.00	1.46E+09
117	0.81	623	0.14	13.40	0.14	13.12	11.45	0.00	1.52E+09
124	0.90	639	0.14	13.40	0.14	13.40	11.45	0.00	1.16E+09

3% pyrite with 6% quartz

Time	pH	Redox	Iron Concentration kgFe/m^3				Iron release		Total count
			Suspension		Supernatant		kgFe/m^3		
hours			Fe^{2+}	Fe^{tot}	Fe^{2+}	Fe^{tot}	Fe^{tot}	Fe^{2+}	cells/ml
2	1.45	492	0.28	1.40	0.28	1.40	1.40	0.28	3.02E+08
20	1.37	521	0.14	2.23	0.14	2.23	2.23	0.00	3.88E+08
46	1.21	520	0.28	3.91	0.28	3.63	3.91	0.28	7.06E+08
52	1.14	527	0.28	4.19	0.28	4.19	4.19	0.28	7.31E+08
68	1.08	542	0.28	5.59	0.28	5.59	5.59	0.28	1.00E+09
75	1.08	550	0.28	6.42	0.28	6.42	6.42	0.28	1.33E+09
93	1.00	565	0.14	8.38	0.14	8.38	8.38	0.00	1.55E+09
99	1.08	577	0.14	9.22	0.14	9.22	9.22	0.00	1.56E+09
117	1.08	605	0.14	11.17	0.14	10.61	11.17	0.00	1.84E+09
123	1.01	625	0.14	12.29	0.14	11.73	12.29	0.00	1.84E+09
130	1.15	645	0.14	12.01	0.14	11.73	12.01	0.00	1.36E+09

3% pyrite with 15% quartz

Time	pH	Redox	Iron Concentration kgFe/m^3				Iron release		Total count
			Suspension		Supernatant		kgFe/m^3		
hours			Fe^{2+}	Fe^{tot}	Fe^{2+}	Fe^{tot}	Fe^{tot}	Fe^{2+}	cells/ml
2	1.65	475	0.42	1.40	0.42	1.40	1.40	0.42	1.69E+08
21	1.49	499	0.28	2.23	0.28	1.95	2.23	0.28	4.27E+08
46	1.42	519	0.28	4.19	0.28	3.91	4.19	0.28	6.59E+08
52	1.38	527	0.28	5.03	0.28	4.47	5.03	0.28	6.25E+08
73	1.35	539	0.28	6.42	0.28	5.59	6.42	0.28	1.10E+09
82	1.39	542	0.14	6.98	0.14	6.70	6.98	0.14	1.34E+09
94	1.34	565	0.14	7.82	0.14	7.26	7.82	0.14	1.34E+09
102	1.02	575	0.14	8.66	0.14	8.66	8.66	0.14	1.44E+09
119	0.82	628	0.14	11.17	0.14	11.17	11.17	0.14	1.59E+09
127	1.07	656	0.14	12.29	0.14	11.73	12.29	0.14	1.60E+09
142	0.92	650	0.14	11.73	0.14	11.73	11.73	0.14	1.59E+09

3% pyrite with 21% quartz

Time	pH	Redox	Iron Concentration kgFe/m^3				Iron release		Total count
			Suspension		Supernatant		kgFe/m^3		
hours			Fe^{2+}	Fe^{tot}	Fe^{2+}	Fe^{tot}	Fe^{tot}	Fe^{2+}	cells/ml
2	1.43	495	0.28	1.40	0.28	1.40	1.40	0.28	3.13E+08
21	1.26	521	0.28	2.23	0.28	2.23	2.23	0.28	4.98E+08
46	1.03	528	0.28	4.19	0.28	3.63	4.19	0.28	5.83E+08
55	1.03	525	0.28	5.03	0.28	4.75	5.03	0.28	8.28E+08
69	0.95	536	0.28	5.03	0.28	5.03	5.03	0.28	8.03E+08
75	0.79	541	0.28	5.86	0.28	5.86	5.86	0.28	8.75E+08
92	0.83	547	0.28	6.70	0.28	6.70	6.70	0.28	1.03E+09
99	0.87	553	0.28	7.26	0.28	7.26	7.26	0.28	1.03E+09
117	0.83	562	0.14	8.10	0.14	8.10	8.10	0.14	1.03E+09
125	0.81	566	0.14	8.66	0.14	8.66	8.66	0.14	1.04E+09
141	0.73	578	0.14	9.22	0.14	9.22	9.22	0.14	9.97E+08
148	0.76	580	0.14	9.22	0.14	9.22	9.22	0.14	9.09E+08

3% pyrite with 24% quartz

Time	pH	Redox	Iron Concentration kgFe/m^3				Iron release		Total count
			Suspension		Supernatant		kgFe/m^3		
hours			Fe^{2+}	Fe^{tot}	Fe^{2+}	Fe^{tot}	Fe^{tot}	Fe^{2+}	cells/ml
1	1.46	507	0.14	1.95	0.14	1.95	1.95	0.14	2.64E+08
23	1.39	547	0.14	3.35	0.14	3.07	3.35	0.14	6.00E+08
47	1.31	536	0.28	4.47	0.28	4.47	4.47	0.28	8.34E+08
55	1.16	534	0.28	5.03	0.28	5.03	5.03	0.28	6.88E+08
72	1.19	539	0.28	5.31	0.28	5.03	5.31	0.28	6.42E+08
94	1.14	548	0.14	6.14	0.14	5.86	6.14	0.14	6.91E+08
101	1.03	555	0.14	6.42	0.14	6.42	6.42	0.14	7.91E+08
118	1.01	556	0.14	6.98	0.14	6.98	6.98	0.14	7.41E+08
125	0.95	563	0.14	6.98	0.14	6.98	6.98	0.14	6.53E+08
142	0.94	567	0.14	7.82	0.14	7.82	7.82	0.14	8.09E+08
166	1.08	568	0.14	7.82	0.14	7.82	7.82	0.14	5.09E+08

Comparison of bioleaching experimental results of Nemati and Harrison's work (2000) with the current work

3% pyrite

Nemati and Harrison

Time hours	Iron Released kg Fe /m^3	Microbial cell concentration cell/ml
0	0.00	1.01E+08
20	0.70	1.41E+08
43	2.94	5.06E+08
68	5.88	1.13E+09
98	8.82	1.38E+09
121	9.24	6.00E+08
139	9.94	5.38E+08
164	9.80	5.31E+08

Current Work

Time hours	Iron Released kg Fe /m^3	Microbial cell concentration cell/ml
0	4.25	4.25E+08
22	6.73	6.73E+08
46	9.66	9.66E+08
70	16.56	1.66E+09
93	16.58	1.66E+09
102	14.58	1.46E+09
117	15.17	1.52E+09
124	11.58	1.16E+09

18% pyrite

Nemati and Harrison

Time hours	Iron Released kg Fe /m^3	Microbial cell concentration cell/ml
0	0.00	3.13E+07
23	0.28	5.31E+06
48	0.56	7.50E+06
71	0.70	3.44E+06
96	0.84	1.88E+06
169	1.40	2.63E+07
188	1.54	8.38E+07
212	1.82	1.25E+08
236	2.52	1.78E+08
260	3.08	2.05E+08
291	4.76	1.88E+08
313	5.32	3.38E+08
333	5.60	1.88E+08
356	5.46	1.69E+08
380	5.46	1.35E+08
404	5.60	1.05E+08
428	5.60	5.25E+07
479	5.88	6.56E+07
500	5.88	7.50E+07
525	5.88	5.63E+07

Current Work

Time hours	Iron Released kg Fe /m^3	Microbial cell concentration cell/ml
0	0.00	3.31E+08
22	1.12	4.19E+08
46	2.51	1.83E+08
70	2.79	7.50E+07
93	2.79	1.06E+07

APPENDIX C – Bioleaching experimental results with the addition of air enriched with carbon dioxide

3% pyrite

	with 1% CO_2 added			
Fe release	Biomass concentration	pH	Redox Potential	time
[Fe]kg/m^3	10^8cells /ml		Ag/AgCl	h
0.00	2.3	1.65	520	0
1.68	5.4	1.35	521	23
4.75	11.9	1.17	553	48
7.82	16.7	0.96	574	71
9.77	15.2	0.93	606	95
11.73	17.3	0.87	669	120
11.73	17.4	0.9	670	123

	no CO_2 added			
Fe release	Biomass concentration	pH	Redox Potential	time
[Fe]kg/m^3	10^8cells /ml		Ag/AgCl	h
0.00	4.3	1.59	547	0
0.00	6.7	1.33	504	22
0.00	9.7	1.14	522	46
0.00	16.6	0.97	544	70
0.00	16.6	0.99	586	93
0.00	14.6	1	590	102
0.00	15.2	0.81	623	117
0.00	11.6	0.9	639	124

3% pyrite 21% quartz

	with 1% CO_2 added			
Fe release	Biomass concentration	pH	Redox Potential	time
[Fe]kg/m^3	10^8cells /ml		Ag/AgCl	h
0.00	3.1	1.62	492	0
1.54	5.4	1.38	497	22
2.93	6.1	1.27	494	47
4.19	7.6	1.19	498	71
5.17	11.1	1.14	503	96
5.72	7.7	1.11	501	122
6.00	10.4	1.11	505	143

3% pyrite 21% quartz

	no CO_2 added			
Fe release	Biomass concentration	pH	Redox Potential	time
[Fe]kg/m^3	10^8cells /ml		Ag/AgCl	h
0.00	3.3	1.62	538	0
1.40	5.2	1.32	514	22
2.51	4.2	1.20	508	46
3.07	3.3	1.16	505	71
3.91	4.4	1.15	498	96
4.75	3.6	1.16	495	119
4.47	2.7	1.10	491	143
4.75	2.3	1.14	493	168

3%pyrite, 24% quartz

	with 1% CO_2 added			
Fe release	Biomass concentration	pH	Redox Potential	time
[Fe]kg/m^3	10^8cells /ml		Ag/AgCl	h
0.00	3.1	1.53	487	1
1.40	6.8	1.33	520	24
3.63	9.2	1.19	527	47
4.47	9.5	1.15	531	54
5.59	8.4	1.08	541	72
5.86	11.7	1.10	543	81
6.98	13.6	1.07	571	95
8.10	12.4	1.04	581	120
8.66	11.8	1.01	559	145
8.94	12.7	0.99	563	154
8.94	9.9	0.99	573	169

	no CO_2 added			
Fe release	Biomass concentration	pH	Redox Potential	time
[Fe]kg/m^3	10^8cells /ml		Ag/AgCl	h
0.00	3.5	1.46	507	1
1.68	6.7	1.39	547	24
3.07	5.4	1.31	536	47
3.35	4.7	1.16	534	54
3.35	3.8	1.19	539	72
3.63	4.3	1.14	548	81
4.19	3.6	1.03	555	95
4.47	3.0	1.01	556	120
4.19	3.4	0.95	563	145
4.75	3.5	0.94	567	154
4.19	2.7	1.08	568	169

APPENDIX D – Bioleaching experimental results at various agitation rates using 3% pyrite in the presence of 15% quartz

560 rpm

Time hours	Iron release kg/m^3	Microbial cell concentration 10^8 cells/ml	pH	Redox Potential Ag/AgCl
2	0.00	1.7	1.65	475
21	0.84	4.3	1.49	499
46	2.79	6.6	1.42	519
52	3.63	6.6	1.38	527
73	5.03	11.0	1.35	539
82	5.59	13.4	1.39	542
94	6.42	13.4	1.34	565
102	7.26	14.4	1.02	575
119	9.77	16.0	0.82	628
127	10.89	16.0	1.07	656
142	10.33	15.9	0.92	650

660rpm

Time hours	Iron release kg/m^3	Microbial cell concentration 10^8 cells/ml	pH	Redox Potential Ag/AgCl
0	0.00	4.6	1.60	551
24	1.95	6.9	1.35	506
42	4.75	9.4	1.16	524
67	6.28	12.4	1.05	546
91	9.49	14.6	1.00	568
116	10.89	15.6	0.92	595
140	11.45	13.6	0.90	609
162	10.75	9.3	0.92	610

760rpm

Time hours	Iron release kg/m^3	Microbial cell concentration 10^8 cells/ml	pH	Redox Potential Ag/AgCl
0	0.00	3.1	1.6	505
19	1.26	4.8	1.36	501
44	1.54	2.6	1.28	444
67	1.54	1.7	1.26	430
92	1.68	0.7	1.28	429
115	1.40	0.7	1.28	430

APPENDIX E – Bioleaching experimental results for different inoculum states using 3% pyrite and 15% quartz

Shake flask

Time hours	Iron concentration (kg /m^3)	Microbial cell concentration cells/ml	pH	Redox Potential Ag/AgCl
0	3.35	5.56E+08	1.19	513
26	4.19	4.01E+08	1.18	484
48	4.75	2.48E+08	1.17	475
72	4.75	1.34E+08	1.11	470
97	4.75	9.19E+07	1.20	473
145	4.75	1.04E+08	1.20	472

STR

Time hours	Iron concentration (kg /m^3)	Microbial cell concentration cells/ml	pH	Redox Potential Ag/AgCl
0	0.84	4.27E+08	1.49	499
23	2.79	6.59E+08	1.42	519
30	3.63	6.25E+08	1.38	527
51	5.03	1.10E+09	1.35	539
60	5.59	1.34E+09	1.39	542
71	6.42	1.34E+09	1.34	565
79	7.26	1.44E+09	1.02	575
96	9.77	1.59E+09	0.82	628
104	10.89	1.60E+09	1.07	656
119	10.33	1.59E+09	0.92	650

APPENDIX F – Size Distribution of Pyrite and Quartz